INTRODUCTION

Nature entrusts peptides with numerous tasks ranging from passing on messages as peptide hormones to priming the immune system, tuning metabolism and protein degradation or defending microorganisms as antibiotic agents. In addition, researchers have identified a variety of peptides with artificial biological functions that are not represented by naturally occurring molecules, e. g. receptor antagonists or inhibitors of protein-protein interactions. These peptides or their derivatives are starting points for drug development and, indeed, a number of peptides or peptide-derived drugs have already made their way into the clinic. Compared to the standard properties of drug-like small molecules matching the "rule of five", which are today's preferred formats, peptide-based drugs sometimes overcome the barrier of "undruggable targets" and are often extremely potent. Furthermore, many peptides are highly specific and do not accumulate in the body since they have short half-life. As a consequence, peptides often show less systemic toxicity compared to small molecules. In addition, peptides are ideal, rapidly accessible lead structures for drug-target validation as well as further drug development due to their modulator structure, variable presentation of different functional groups and easy to prepare, either chemically or biologically. Despite their favourable properties, peptide-based drugs are under-represented in the pharmaceutical market. This discrimination is usually due to their poor bioavailability, which sometimes necessitates non-oral administration or even special medical devices such as inhalers. Another related major disadvantage of peptides is their low metabolic stability due to proteolytic degradation. In addition, costs of goods for the drug substance are sometimes tremendous. Therefore, there is considerable interest to transform the "active principle" of biologically active peptides into small molecules with improved pharmacokinetics properties.

The Role of Somatostatin

" Non c'è nulla interamente in nostro potere,
se non i nostri pensieri. "

René Descartes
(1596 – 1650)

The peptide hormone somatostatin (SRIF) is a cyclic tetradecapeptide whose primary structural formula showed in Figure 1 was isolated from ovine hypothalamus[1] in 1973 and firstly synthesized by Rivier.[2]

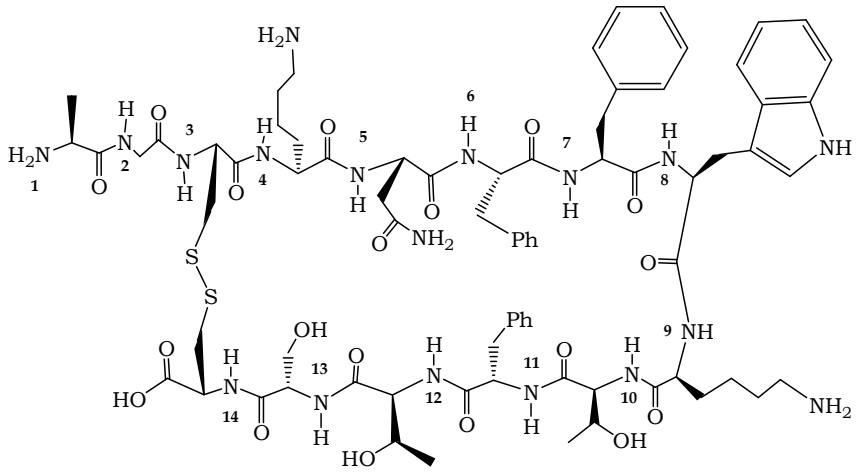

Figure 1. SRIF-14.

Later on an amino-terminally extended type, Somatostatine-28 (SRIF-28) was discovered in the gut.[3] The highly potent somatostatin peptides SRIF-14 and SRIF-28 are generated as C-terminus products from prosomatostatin.[4] SRIF-14 and 28 are predominantly produced by neurones and secretory cells in the central and peripheral nervous system and in the gastrointestinal tract. SRIF are unique in their broad inhibitory effects on both endocrine secretion, for example, on growth hormone (GH), insulin, glucagon, gastrin, cholecistokinin, Vasoactive Intestinal Peptide (VIP) and secretin and exocrine secretion for example, of gastric acid, intestinal fluid and pancreatic enzymes.[5,6] SRIF induces its biological effects, all inhibitory in nature, by a family of structurally related, G-protein-coupled, transmembrane receptors (
Figure 2) located in pituitary, pancreas, gastrointestinal tract, thyroid and immune cells. Somatostatin receptors (sst) have also been localized in various tumour cells for example, breast cancer cells, neuroblastoma, glioma and leukemic and myeloma cell

[1] Burgus, R.; Brazeau, P.; Vale, W. W. Isolation and Determination of the Primary Structure of Somatostatin (a Somatotropin Release Inhibiting Factor) of Bovin Hypothalamic Origin. *Advances in Human Growth Hormone Research*; U. S. Government Printing Office, DHEW, Publ No. (NIH) **1973**, *74-612*, pp144-158.
[2] Rivier, J. Somatostatin: Total Solid Phase Synthesis. *J. Am. Chem. Soc.* **1974**, *96*, 2986-2992.
[3] Pradayrol, L.; Joernvall, H.; Mutt, V.; Ribet, A. N-Terminally Extended Somatostatin: the Primary Structure of Somatostatin-28. *FEBS Letters.* **1980**, *109*, 55-58.
[4] Beniot, R.; Esch, F.; Bennett, H. P. J. Processing of Somatostatin. *Metabolism.* **1990**, *39*, 22-25.
[5] Reichlin, S. Somatostatin. *N. Engl. J. Med.* **1983**, *309*, 1495-1501.
[6] Reichlin, S. Somatostatin. (Second Part). *N. Engl. J. Med.* **1983**, *309*, 1495-1501.

lines.[7] Signaling through SRIF receptors is complex; the binding of the ligand to sst induces G_i-protein activation and signalling through various pathways is showed in Figure 2.

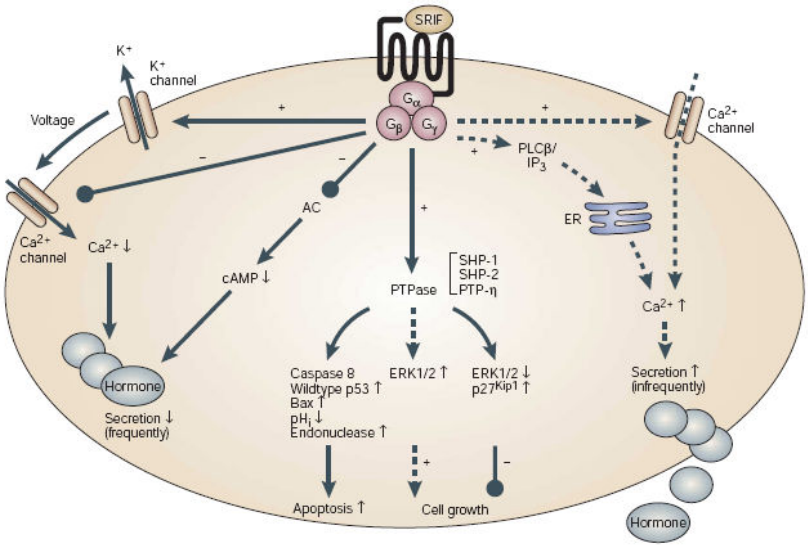

Figure 2. SRIF receptor-mediated modulation of signalling cascades leading to changes in hormone secretion, apoptosis and cell growth.[8]

In mammalian, six distinct somatostatin receptor subtypes, termed sst_1, sst_2 A sst_2 B, sst_3, sst_4 and sst_5, have so far been isolated by recombinant Deoxyribonucleic acid (DNA) technology (Figure 3).[9,10,11] Their identification in the early 1990s was a major step forward in elucidating the SRIF signalling system. During recent years, researchers were urged to find correlation between cloned and native receptors and to assign specific function to individual receptor subtypes.[12] The specific functional roles of $sstr_{1-5}$ receptors are under extensive investigation. In addition to normal tissues, sst are over-expressed by gastro-intenteropancreatic (GEP) tumours, pituitary tumours, small-cell lung tumours, carcinoid tumours, prostate carcinoma, breast carcinoma, renal carcinoma

[7] Patel, J.C. Molecoular Pharmacology of Somatostatin Receptor Subtypes. *J. Endocrinol. Invest.* **1997**, *20*, 348-367.
[8] Weckbecker, G.; Lewis, I.; Albert, I.; Schmid, A. H.; Hoyer, D.; Bruns, C.; Opportunities in Somatostatin Research: Biological, chemical and therapeutic aspects. *Nat. Rev.* **2003**, *2*, 999-1017.
[9] Yamada, Y.; Post, S.; Wang, K.; Tager, H.; Bell, G. I.; Seino, S. Cloning and Functional Characterization of a Family of Human and Mouse Somatostatin Receptors Expressed in Brain, Gastrointestinal Tract and Kidney. *Proc. Natl. Acad. Sci.* USA **1992**, *89*, 251-255.
[10] Rayonor, K.; O'Carroll, A.; Kong, H. Characterization of Cloned Somatostatin Receptors sst_4 and sst_5. *Mol. Pharmacol.* **1993**, *44*, 385-392.
[11] Meyerhof, W. The Elucidation of Somatostatin Receptor Functions: a Current View. *Rev. Physiol. Biochem. Pharmacol.* **1998**, *133*, 55-108.
[12] Olias, G.; Viollet, C.; Kusserow, H.; Epelbaum, J.; Meyerhof, W. Regulation and Function of Somatostatin Receptors. *J. of Neurochem.* **2004**, *89*, 1057-1091.

and frequently nervous system tumours and medullary carcinoma of thyroid. Sst_2 is the most frequently expressed subtype, followed by sst_1, sst_3, sst_4 and finally by sst_5.

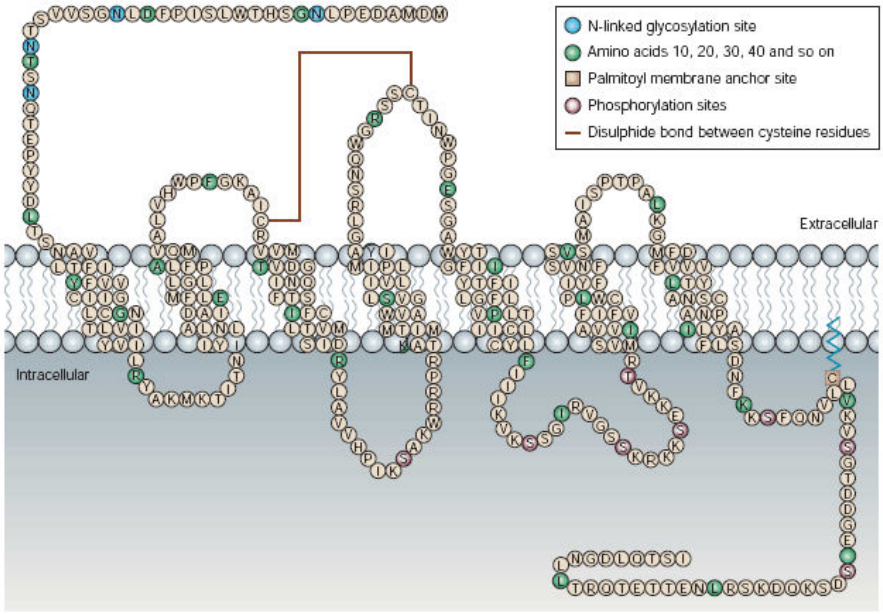

Figure 3. Structure of SRIF receptors exemplified by subtype $sstr_{2A}$ receptor.[8]

Recently, several laboratory found that sstr-expressing tumours frequently contain two or more sst subtypes, and discovered that sst subtypes might form homo/heterodimers to create a novel receptor with different functional characteristics, expanding the array of selective sst activation pathway and subsequent intracellular signalling cascade.[13]

The co-expression of multiple sst subtypes in malignant and normal cells has recently been investigated by Reubi *et al.*[14] They evaluated approximately 200 tumours for their receptors subtype protein expression by competition binding experiments using subtype-selective ligands to displace [^{125}I]-[Leu^8, D-Trp^{22}, Tyr^{25}]-sst-28. The majority of the tested tumours predominantly expressed sst_2. Prostate carcinomas and sarcomas preferentially expressed sst_1. Most inactive pituitary adenomas expressed sst_3 and to lesser extend sst_2 while GH-secreting pituitary adenomas expressed sst_2 and sst_5. GEP tumours and phaeochromocytomas frequently expressed sst_2 and/or sst_1. Regarding the molecular mechanisms involved in SRIF antineoplastic activity, both indirect and direct effects via specific sstr expressed in the target cells have been described.

[13] Froidevaux, S.; Ebarle, A. N. Somatostatin Analogs and Radiopeptides in Cancer Therapy. *Biopolymers Peptide Science*, **2002**, *66*, 161-183.
[14] Reubi, J. C.; Waser, B.; Schaer, J. C.; Laissue, J. A. Somatostatin Receptor sst1-sst5 Expression in Normal and Neoplastic Human Tissues Using Receptor Autoradiography with Subtype-Selective Ligands *Eur. J. Nucl. Med.* **2001**, *28*, 836-846.

Direct action may result by the interaction of the ligand with sst that cause the blockade of mitogenetic growth signal or induce apoptosis. Indirect effects may be the results of reduced or inhibited secretion of growth promoting hormones and growth factors, that stimulate the growth of various type of cancer, also inhibition of angiogenesis or influence on the immune system are important factors.

1.1. Clinical use of Somatostatin analogues

The demonstration of the broad antisecretory action of natural SRIF in the 1970s drove a number of early clinical studies to characterize the potential therapeutic role of natural SRIF, mainly in acromegaly, diabetes and gastrointestinal disorders. SRIF can decrease elevate concentration of GH in acromegalic patient, this evidence prepared the ground for the subsequent clinical use of SRIF analogues in this type of tumour.[5,6] In patient with type I diabetes, continuously infused SRIF resulted in a lowering of blood glucose.[15] However, neither SRIF nor any of somatostatin analogues have been approved as antidiabetic agents. Similarly, despite the demonstration gf numbers of numerous effects of SRIF on gastrointestinal mobility, secretion and absorption, its clinical usefulness for treating gastrointestinal disorders has been limited. Promising early studies showed beneficial effects of SRIF in gastric ulcer and gastritis, haemorrhagic pancreatitis and on tissue damage caused by toxic agents. New SRIF analogues with a more SRIF-like broad sstr binding²profile should be re-investigated. So far, only SRIF-14 (Stilamin) and two analogues, octreotide (SMS 201-995; Sandostatin) and Lanreotide (BIM 23014; Somatuline), are approved for clinical use; Vapreotide (RC-160; Octastatin) is still in Phase II studies. The binding affinity of the analogues compared with SRIF-14 and SRIF-28 are given in table 1.

Compound	***Sstr$_1$***	***Sstr$_2$***	***Sstr$_3$***	***Sstr$_4$***	***Sstr$_5$***
SRIF-14	1.1	1.3	1.6	0.53	0.9
SRIF-28	2.2	4.1	6.1	1.1	0.07
Octreotide	>1000	2.1	4.4	>1000	5.6
BIM 23014	>1000	1.8	43	66	0.62
RC-160	>1000	5.4	31	45	0.7

Table 1. Binding affinities[16] (K_i) nM of clinically useful Somatostatin analogues at sst_{1-5} receptors.

[15] Gerich, J. E.; Lorenzi, M; Schineider, V.; Forsham, P. H. Effect of Somatostatin on Plasma Glucose and Insulin Reponses to Glucagon and Tolbutamide in Man. *J. Clin. Endocrinol. Metab.* **1974**, *39*, 1057-1060.
[16] Patel, J. C.; Srikant, C. B. Subtype Selectivity of Peptide Analogs for All Five Cloned Human Somatostatin Receptors (sst_{1-5}). *Endocrinology*. **1994**, *135*, 2814-2817.

The metabolically unstable SRIF14 is used for certain acute indications, such as acute oesophagel vertical bleedings,[17] whereas the SRIF analogues are mainly use in chronic setting. Ocreotide and Lanreotide are available as long acting release formulation.[18,19] Octreotide and Lanreotide are approved For treating pituitary adenomas and GEP tumours.[20,21] Current research is exploring additional indication for these classical drugs as well as for new SRIF analogues. In the clinical application, not only binding of the radiolabeled somatostatin analogues to the receptor is important but also internalization of the receptor–ligand complex for successful *in vivo* targeting of tumoural peptide receptors using radiopeptides.[22, 23] Therefore, during the course of optimal development of new radiopeptide analogues for *in vivo* receptor targeting, peptide need to be tested not only for receptor binding and biodistribution but also for their receptor internalization properties. Localization of neuroendocrine tumours in patients by standard technique such as ultrasonography or computed tomography is often very difficult because of the frequently small size of such tumours. Visualization of sst in neuroendocrine tumours was therefore considered an alternative approach, provided that SRIF radiopharmaceuticals suitable for scintigraphy are available and density of sst in endocrine tumours is high enough for this type of imaging. The first radioactive SRIF analogues used for external imaging was [^{123}I]-[Tyr^3]-octreotide (OctreoTher).[24] More recently, several novel chelator attachment at the N-terminus of SRIF analogues for labelling with radio-metals were designed and studied in the clinic. In most case a bifunctional chelating agent (BFCA), as DTPA or DOTA (Figure 4.), were use in order to chelate the radio-metals and to conjugate to the drug with covalent bond. [^{111}In]-[DTPA D-Phe^1]-octreotide[25] was the first radiopeptide explored in patients

[17] Avgerios, A.; Nevens, F.; Raptus, S.; Fevery, J. Early Administration of Somatostatinand Efficacy of Sclerotherapy in Acute Oesophageal Vertical Bleeds: the European Acute Bleedings Oesophageal Vertical Episodes (ABOVE) Randomised Trial. *Lancet*. **1997**, *350*, 1495-1499.

[18] Coron, P.; Morante-Ramons, I.; Cognem M; Jaquet, P. Three Years Follow-Up of Acromegalic Patient Treated with Intramuscolar Slow-Realease Lanreotide. *J. Clin. Endocrinol. Metab.* **1997**, *82*, 18-22.

[19] Lancranjan, I.; Atkinson, A. B. Results of an European Multicentre study with Sandostatin LAR in Acromegalic Patient. Sandostatin LAR Group. *Pituitary*. **1999**, *1*, 105-114.

[20] Karashima, T.; Cai, R. Z.; Shally, A. V.; Effects of Highly Potent Octapeptide Analogs of Somatostatin on Growth Hormone, Insulin and Glucagon Release. *Life Sci.* **1987**, *41*, 1011-1019.

[21] Lamberts, S. W. J.; Krenning, E. P.; Reubi, J. C. The Role of Somatostatin and its Analogs in the Diagnosis and Treatment of Tumors. *Endocrine Rev.* **1991**, *12*, 450-482.

[22] Reubi, J. C. Peptide receptors as molecular targets for cancer diagnosis and therapy. *Endocrinol Rev.* **2003**, *24*, 389-427.

[23] Kwekkeboom, D. J.; Krenning, E. P.; De Jong, M.; Peptide Receptor imaging and therapy. *J Nucl. Med.* **2000**, *41*, 1704-1713.

[24] Krenning, E. P.; Bakker, W. H.; Breeman, W. A; Koper, J. W.; Kooij, P.P.; Ausema, L.; Lameris, J. S.; Reubi, J. C.; Lamberts, S. W. Localisation of Endocrine-Related Tumours with Radioiodinated Analogue of Somatostatin. *Lancet*. **1989**, *1*, 242–244.

[25] Bakker, W. H.; Albert, R.; Bruns, C.; Breeman, W. A.; Hofland, L. J.; Marbach, P.; Pless, J.; Pralet, D.; Stolz, B.; Koper, J.; et al. [^{111}I]-[D-Phe^1]-Octreotide a potential radiopharmaceutical for imaging of somatostatin receptor positive tumor: synthesis, radiolabelling and in vitro validation. *Life Sci.* **1991**, *49*, 1583-1591.

which contains a chelator-bound radiometal. This radiopharmaceutical is now commercially available as OctreoScan and used routinely in the clinic for tumour imaging of sstr-expressing neuroendocrine tumours.[26]

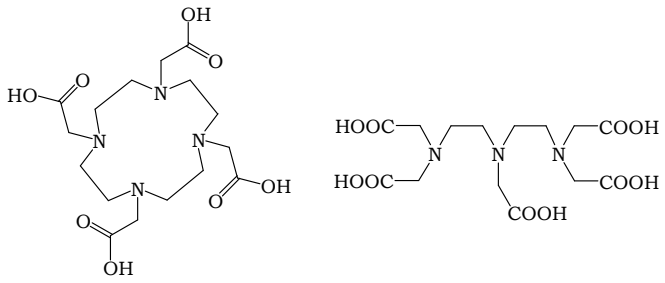

Figure 4. Bifunctional chelating agents: a. DOTA and b. DTPA.

Other [^{111}I]-labelled [DTPA D-Phe^{1}]-octreotide analogues containing hydrolysable linker group were examined, with little advantage over OctreoScan. DOTA-octreotide analogues displayed more favourable *in vivo* distribution than OctreoScan and are more suitable for internal radiotherapy.[27] It has also been shown that sstr scintigraphy using this agent is the most sensitive method for localization of primary and metastatic diseases in endocrine pancreatic tumour and carcinoid insulinomas.[28] New conjugates may show higher sensitivity with regard to the localization of tumour and metastases. [^{111}I]-DOTA-TOC and [^{90}Y]-DOTA-TOC have shown to be effective targeting and therapeutic agent in animal model and patient.[29] In addition, replacement of the alcohol group at C-terminus of octa-peptide by carboxylic acid group led to increase sst_2 affinity and [^{177}Lu-DOTA]- D-Phe^{1}-Tyr^{3}-Thr^{8}-octreotide ([^{177}Lu-DOTA-TATE]) showed higher tumour uptake than [^{111}In-DTPA].[14] These new radio-peptide bind with high affinity only to sst_2, no affinity to sst_4 and low with sst_3 and sst_5. Although the majority of tumour studied expressed mainly sst_2, recent literature data indicate that also sst_1 and

[26] Kenning, e. P. Kwekkeboom, D. J.; Bakker, W. H.; Breeman, W. A.; Kooij, P. P.; Oei, H. Y.; van Hagen, M.; Postema, P. T.; de Jong, M.; Reubi, J. C.; *et. al*. Somatostatin receptor scintigraphy with [^{111}In-DTPA-D-Phe^{1}]- and [^{123}I-Tyr^{3}]-octreotide: the Rotterdam experience with more than 1000 patients *Eur. J. Nucl. Med.* **1993**, *20*, 716-731.

[27] Froidevaux, S.; Heppeler, A.; Eberle, A. N.; Meier, A. M.; Häusler, M.; Beglinger, C.; Béhé, M.; Powell, P.; Mäcke H. R. Preclinical Comparison in AR4–2J Tumor-Bearing Mice of Four Radiolabelled 1,4,7,10-Tetraazacyclododecane-1,4,7,10-Tetraacetic Acid-Somatostatin Analogs for Tumor Diagnosis and Internal Radiotherapy. *Endocrinology*. **2000**, *141*, 3304-3312.

[28] Gibril, F.; Reynolds, J. C.; Doppman, J. L.; et. al. Somatostatin Receptor Scintigraphy: Its Sensitivity Compared with that of Other Imaging Methods in Detecting Primary and Metastatic gastrinomas-a Prospective study. *Ann. Inter. Med.* **1996**, *125*, 24-26.

[29] Otte, A.; Muller-Brand, J.; Dallas, S.; Nitzshe, E.; Herrmann, R.; Maecke, H. Yttrium-90-labelled Somatostatin-Analogue for Cancer Treatment. *Lancet*. **1998**, *351*, 417-418.

sst_3, sst_5 may be present in the same human tumours. To extend biological activity profile of radiolabelled somatostatin analogues, same authors investigated several radiopeptides. [^{111}In/^{90}Y- DOTA-1-Nal^3-octreotide] (^{111}In/^{90}Y- DOTA-NOC) was one of the most interesting peptide; it has improved affinity to sst_2 and high affinity to sst_3 and sst_5 and potentially extend the spectrum of accessible tumours in diagnosis and internal radiotherapy.[30] As described before ^{111}In, ^{90}Y and ^{177}Lu are the most common radio-metals used for diagnosis and therapy. Other radio-metals, as ^{99m}Tc, ^{64}Cu and ^{68}Ga, are recently investigated to improve distribution properties and tumour imaging. ^{99m}Tc has favourable properties as low cost production and short half-life (6 h), some ^{99m}Tc-analogues showed good performance in identification of sst-positive tumours.[31] Several [^{64}Cu]-labelled somatostatin analogues were synthesized and showed favourable biodistribution in animal models and good performance in PET imaging in patients; however the use of ^{64}Cu relies on the availability of a cyclotron.[32] Another interesting positron emitter is ^{68}Ga which is produced by a ^{68}Ge/^{68}Ga generator available at most PET centres.[33] In the table below we displayed the most common radio-metals used to obtain radiopharmaceuticals.

[30] Wild, D.; Shmitt, J. S.; Ginj, M.; Maecke, H. R.; Bernard, B. F.; Krenning, E.; de Jong, M.; Wenger, S.; Reubi, J. C. DOTA-NOC, a High-Affinity Ligand of Somatostatin Receptor Subtype 2, 3 and 5 for Labelling with various Radiometals. *Eur. J. Nucl. Med.* **2003**, *30*, 1338-1347.

[31] Virgolini, I.; Leiner, M.; Handermaker, H.; et. al. Somatostain Receptor Subtype Specificity and in vivo Binding of a Novel Tumor Tracer ^{99m}Tc-P829. *Cancer Res*. **1998**, *58*, 1850-1859.

32 Sprague, J. E.; Peng, Y.; Sun, X.; Weisman, G. R.; Wong, E. H.; Achilefu, S.; Anderson C. J. Preparation and Biological Evaluation of Copper-64–Labeled Tyr^3-Octreotate Using a Cross-Bridged Macrocyclic Chelator. *Clinical Cancer Research* **2004**, *10*, 8674-8682.

[33] Froidevaux, S.; Eberle, A. N.; Christe, M.; Sumanovski, L.; Heppeler, A.; Schmitt, J. S.; Eisenwiener , K.; Beglinger , C.; Mäcke , H. R. Neuroendocrine tumor targeting: Study of novel gallium-labeled somatostatin radiopeptides in a rat pancreatic tumor model. *Int. J. Cancer.* **2002**, *98*, 930-937.

Radio-nuclide	Physical half-life	Particle Energy (MeV)	Maximum tissue range
^{32}P	14.3 d	β (1.71)	8.7 mm
^{67}Cu	2.58 d	β (0.54), γ (0.185)	1.8 mm
^{90}Y	2.67 d	β (2.28)	12.0 mm
^{105}Rh	1.48 d	β (0.57), γ (0.320)	1.9 mm
^{109}Pd	13.6 h	β (1.0)	4.6 mm
^{111}Ag	7.47 d	β (1.05), γ (0.34)	4.8 mm
^{125}I	60.0 d	γ (0.027)	10 nm
^{131}I	8.04 d	β (0.6), γ (0.364)	2.0 mm
^{177}Lu	6.7 d	β (0.497), γ (0.208)	1.5 mm
^{186}Re	3.77 d	β (1.08), γ (0.131)	5.0 mm
^{188}Re	16.95 h	β (2.13), γ (0.155)	11.0 mm
^{198}Au	2.7 d	β (0.97), γ (0.411)	4.4 mm
^{211}At	7.2 h	α (6.8)	65 μm
^{212}Bi	1 h	α (7.8), γ (0.72)	70 μm
^{99m}Tc	6 h	γ (0.143)	6.7 mm
^{64}Cu	12.7 h	β (0.573), γ (1.34)	10 μm

Table 2. Radio-nuclides physical half-life, decay and maximum penetration.

Peptide Design

" Lo scienziato non è l'uomo che fornisce le vere risposte:
è quello che pone le vere domande. "

Claude Levi Strauss
(1908-2009)

The design of a chemical library will depend on whether it is destined for a discovery screen against a novel target, in which case diversity is key, or whether it will explore the SAR around a particular chemotype for a specific target. Will the library be based on a novel scaffold, or derived from a peptide or natural product? Should it be prepared by automated, parallel techniques, or can a biosynthetic pathway be pressed into service? Often there is no right answer to these questions, and debate is likely to continue for a long time on the key issue of "diversity": how is it measured, how is it designed and, ultimately, what does it mean in the context of a chemical collection? Nuclear Magnetic Resonance (NMR)-based techniques have emerged as the most powerful of the methods used to detect low-affinity ligands in biological systems. In *silico* predictive methods have become available to asses very large compound datasets, helping scientists to classify and rank compound collections or library designs according to their predicted properties or compliance with established rules. In order to discover new drugs, new chemical entities are needed. These compounds need to be designed or sourced. Where do the new chemical entities come from? The production of focused compounds is nowadays benefiting greatly from recent developments of in *silico* tools for drug design. Many cheminformatics and bioinformatics approaches have been recently developed to assist in the design and synthesis of relevant compounds. Computer-based lead finding and feature-based pharmacophore algorithms are used for designing and optimizing as many chemical scaffold properties as possible. Quantitative structure-activity relationship (QSAR) analysis, clustering and principal component analysis are mathematical tools which are routinely utilized to optimize, render and cluster the 2D and 3D structures of chemical entities and correlate them with biological activity.[34] The calculated physiochemical information for the compounds of interest is evaluated and correlated with what is knew about the structure of the target itself. All of this insight are fed back into the design of a set of compounds that are optimized for the desired target and appropriate physical characteristics (natural product-likeness, drug-likeness) within a diversity set. Even when the structure of the biological target is not readily available, cheminformatics approaches can still be useful in library design based on known pharmacophoric features of the chemical scaffolds.

[34] Kubinyi. H. Combinatorial and computational approaches in structure-based drug design. *Curr. Opin. Drug. Disc. Dev.* **1998**, *1* (1), 16.

2.1 The Rational Approach

Rational approach takes into account all available information about the target-ligand system in question, to narrow down the chemical space of potential small molecule ligands. Structure-based methods utilise information of the 3D structure of the target protein. This information can be used as a template for docking experiments in which libraries of small molecules are fitted into the binding site of the target. Ligand based design depends on structural information about ligands. This ligand structure is either known from experimental techniques, such as X-ray crystallography or NMR spectroscopy, or can be deduced from other ligands with known structure, such as protein, or from SAR data and sequence information about the ligands. The sequence based approach was employed since the beginning of SRIF discovery to obtain new active peptides, starting from the native natural molecule. This approach involves scanning the entire sequence of protein with overlapping peptides, usually not longer than 15 amino acids (peptide scan), which are screened for interactions with a binding partner. The sequence common to the interacting peptides is the binding site and such peptides often inhibit the respective protein-protein interaction. Once the primary structure of the biologically active peptide has been determined, the first step is to identify the smallest active fragment required for biological activity. This step involves the preparation of truncated peptides in which amino acids from the amino and carboxyl termini have been removed, one at a time. Subsequently, the influence of each individual amino acid on the biological activity is determined by systematically replacing each residue in the peptide with specific amino acids, such as alanine or D-amino acids.[35,36] After the SAR of each amino acid in the peptide has been explored, the bioactive conformation is investigated by introducing constraints at various positions in the peptide to reduce its conformational flexibility. In the final step, the essential amino acid side chains are positioned on carefully selected non-peptide scaffolds to correspond with the derived model of the bioactive conformation (Scheme 1).[37] Biologically active peptides often contain a well-defined core of the key residues. Peptides are typically highly flexible, but should be as rigid as possible for the transformation process for two reasons: the binding-free energy of a peptide interacting

[35] Brown, M.; Rivier, J.; Vale, W. Somatostatin: Analogs with Selected Biologic Activity. *Science*. **1977**, *196*, 1467-1469.
[36] Vale, W.; Rivier, J.; Ling, N.Brown, M. Biologic and Immunologic Activities and Application of Somatostatin Analogs. *Metab. Clin. Exp.* **1978**, *27*, 1391-1401.
[37] V. J. Ruby. Designing peptide receptor agonists and antagonists. *Nat. Rev. Drug Discov*. **2002**, *1*, 847.

with a binding partner can be improved, and even more important a rigid conformation helps in generating a peptide-based pharmacophore model because functional groups involved in activity are already prepositioned and can be assigned in three dimensions, preferably by NMR techniques.

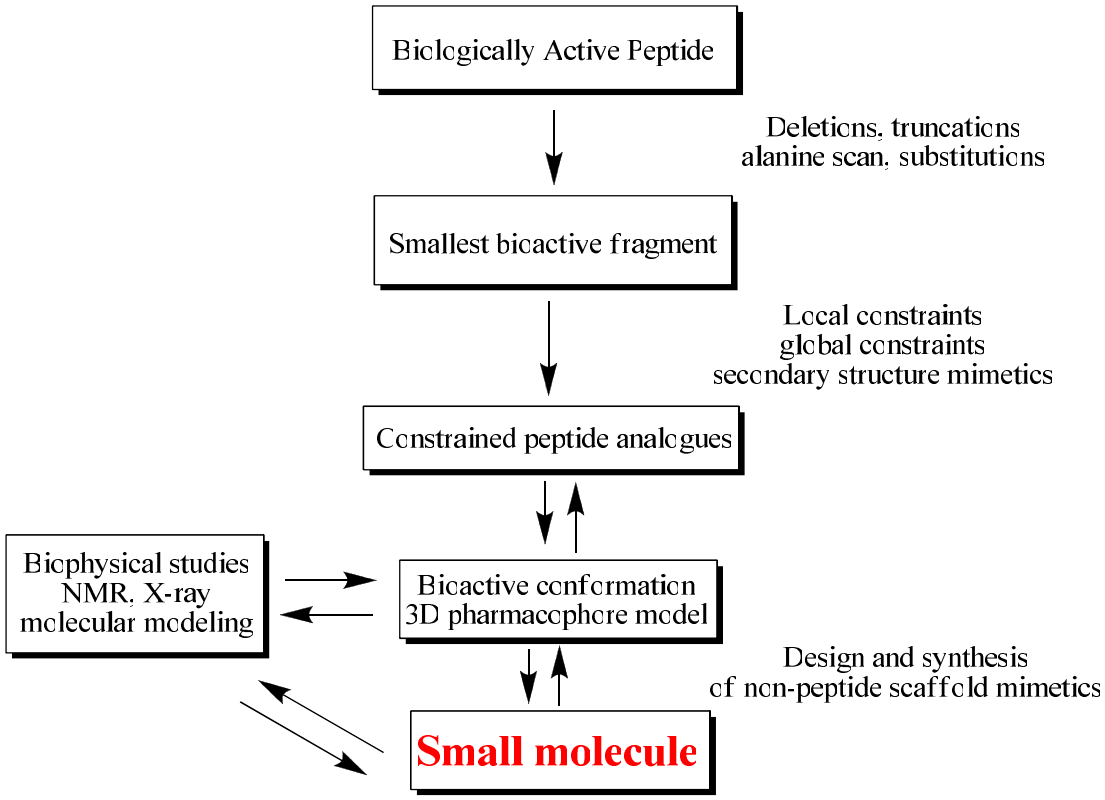

Scheme 1. Strategy for transforming peptides into small molecules.

Conformational flexibility can be reduced by introducing local and/or global constraints at various positions in the peptide. Local conformational constraints can be achieved by incorporating modified amino acids (D-, N-methyl, α-methyl, cyclic, α,β-dehydro, β-substituted amino acids), replacing the amide moiety by isosteres (CH=CH, CH_2CH_2, CH_2NH, etc) and short range cyclizations, either within a single amino acid (proline or proline mimetics) or between adjacent residues. Cyclization can impose significant conformational restrictions on the peptide backbone and the location of attached side chains. The most common examples of side chain to side chain cyclization include the formation of disulfide bridges between cysteine and the formation of lactam bridges between glutamic/aspartic acid and lysine residues. Since SRIF was discovered in 1973, the rational approach, in particular the sequence based design, has suggested new SRIF analogue structures, agonist and antagonist both. To overcome the

therapeutic limitation of SRIF-14, namely its very short plasma half-life of 3minutes,[38] since its discovery, much works have been done to ascertain the minimum structural requirements for biological activity. In the group with D-amino acid substitution, replacing Trp^8 with D-Trp^8 (numbering is referred to SRIF-14) increased the potency by 6-8 times (inhibition of GH *in vitro* and glucagon and insulin *in vivo*).[39] [D-Trp^8]-SRIF was the first analogue reported possessing significantly higher potency than somatostatin. Its high potency might reflect the stabilization of a more active conformation or may result from a greater resistance of the peptide to degradation. D-Trp^8 substitution seems to be critical for the potency of SRIF analogues, as it has been used in all somatostatin analogues but sst_3 antagonist.[40] Substitution of Ala for Gly^2, Lys^4, Asn^5, Thr^{10}, Thr^{12} or Ser^{13} did not markedly reduce biological activity, indicating that the functional groups of these residues are expendable. Replacement of Phe^6, Phe^7, Trp^8, Lys^9 or Phe^{11} by alanine decreased the GH inhibiting potency of the resultant analogues. Based on these results Vale *et al.* found that the smallest peptide active to inhibit GH secretion was a cyclic peptide (Figure 5).[41] This finding reinforced the view of the importance of the 6-11 amino acid region in somatostatin and provided a simplified model peptide for further studies.

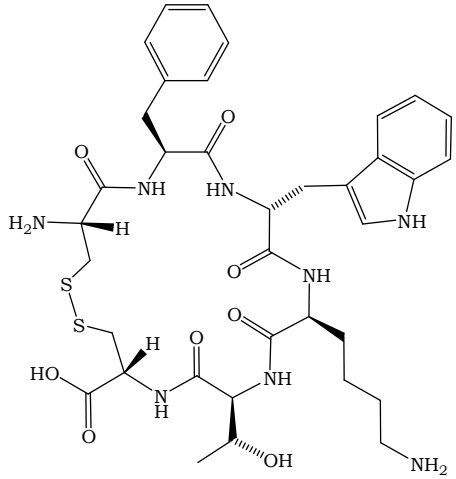

Figure 5. Smallest peptide active to inhibit GH

[38] Patel Y. C.; Wheatley, T. i*n Vivo* and *in Vitro* Plasma Disappearence and Metabolism of Somatostatin-28 and Somatostatin-14 in the Rat. *Endocrinology*. **1983**, *37*, 632-634.
[39] Rivier, J.;.Brown, M.; Vale, W. D-Trp8-somatostatin: an analog of somatostatin more potent than the native molecule. *Biochem Biophys Res Commun*. **1975**, *65*, 746–751.
[40] Reubi, J. C.; Schaer J. C.; Wanger, S.; Hoeger, C.; Herchegyi, J.; Waser, B.; Rivier, J. Sst_3-selective Potent Peptidic Somatostatin Receptor Antagonists. *PNAS*. **2000**, *97*, 13973-13978.
[41] Vale, W.; Brown, M; Rivier, C.; Perrin, M.; Rivier, J. Development and Application of Analogs of LRF and Somatostatin. In Brain Peptides: A New Endorinology. Eds Gotto, A. M. Jr; Peck, E. J. Jr; Boyd, A. E. **1979**, Elsevier Scientific, Amsterdam, pp 71-88.

2.1.1 Somatostatin agonists

Based on the model sequence in Figure 5. , Vale *et al.* synthesized a series of octa- and nona-peptide analogues, which all contained the Phe^7-D-Trp^8-Lys^9-Thr^{10} fragment found to be the pharmacophore sequence of SRIF. Residues D-Trp^8-Lys^9 were essential, whereas Phe^7 and Thr^{10} can undergo minor substitutions e.g. Phe^7 can be replaced with Tyr while Thr^{10} can be substituted with Ser or Val. Veber *et al*. synthesized a series of reduced-size analogues, within the most interesting was the highly active hexa-peptide analogue L-363, 301 (Figure 6).

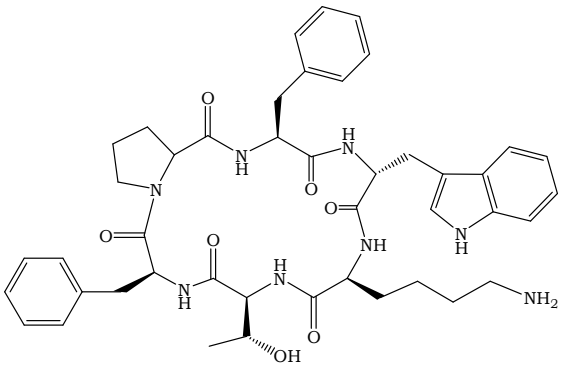

Figure 6. L-363, 301.

Proline at position 6 was used to form the cyclic hexa-peptide derivative trough an amide linkage. This molecule showed higher biological activity than native SRIF in inhibiting the release of GH, insulin and glucagon. From NMR studies Veber and colleagues proposed a type II' β-turn about the tetra-peptide sequence Phe^7-D-Trp^8-Lys^9-Thr^{10}, which they considered to be the biologically active portion interacting with the receptor.[42,43] The II' β-turn is expected to arise from the particular amino acid sequence of the tetra-peptide portion (D-amino acid at position i+1 ad L-amino acid at position i+2).[44,45] From the Nuclear Overhauser Effects (NOE) and restraint molecular dynamic it can be seen that the turn structure is important for the proper orientation of the adjacent Phe, Trp and Lys. The biologically active analogues have the side chains of

[42] Nutt, R.; Veber, D. F.; Curley, P.; Saperstein, R.; Hirshmann, R. Somatostain Analogs which Define the Role of the Lysine-9 Amino Group. *Int. J. Peptide Protein Res.* **1983**, *21*, 66-73.
[43] Veber, D. F.; Saperstein, R.; Nutt, R.; *et al*. A Super Active Cyclic Hexa-peptide Analogs of Somatostatin. *Life Sci.* **1984**, *34*, 1371-1378.
[44] Lewis, P. N.; Momany, F. A.; Scheraga, H. A. Folding of Peptide Chains in Proteins: A Proposed Mechanism for Folding. *Proc. Nat. Acad. Sci. USA*. **1971**, *68*, 2293-2297.
[45] Hutchinson, E. G.; Thorton, J. M. A Revised Set of Potentials β-turn Formation in Proteins. *Protein Sci.* **1994**, *3*, 2207-2216.

Lys and D-Trp extended away from the 18-membered ring in close proximity to each other. The absence of the II' β-turn at the D-Trp-Lys disrupt the side-chain array produced inactive molecules. So the role of the bridging region is to stabilize the II' β-turn and help to maintain the proper orientation of the side-chains of Lys and D-Trp. Bauer *et al.* chose as a conformationally adequate surrogate for somatostatin sequence the cyclic hexa-peptide described first by Vale,[41] c[Cys- Phe-D-Trp-Lys-Thr-Cys], which, however, showed only 1/1000 times the potency of the activity of SRIF in pituitary cell culture *in vitro*. They proceeded to prepare close analogues of this hexa-peptide in search of peptides that would inhibit the secretion of GH and be more stable than somatostatin by incorporating additional residues at both ends of the molecule. One of the residues of SRIF thought to be important is Phe^6, which was replaced by Cys in the cyclopeptide. D-Phe added to the N-terminus of hexa-peptide proved to be very advantageous for activity. The aromatic side chain of this additional amino acid can occupies at least some of the conformational space available to Phe^6 in somatostatin and also protects the disulphide bridge against enzymatic attacks. Addition of the amino alcohol Thr-ol to the cyclo-hexa-peptide C-terminus further increase the activity. The resulting octa-peptide (Figure 7.), named SMS 201-995 or octreotide or sandostatin, was characterized by a greater duration of action and half-life (117 min), great metabolic stability and higher selectivity in GH inhibition compared with insulin and glucagone.[46,47]

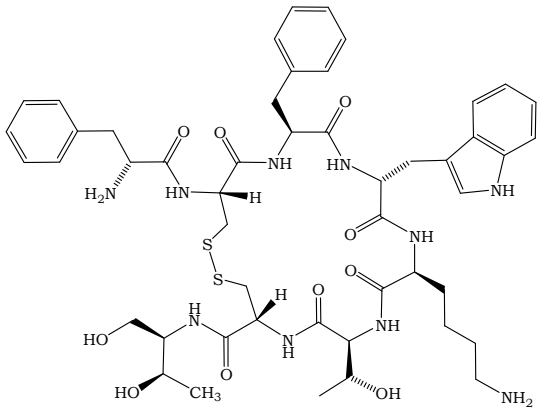

Figure 7. Octreotide, SMS-201-995.

[46] Bauer, W.; Briner, U.; Doepfner, W.; *et al*. SMS-201-995; a very Potent and Selective Octapeptide Analogue of Somatostatin *Life Sci.* **1982**, *31*, 1133-1140.
[47] Marbach, P.; Briner, U.; Lemaiire, M.; Shweizer, A.; Terasaki T. From Somatostatin to Sondatostatin: Pharmacodinamycs and Pharmacokinetics. *Metab.Clin. Exp.* **1992**, *41*, 7-10.

Octreotide, which is 70 time more potent in inhibiting GH *in vivo* than SRIF and 3 time more potent *in vitro,* is protected against enzymatic degradation by the D-Phe residues at N-terminus and by the amino alcohol at the C-terminus. SMS-201-995 was introduced into clinical practice in 1987 for treatment of hormone-secreting pituitary adenomas and GEP tumours.[48] The high potency of octreotide encouraged many investigators to use this octa-peptide as a parent compound for further modifications. Schally and co-workers synthesized 200 octa-peptide amide analogues of somatostatin. They contained Phe^3 and Thr^6 or Tyr^6 and Val^6 and were modified at N-terminus and at C-terminus. One of the synthesized analogues, named RC-160 or vapreotide (Figure 8.), showed a high potency and long duration of action for inhibiting of GH release *in vivo*, and much lower activity for the suppression of insulin, glucagon and gastric acid secretion.[49]

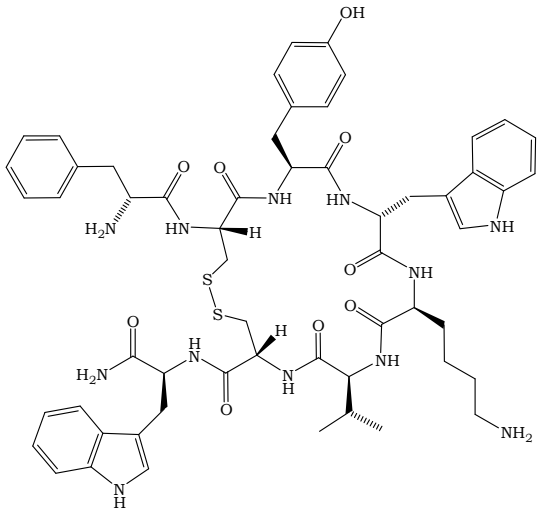

Figure 8. RC-160 Vapreotide.

Another series of octa-peptide analogues was synthesized by Coy and co-workers, the most active analogue of this series was BIM 23014 or lanreotide (Figure 9.) which shows some selectivity in binding to the $sstr_5$ over the $sstr_2$ subtype.[50]

[48] Lamberts, S. W. J.; van der Lay, A. J.; de Herder, W. W.; Hofland, L. J. Octreotide. Drug Therapy. *New Engl. J. Med.* **1996**, *334*, 246-254.
[49] Cai, R. Z.; Karashima, T.; Guoth, J.; Szoke, B.; Olsen, D.; Schally, A. V. Superactive Octapeptide Somatostatin Analogs Containing Tryptophan in position 1. *Proc. Natl. Acad. Sci. USA*, **1987**, *84*, 2502-2506.
[50] Murphy, W. A.; Lance, V. A.; Moreau, S.; Moreau, J. P.; Coy, D. H. Inhibition of Rat Prostate tumor growth by an Octapeptide Analog of Somatostatin *Life Sci.*, **1987**, *40*, 2515-2522.

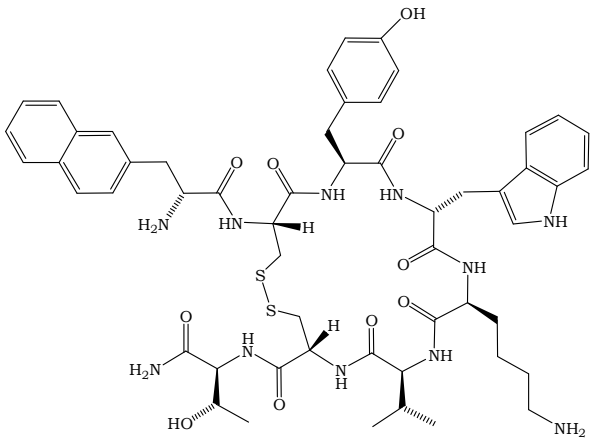

Figure 9. BIM 23014 lanreotide.

Based on L-363,301 Veber and co-workers synthesized MK-678 or segletide (Figure 10.) which showed at least 10-fold greater potency than the parent compound in all biological tests and 50-100 times the potency of SRIF for inhibition of glucagon, insulin and GH release.[51] MK-678 showed an even more selective binding affinity profile than octreotide, with higher-affinity binding to $sstr_2$ and reduced affinity for $sstr_3$ and $sstr_5$.

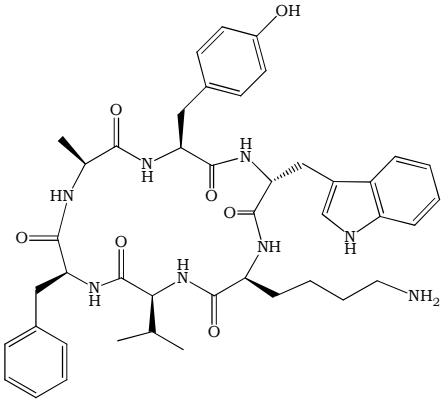

Figure 10. MK-678 segletide.

Later on Mattern *et al.* investigated the biological activity and conformational behaviour of L-363,301 analogues. Novel arylalkyl peptoid residues, N-benzylglicine and (*R*) and (*S*)-*β*-methyl-benzylglycine, which can induced *cis*-amide bonds were introduced instead of Pro^6 in the parent L-363,301 to further investigate the role of the bridging region.[52,53] Changing in selectivity and biological activity of the new analogues

[51] Veber, D. F.; Sapertstein, R.; Nutt, R. F. A Super Active Cyclic Hexapetide Analog of Somatostatin. *Life Sci.* **1984**, *34*, 1371-1378.
[52] Mattern, R. H.; Tran, T. A.; Goodman, M. Conformational Analysis of Somatostatin-Related Cyclic Hexapeptide Containing Peptoid Residues. *J. Med. Chem.* **1998**, *41*, 2686-2692.

suggested the importance of an hydrophobic residue in position 6. Comparing the binding activity of the new peptoid analogues the author underlined that arylalkyl residues near the side-chain of Phe^{11} could increase the binding with sst_2. The orientation of the aryl chain of the peptoid residues parallel to the aromatic portion of Phe^{11} is well tolerated by $sstr_2$, and destroyed the affinity toward sst_3 and sst_5. All this modification of L-363,301 provided new conceptual avenues to follow in structure activity relationship studies. However, they did not contribute to finding more potent or clinically useful somatostatin analogues.

A new promising molecules is SOM230, which possesses almost equal affinity for all receptors subtypes. This analogue, based on a cyclo-hexa-peptide template, incorporates novel functionalized side-chain, such as tyrosyl-benzyl, to mimic Phe^6, Phe^7 and Phe^{11} residues, and hydroxyproline with a basic extension to mimic Lys^4 of SRIF-14. SOM230 can be considered as almost universal SRIF agonist (Figure 11.). *In vitro* studies indicate that this analogue is a potent inhibitor of GH release from human GH-secreting pituitary adenomas and prolactin (PRL) release from mixed GH/PRL-secreting tumours and prolactinomas.

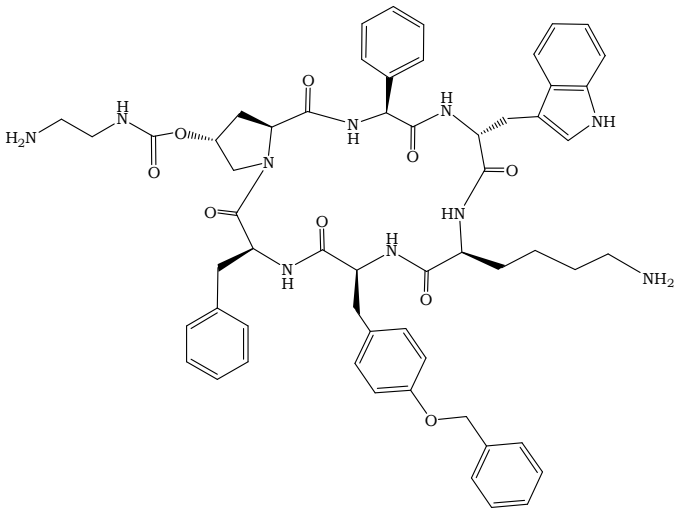

Figure 11. SOM230 first universal SRIF agonist.

Other studies demonstrated SOM230 is a highly potent inhibiting of GH/IGF-1 axis in rat, dogs and monkeys, as well as in healthy human subjects and acromegalic

[53] Mattern, R. H.; Moore, S. B.; Tran, T. A.; Rueter, J. K; Goodman, M. Synthesis, Biological Activities and Conformational Studies of Somatostatin Analogs. *Tetrahedron* **2000**, *56*, 9819-9831.

patient.[54,55] Approaches for developing selective analogues could also be based on intermediate SRIF-14/octa-peptide template. The undeca-peptide CH-275 (Figure 12.) incorporates I-Amp in the *β*-turn and shows high-affinity binding to sst_1 but not bind to the other four subtypes.[56]

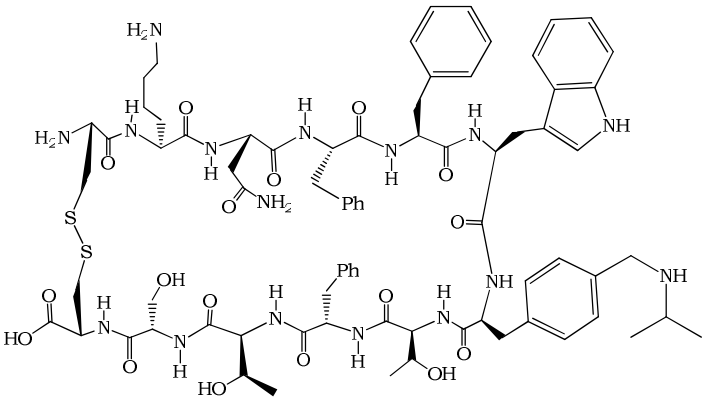

Figure 12. CH-275 sst_1 selective analogue.

The rationale behind this approach was that the introduction of conformational constraints, induced by incorporating N-methylated amino acids, would limit the multiple bioactive conformations of SRIF-14, thereby providing the selective SRIF-14 template-based analogues with high affinity for $sstr_1$.[57] Furthermore, ring chemistry, size and position of the bridging units exert strong effects on sstr binding, as shown in a study of a novel cyclic-backbone-based somatostatin analogue PTR3173 (Figure 13. which selectively inhibits growth hormone but not insulin and glucagon, and which has been clinically evaluated.[58]

[54] Lewis, I.; Bauer, W.; Albert, R.; Chandramouli, N.; Pless, J.; Weckbecker, G.; Bruns, C. A Novel Somatostatin Mimic with Broad Somatotropine Release Inhibitory Factor Receptor Binding and Superior Therapeutic Potential. *J. Med. Chem.* **2003**, *46*, 2334-2344.

[55] Hoflan, L. J.; van del Hoek, J.; van Koetsveld, P. M.; Herder, W. W.; Waaijers, M.; Sprij-Kooij, D.; Bruns, C.; Weckbecker, G.; Feelders, R.; vander Lely, A. J.; et al. The Novel Somatostatin Analog SOM230 is a Potent Inhibitor of Hormone Release by Growth Hormone-and Prolactine-Secretion Pituitary Adenomas *in vitro*. *J. Clin. Endocrinol. Metab.* **2004**, *89*, 1577-1585.

[56] Rivier, J. E.; Hoeger, C.; Erchegyi, J.; Gulyas, J.; DeBoard, R.; Craig, A. G.; Koerber, S. C.; Wenger, S.; Waser, B.; Schaer, J. C.; Reubi J. C.; Potent Somatostatin Undecapeptide Agonists Selective for Somatostatin Receptor 1 (sst1). *J. Med. Chem.* **2001**, *44*, 2238-2246.

[57] Rajeswaran, W. G.; Hocart, S. J.; Murphy, W. A.; Taylor, J. E.; Coy D. H. *N*-Methyl Scan of Somatostatin Octapeptide Agonists Produces Interesting Effects on Receptor Subtype Specificity. *J. Med. Chem.* **2001**, *44*, 1416-1421.

[58] Afargan, M.; Janson, E. T.; Gelerman, G.; Rosenfeld, R.; Ziv, O.; Karpov, O.; Wolf, A.; Bracha, M.; Shohat, D.; Liapakis, G.; Gilon, C.; Hoffman, A.; Stephensky, D.; Oberg, K.; Novel Long-Acting Somatostatin Analog with Endocrine Selectivity: Potent Suppression of Growth Hormone But Not of Insulin. *Endocrinology*. **2001**, *142*, 477-486.

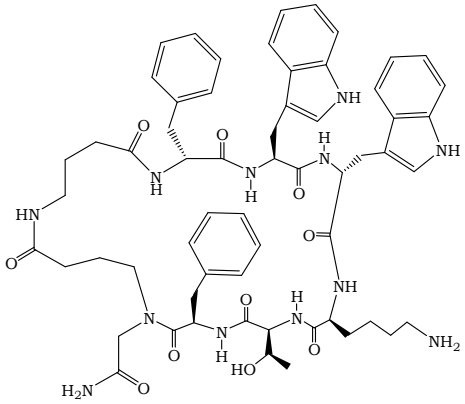

Figure 13. PTR3173 cyclic- backbone analogue.

2.1.2 Somatostatin antagonists

The full versatility of octa-peptide template has been demonstrated with the discovery of peptidic sst_2-breacking analogues, such as the cyclic octa-peptide CYN-154806 (Figure 14.), the first SRIF peptide antagonist that binds to sst_2 with nanomolar affinity, and exhibits intermediate affinity for sst_5.[59]

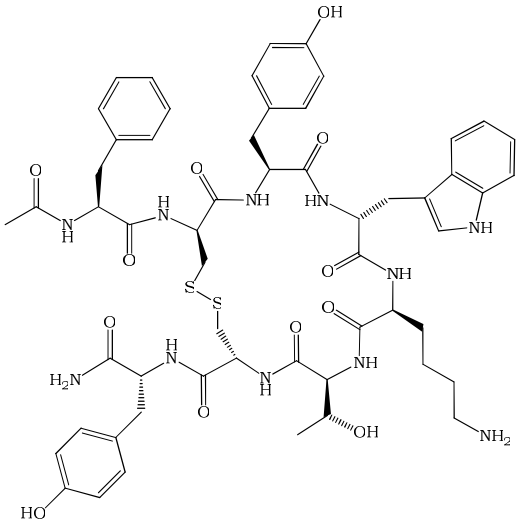

Figure 14. CYN-154806 first SRIF antagonist.

The octa-peptide antagonist sst_3-ODN-8 (Figure 15.), in which the conformation-restricting N-methyl-2-amino-2-napthoyl-aminoglycine replaces D-Trp[8], binds

[59] Bass, R. T.; Buckwalter, B. L.; Patel, B. P.; Pausch, M. H.; Price, L. A.; Strnad, J.; Hadcock J. R.; Identification and Characterization of Novel Somatostatin Antagonists. *Mol. Pharmacol.* **1997**, *50*, 709-715.

selectively and with high affinity to sst_3 and antagonizes SRIF-induced inhibition of c-AMP accumulation. Sst_3-ODN-8 enabled functional investigation of $sstr_3$ and demonstrated the utility of strategies based on restricting conformational freedom.[40] Although there is a consensus that antagonists generally do not trigger the internalization of G-protein–coupled receptors, examples exist of peptide receptor antagonists that do stimulate internalization, such as cholecystokinin-, 5-HT2A-, endothelin- and neuropeptide Y–analogism.[60,61] In the somatostatin receptor field, a recent report indicated that somatostatin receptor agonists, but not somatostatin receptor antagonists, are able to internalize the somatostatin receptor subtype 2.[62]

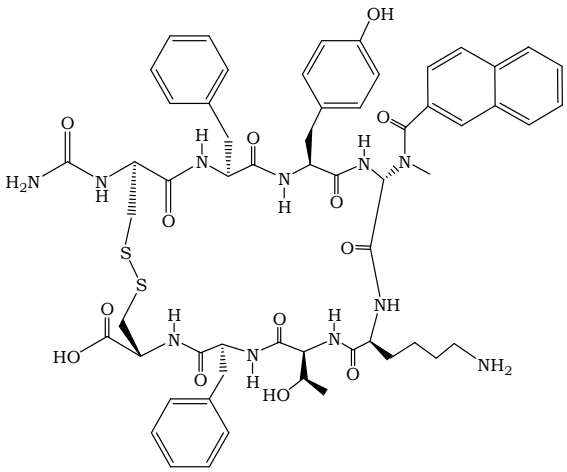

Figure 15. Sst_3-ODN-8 selective sst_3 antagonist.

Many studies describing new radiopeptides for in vivo targeting do not give experimental evidence of whether these radioligands are agonists or antagonists. Sst_3 somatostatin receptor subtype and sst_5 are internalized to a much higher extent than its sst_1 or somatostatin receptor subtype sst_4.

[60] Gray J. A., Roth B.L. Paradoxical trafficking and regulation of 5-HT(2A) receptors by agonists and antagonists. *Brain Res Bull.* **2001**, 56, 441–451.
[61] Pheng L.H., Dumont Y., Fournier A., Chabot J. G., Beaudet A., Quirion R. Agonist and antagonist-induced sequestration/internalization of neuropeptide Y Y1 receptors in HEK293 cells. *Br J Pharmacol.* **2003**, *139*, 695–704.
[62] Liu Q., Cescato R., Dewi D.A., Rivier J., Reubi J.C., Schonbrunn A. Receptor signaling and endocytosis are differentially regulated by somatostatin analogs. *Mol Pharmacol.* **2005**, *68*, 90–101.

2.2 NMR conformational analysis approach

The first NMR experiments with biopolymers were described over 30 years ago. Initial progress was slow because of limitations imposed both by the available instrumentation and by the lack of suitable samples of biological macromolecules. ^{1}H-NMR assignments have been described to date for more than 7598 small proteins. Listing of chemical shifts obtained from systematic studies of amino acid residues in model peptides are also available for ^{13}C and ^{1}H NMR (Table 3.).[63]

Residues	Code	NH	αH	βH	Ot ers	
Gly	G	8.39	3.97			
Ala	A	8.25	4.35	1.39		
Val	V	8.44	4.18	2.13	γ CH$_3$	0.97, 0.94
Ile	I	8.19	4.23	1.90	γ CH$_2$ γ CH$_3$ δ CH$_3$	1.48, 1.19 0.95 0.89
Leu	L	8.42	4.38	1.65, 1.65	γ H δ CH$_3$	1.64 0.94, 0.90
Pr (trans)	P		4.44	2.28, 2.02	γ CH$_2$ δ CH$_2$	2.03, 2.03 3.68, 3.65
Ser	S	8.38	4.50	3.88, 3.88		
Thr	T	8.24	4.35	4.22	γ CH$_3$	1.23
Asp	D	8.41	4.76	2.84, 2.75		
Glu	E	8.37	4.29	2.09, 1.97	γ CH$_2$	2.31, 2.28
Lys	K	8.41	4.36	1.85, 1.76	γ CH$_2$ δ CH$_2$ ε CH$_2$ ε NH$_3$	1.45, 1.45 1.70, 1.70 3.02, 3.02 7.52
Arg	R	8.27	4.38	1.89, 1.79	γ CH$_2$ δ CH$_2$ NH	1.70, 1.70 3.32, 3.32 7.17, 6.62
Asn	N	8.75	4.75	2.83, 2.75	γ NH$_2$	7.59, 6.91
Gln	Q	8.41	4.37	2.13, 2.01	γ CH$_2$ δ NH$_2$	2.38, 2.38 6.87, 7.59
Met	M	8.42	4.52	2.15, 2.01	γ CH$_2$ ε CH$_3$	2.64, 2.64 2.13
Cys	C	8.31	4.69	3.28, 2.96		
Trp	W	8.09	4.70	3.32, 3.19	2H 4H 5H 6H 7H NH	7.24 7.65 7.17 7.24 7.50 10.22
Phe	F	8.23	4.66	3.22, 2.99	2,6H 3,5H 4H	7.30 7.39 7.34
Tyr	Y	8.18	4.60	3.13, 2.92	2,6H 3,5H	7.15 6.86
His	H	8.41	4.63	3.26, 3.20	2H 4H	8.12 7.14

Table 3. ^{1}H chemical shifts for the 20 common amino acid residues.

[63] Wütrich, K.; *NMR of protein and nucleic acids*. **1986**. Wiley, New York.

One of the principal role of the NMR investigation is the knowledge of the bioactive conformation. A NMR data set for protein structure determination contains a precisely known number of constraints and the precision of these constraints is also clearly defined. Conformational analysis resume some fundamental steps, in order to comprehend the peptide or protein structure (Scheme 2).

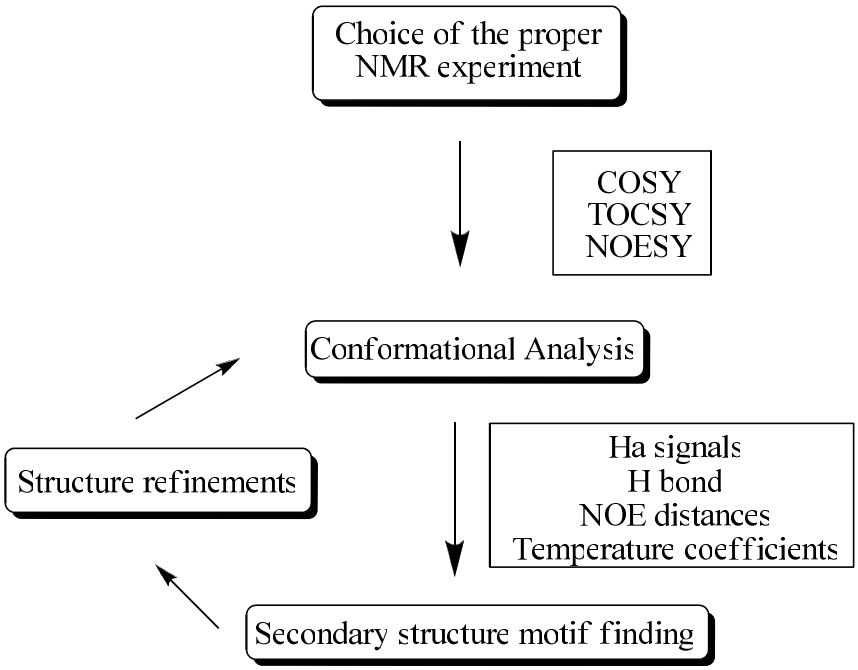

Scheme 2. The NMR conformational analysis approach.

2.2.1 NMR Experiments

Only a fraction of the NMR data are needed for obtaining the resonance assignments: NOE and intermolecular interactions. For resonance assignments of small peptides usually a set of three different spectra is recorded: a COSY, a TOCSY and the NOESY.

COSY is the standard experiment for studies of scalar spin-spin coupling connectivity. A single COSY spectrum presents a map of the complete scalar coupling (through bond) network in a macromolecular structure. The COSY experiment is therefore almost exclusively used for smaller peptides. Positions of cross peaks in the COSY are characteristic for the amino acids and can be classified. The backbone NH-Hα spectra is of special interest, since it presents a fingerprint of the amino acid

sequence. Each L-amino acid residue contributes a single NH-Hα cross peak, and each Gly gives either two cross peaks, or a single cross peak with unique multiplet fine structure. N-terminal amino protons cannot be observed due to very rapid exchange with the solvent. Scalar coupling can only be observed between protons separated by not more than three bonds (^{3}J).

A TOCSY experiment contains all cross peaks due to protons of the same spin system. Protons from different amino acids always belong to different spin system, because there is no scalar coupling across the amide bond. Analysis of spin systems allows to decide to which type of amino acids the spin system belongs.

Cross peaks in the NOESY are due to dipolar couplings resulting from interaction of spins *via space* and hence only dependent on the distance but non on the number of intervening bonds. Dipolar couplings are average to zero in solution but give rise to the very important relaxation phenomena, one of which is the NOE. The strong dependence of the cross peaks intensity on the distance separation explains why this parameter is the most useful for structure determination. Similarly to the situation encountered in TOCSY/COSY spectra, peaks may be classified according to in which region of the spectrum they are found. Sequential resonance assignment means connecting spin systems in their sequential order. Considering the fact that scalar couplings will never occur between protons of different amino acids it is clear that NOEs must be used for that purpose. Since NOEs may be found between all protons close in space the use of them introduces some ambiguity. For sequential correlations usually a set of peaks are used, largely depending on the secondary structure in the corresponding segment. For most values of J more than one solution exists.

Scalar couplings may be used to define dihedral angle restraint range, which sometimes helps to improve convergence of the structure calculation.[64,65] Similar to COSY, the NOESY cross peaks connect individual diagonal peaks. Numerous NOESY cross peaks are expected to occur in the same locations as COSY cross peaks, since hydrogen atoms connected by scalar coupling are usually also located at a short through-space distance. In addition, spectral regions that are nearly or completely empty in the COSY spectrum, may be crowded with NOESY cross peaks. A NOE between two hydrogen atoms (or groups or hydrogen atoms) is observed if these hydrogens are located at a shorter distance than approximately 5.0 Å from each other in the molecular

[64] Cavanagh, J.; Fairbrother, W. J.; Palmer, A. J.; Skelton, N. J.; Protein NMR Spectroscopy Principles and Practice. **1996**. Academic Press.
[65] Bax, A.; Two –Dimensional NMR and Protein Structure. *Ann., Rev., Bioch*. **1989**, 58, 223-256.

structure. Combined with resonance assignments these distance constraints can be attributed to specified sites along the polymer chain and hence the NOE experiments define the formation of loops by chain segments of variable lengths. There are two principal way for peptide to assign the protonic resonance; one of this is the sequential assignment for a polypeptide chain can conceptually be considered as a 2-step process:

- Intraresidual ^{1}H-^{1}H connectivity established by scalar spin-spin couplings.
- Inter-residue connectivity established by sequential NOEs.[66]

Each amino acid residue represents a "spin system", i.e. it consists o fan array of hydrogen atoms including an amide proton (HN), an α-proton (Hα) and the side chain protons, which can be connected by steps over three or less covalent bonds through the observation of scalar spin-spin ("through-bond") couplings. Conversely, hydrogen atoms located in sequentially neighboring amino acid residues are separated by at least four covalent bonds. Pairs of neighboring residues in the sequence can therefore only be connected *via* NOEs, manifesting short through-space distance, such as $d_{\alpha N}$ and d_{NN}.[67]

Spectra are usually recorded in 90% H_2O and 10% D_2O. The very strong water signal must be experimentally suppressed and the residual water usually appears in the middle of the spectrum. It may obscure peaks close to the water resonance (such as the Hα protons). For all the classes of peptides or proteins useful structural information can only be expected when conditions in the NMR sample match the natural biological environment as closely as possible. Although solvent mixtures, like chloroform/methanol, may help to perfectly solubilize these peptides, their structure may be quite different from those of the membrane-bound form. Cell surfaces display an enormous complexity. A perfect model to study the interaction of a peptide with a biological membrane would require knowledge about the cell membrane composition in that particular tissue. Even if such information were available it will most probably not be possible to fully mimic the biological environment.[68]

The result of a biomolecular structure determination, by solution nuclear magnetic resonance spectroscopy, is typically a family of structural models describing the accessible molecular conformations. This family, or *ensamble*, of structure models

[66] Noggle, J. H. ; Schirmer, R. E.; The Nuclear Overhouser Effect; **1971**. Academic Press, New York.
[67] Wagner, G.; Anil-Kumar, and Wütrich, K.; Systematic application of two-dimensional ^{1}H nuclear magnetic resonance techniques for studies of proteins 2: combined use of correlated spectroscopy and nuclear Overhouser spectroscopy for sequential assignments of backbone resonances and elucidation of polypeptide secondary structures.. *Eur. J. Bioc.* **1981**, *114*, 375-384.
[68] Zerbe, O.; BioNMR in Drug Research; **2002**, Wiley-VCH.

should agree as a whole with the experimental NMR data used in the procedure, as well as other additional data. Derivation of such structural restraints from NMR spectra is complicated because of spectral overlap, spin diffusion, local dynamics and interconverting conformations have to be taken into account.

2.2.2 Conformational Analysis

The function of a biologically active peptide is often dictated by its three-dimensional structure. Such preferred conformations might be similar to the binding conformation in target-peptide complexes. Conformational analysis is the study of the conformations of a molecule and their influence on its properties. The conformations of a molecule are traditionally defined as those arrangements of its atoms in space, that can be interconverted purely by rotation around single bond. The conformation of a peptide is its overall three-dimensional structure. If the bond angles and bond lengths are held fixed, the conformation can be described completely by the dihedral angles (also called torsional angles or rotations) about covalent bonds.[69,70] For this reason many experimental methods have been developed for studying conformations of peptide molecules. Theoretical methods are also valuable in the conformational analysis of peptides. With this information, can the desired conformational features be designed into a peptide? That is, given a peptide having certain conformational characteristics and certain desired biological activity, can other peptides be designed (and synthesized) having similar physical and biological properties? Knowledge of the molecular structure in solution is highly relevant. In the NMR experiments, solution conditions such as the temperature, pH and salt concentrations can be adjusted so as to closely mimic a given physiological fluid. Amino acid interactions and conformations are due to amino acids sequence. Once sequence-specific resonance assignments have been obtained, specific location in the sequence could be confirmed by further NMR measurements, such as:

NOEs. The intensity of the NOE is related to the product of the inverse sixth power of the internuclear distance. Although the NOE is a common phenomenon for all combinations of closely spaced nuclear spins, NOEs between pairs of hydrogen atoms are prime interest for structural studies. A ^{1}H-^{1}H NOE is related to the "through-space" distance between a pair of atoms that are either not at all linked by covalent bonds

[69] Popov, E. M.; Lipkind, G. M.; *Mol Biol*.; **1971**, *5*, 496-505.
[70] Ranachandran, G. N.; Ramachrishnan, C. M.; Sasisekharan, V. *J. Mol. Biol.,* **1963**, 7, 95-99.

(intermolecular NOE) or that may be far apart in the amino acid sequence of a polypeptide chain.

The formation of hydrogen bonds between backbone amide protons and backbone carbonyl oxygens is an outstanding trait of the common polypeptide secondary structures. Each secondary structure is characterized by a specific pattern of hydrogen bonds. The location of hydrogen bonds is used in the determination of protein structures by NMR.

The amide proton exchange rates are seldom measured; the preference is to use the temperature dependence of the NH shift for the same purpose. There are two reasons for this: the first one is that many peptide NMR studies are carried out in DMSO, where exchange doesn't occurs; the second one is that for many peptides in water or methanol, exchanges are so rapid that they are only measurable by saturation transfer experiments, which are technically harder than simple observation of exchange. The H end of the hydrogen bond is indicated by slow NH exchange rates. In D_2O solution the labile protons can be replaced by deuterium, so that the ^1H NMR spectrum contains only the resonance lines of the carbon-bound hydrogen atoms.

The ^3J coupling constants: in particular ^3J Hα-HN gives information about the dihedral angles of a molecule. By the Karplus equation it is possible to obtain the ϕ value of amino acid. Nevertheless it is important to remind that different dihedral angles values appertain to the same J constant when its value is intermediate.

The Temperature Coefficients : the temperature dependence of the amide proton chemical shift ($\Delta\delta_{HN}/\Delta T$) has been shown to correlate with the presence of intramolecular hydrogen bonds.

The development of methods for calculating conformations of peptide molecules originated in the early and middle 1960s. Given a set of equations and parameters, the conformational energy could be calculated for appropriately chosen conformations. By comparing the relative energies of all possible or all reasonable conformations, the lowest-energy conformation(s) could then be identified as the preferred or most probable structure(s). This would be a simple task if peptides existed predominantly in only one minimum-energy conformation (the global minimum. Ramachandran and co-workers developed an elegant method for expressing the allowed and disallowed regions of conformational space using "conformational maps": the Ramachandran

maps. These are plots showing the boundaries between the allowed and disallowed conformations as a function of two variables, ϕ and ψ.[71,72]

2.2.3 Matching the Secondary Structure motif

The occurrence of certain patterns of NMR parameters along the polypeptide chain is then indicative of particular secondary structure. This is dominated by energetically favored torsion angles ψ, φ together with additional stabilizing factors such as hydrogen bonds and hydrophobic contacts (Table 4). The most important dihedral angles in the context of peptide conformations are:

Parameter	α-helix	3_{10}-helix	γ-turn	*β*-turn II	*β*-turn II'
φ (°)	-63	-57	-70	-60	60
ψ (°)	-42	-30	70	120	-120
n	3.63	3.24	2.20		

Table 4. Average Parameters for Peptide Helices Based on α-Amino Acids.

φ: is the torsional angle described by the four atoms C'-N-C_α-C', that is, rotations about the N-Cα bond.

ψ: is described by the atoms N-C_α-C'-N, that is, rotation about the C_α-C' bond.

The nomenclature of secondary structure is usually described as n_m, where *n* is the number of amino acid residues per helical turn, and *m* is the number of atoms involved in the pseudo cycle generated by the intramolecular H-bond.

The most commonly found 3D-structures in a system of four linked peptide units are the 1←3, 1←4 and 1←5, intramolecularly H-bonded conformations. As they are pseudo cyclic forms and have different *m* values, these structures are also called C_7, C_{10} and C_{13} conformations, respectively. An alternative nomenclature of common use for these structures is *γ-turn*, *β-turn* and *α-turn* respectively. Reverse turns have often been implicated as recognition elements for peptide-receptor interactions and therefore introducing turn mimetics into peptides is an important strategy for probing bioactive

[71] Lewis, P. N.; Momany, F. A.; Scheraga, H. A. Folding of Polypeptide Chains in Proteins: A Proposed Mechanism for Folding. *PNAS*, **1971**, *68*, 2293-2297.
[72] Nemethy, G.; Scheraga, H. A. Theoretical determination of sterically allowed conformations of a polypeptide chain by a computer method. *Biopolymers*, **1965**, *3*, 155-184.

conformations. Reverse turns are classified according to the number of amino-acid residues involved as γ-turns (three amino acids), β-turns (four amino acids), α-turns (five amino acids) or π-turns (six amino acids). The most common secondary structures found in peptides and proteins are:

Helix. Helical structures originated from consecutively repeating these intramolecularly H-bonded conformations are called 2.2_7 or ***γ-helix***, ***3_{10} helix*** and 3.6_{13} or ***α-helix***, respectively, where the values 2.2, 3.0 and 3.6 correspond to their aminoacid residues per helical turn. These turns and helices are all characterized by a right handed screw sense if based on amino acids with the usual L-configuration at the α-carbon.[73,74] The classical α-helix is the most common regular secondary structure of peptides and proteins. The other principal long-range helical structure that occurs in peptides and in proteins is the 3_{10}-helix.[75,76] This ternary helix is more tightly bound and more elongated than the α-helix. The sets of φ, ψ torsion angles of the α and 3_{10} helices do not differ much, falling within the same region of the Ramachandran map (helical region). The 3_{10}-helix is less stable than the α-helix. Indeed, its Van der Waals energy is less favourable and the H-bond geometry is not optimal. Helix are featured by strong NOE.

However, there is no disallowed region of the ϕ, ψ space completely separating these two regularly folded secondary structures. Thus, the α-helix may be gradually transformed in to a 3_{10}-helix (and vice versa) maintaining a nearly helical conformation of the chain throughout.

[73] Crisma, M.; Formaggio, F.; Moretto, A.; Toniolo, C.; Peptide Helices Based on α-Amino Acids. *Biopolymers*. **2006**; *84*, 3-12.
[74] Toniolo, C. *Crit. Rev. Biochem.* **1980**; 9, 1-4.
[75] Toniolo, C.; Benedetti, E.; The Polipeptide 3_{10} Helix. *Trends. Biochem Sci.***1991;** *16*, 350-353.
[76] Karle, I. L.; Balaram, P.; Structural characteristics of .alpha.-helical peptide molecules containing Aib residues *Biochemistry*. **1990**; *29*, 6747-6756.

NH_i-NH_{i+1}, NH_i-NH_{i+2}, $H_{\beta i}$-NH_{i+1}, $H_{\alpha i}$-NH_{i+3}, $H_{\alpha i}$-NH_{i+4}, $H_{\alpha i}$-$NH_{\beta i+3}$ and weak NOE $H_{\alpha i}$-NH_{i+1} (Table 5).

Distance	*α*-helix	3_{10}-helix	*β*	β_p	Turn I[a]	Turn II[a]
$\mathbf{d_{\alpha N}}$	3.5	3.4	2.2	2.2	3.4 *3.2*	2.2 *3.2*
$\mathbf{d_{\alpha N\ (i,\ i+2)}}$	4.4	3.8			3.6	3.3
$\mathbf{d_{\alpha N\ (i,\ i+3)}}$	3.4	3.3			3.1-4.2	3.8-4.7
$\mathbf{d_{\alpha N\ (i,\ i+4)}}$	4.2					
$\mathbf{d_{NN}}$	2.8	2.6	4.3	4.2	2.6 2.4	4.5 2.4
$\mathbf{d_{NN\ (i,\ i+2)}}$	4.2	4.1			3.8	4.3
$\mathbf{d_{\beta N}}$	2.5-4.1	2.9-4.4	3.2-4.5	3.7-4.7	2.9-4.4 3.6-4.6	3.6-4.6 3.6-4.6
$\mathbf{d_{\alpha\beta}}$	2.5-4.4	3.1-5.1				

[a] *For the turns, the first of two numbers applies to the distance between residues 2 and 3, the second to that between residues 3 and 4.*

Table 5. Short (≤ 4.5 Å) sequential and Medium-range ^1H-^1H distances in Polypeptide secondary structures.

β-bend ribbon spiral. In a sequential peptide the alternation of a Pro residue, which disrupts the conventional H-bonding schemes observed in helices (lacking the usual N-H donor group) may give rise to a novel helical structure, called the *β*-bend ribbon spiral.[77] This structure may be considered a variant of the 3_{10}-helix, havin approximately the same helical fold of the peptide chain and being stabilized by intramolecular H-bonds of the *β*-turn type.[78]

γ-Turn. The 1←3 intramolecularly H-bonded peptide conformations (also called C_7 or *γ*-turns) are ring structures that are centred at a single residue and stabilized by an H-bond between the H_{i+2} and O_i atoms.[79,80] A *γ*-turn, which is a more rare reverse turn, is

[77] Karle, I. L.; Filippen-Anderson, J.; Sukumar, M.; Balaram, P.; Conformation of a 16-residue zervamicin IIA analog peptide containing three different structural features: 3(10)-helix, alpha-helix, and beta-bend ribbon. *PNAS.* **1987**; *84*, 5087-5091.

[78] Di Blasio, B.; Pavone, V.; Saviano, M.; Lombardi, A.; Nastri, F.; Pedone, C.; Benedetti, E.; Crisma, M.; Anzolin, M.; Toniolo, C.; Structural characterization of the .beta.-bend ribbon spiral: crystallographic analysis of two long (L-Pro-Aib)n sequential peptides. *J. AM. Chem. Soc.* **1992***; 114*, 6273-6278.

[79] Nemethy, G; Printz, M. P.; The *γ* Turn, a Possible Folded Conformation of the Polypeptide Chain. Comparison with the β Turn. *Macromolecules.* **1972**; *5*, 755-758.

defined by a three-residue turn forming a seven-membered hydrogen bonded-ring between the carbonyl of the I residue and the amide NH of the i+2 residue (Table 5). It exists in two different conformers (equatorial and axial), which are represented on the Ramachandran map by two centrosymmetric points, the coordinates of which are φ ≅ -70°, ψ ≅ 70° (for the more stable, equatorial form, called "inverse *γ*-turn") and φ ≅ 70°, ψ ≅ - 70°(for the less stable, axial form, called "*γ*-turn"). The "inverse *γ*-turn" is quite common in cyclic tetra- and pentapeptides, whereas it has been only very rarely observed in linear peptides. A series of consecutive *γ*-turn generates a *γ*- (or 2.2_7-) helix. This very tightly bound helix has never been experimentally authenticated in any peptide.

β-Turn. *β*-turns are the most common type of non repetitive structure recognized in proteins and they play an important role part in proteins. They provide a direction change for the polypeptide chain and have been implicated in molecular recognition and protein folding.[81] Among 3899 turns that have been identified and classified, only *β*-turns classes I, II, and VII occurred sufficiently frequently to merit an analysis of sequence preferences.[82] Generally hydrophilic residues are more likely to occur in turns than hydrophobic residues, as turns tend to be on the solvent exposed surface of proteins. The most common naturally occurring *β*-turn is usually defined as any tetrapeptide sequence, occurring in a non-helical region, in which the distance between $C_{\alpha i}$ and $C_{\alpha i+3}$ is less than 7 Å. A *β*-turn is often stabilized by a hydrogen bond between the carbonyl function of residue i and the NH-group of residue i+3 to give a 10-membered ring. They are featured by strong NOE $H_{\alpha i}$-NH_{i+1} and the absence of any other *short range* effect. This type of secondary structure could be identified by *long range* signal such as $H_{\alpha i}$-$H_{\alpha Nj}$. In particular H_α-NH NOE signal between i+1 ed i+3 of turn residues is a diagnostic signal for identifying *β*-turn structure (Table 5).

β-Turn II. Proline and tyrosine residues are favoured at i positions, but there is no obvious explanation for this. Proline is also favoured at position i+1 because the φ angle at position (-60°) corresponds to the preferred value for proline. Lysine is also common in this position. This residue do not appear to be involved in any local interactions; rather they form hydrogen bonds with residues elsewhere in the structures or with solvent molecules. Position i+2 is dominated by glycine and to a lesser extent

[80] Matthews, B. W.; The *γ* Turn. Evidence for a New Folded Conformation in Proteins. *Macromolecules*. **1972**; *5*, 818-819.
[81] Venkatachalam, C. M.; Stereochemical criteria for polypeptides and proteins. V. Conformation of a system of three linked peptide units. *Biopolymers*. **1968**; *6*; 1425-1436.
[82] Wilmont, C. M.; Thornton, J. M.; Analysis and prediction of the different types of *β*-turn in proteins. *J. Mol. Biol*. **1988**, *203*, 221-232.

asparagine. At the i+3 position, cysteine, serine and lysine are favoured. Turns involving serine can be stabilized by hydrogen bonding of the serine side chains to the main chain of the first residue in the turn. The lysine side chain is only involved in local hydrogen bonding in about 25% of cases, and most of these involve hydrogen bonds to residue i-1 (the residue before the first residue in the turn).[83] ***β-Turn II'***. It is a secondary structure also involved in *β*-hairpins. Tyrosine shows a significant preference to be in the first position, and valine is more weakly preferred. At position i+1 glycine is favoured. Aspartic acid, asparagines, and serine are all favoured in position i+2. Threonine and glycine are only preferred residues at position i+3 (Figure 16.). The energy barriers between different conformations are low enough to permit rapid conformational exchange. For example, the energy barrier between *α*-helix and *β*-sheet areas is estimated to be approximately 8 Kj mol^{-1} corresponding to virtually unrestricted interconversion. The Random coil is, by common usage, the conformation adopted by "unstructured peptides". It means that the peptide has a range of conformational states available to it that are of similar free energy, and little or no barrier to interconversion between them. The introduction of conformational constraints should influence the backbone conformation, without compromising any crucial side chain interaction with the receptor. A loss in activity after the introduction of a conformational constraint may either be caused by steric hindrance between the ligand and the receptor, due to the added constraint atoms, or by inability of the ligand to adopt the proper conformation.

The question now arises of how reliable secondary structure identification by qualitative delineation of these short distances would be, since it is well know that globular proteins usually contain somewhat distorted secondary structure elements.

[83] Hutchinsons, E. G.; Thornton, J. M.; A revised set of potentials for *β*-turn formation in proteins. *Protein Science*. **1994**, *3*, 2207-2216.

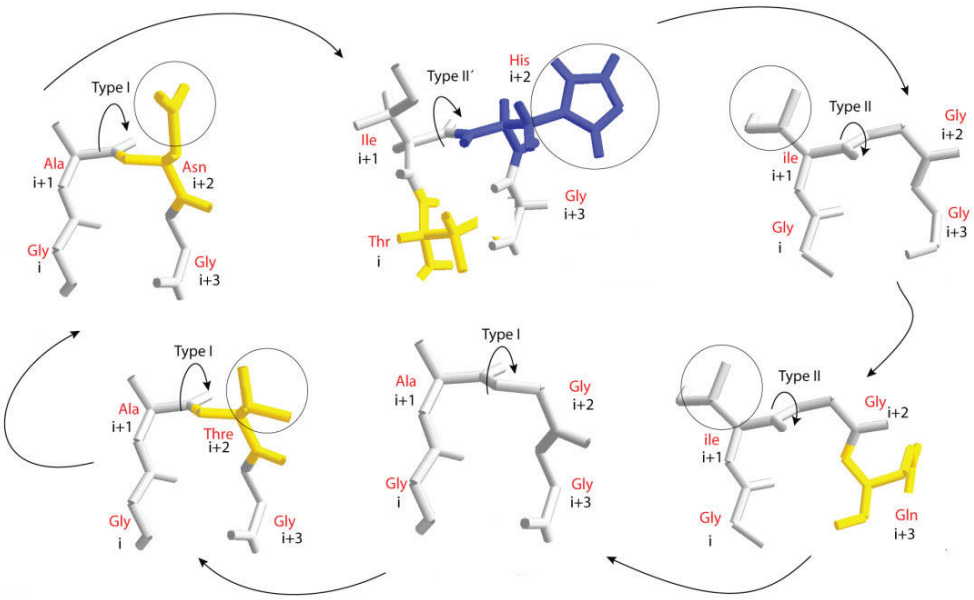

Figure 16. Types of β-turns. β-turns differ from each other based on the orientation the φ and ψ torsional angles of the peptide bond between residues in "i+1" and "i+2" (indicated with curved arrows). Additional differences based on the properties of the residues in the position "i+1" are also observed (in circles). Chains were colored according to the physiochemical properties of amino acids. Hydrophobic residues are colored grey, acidic residues and relatives are yellow, and basic residues are in blue.

In the α helix and the 3_{10} helix one has the H-bonds CO_i-NH_{i+4} and CO_i-NH_{i+3} respectively and in β sheets one observes a dense network of hydrogen bonds between neighbouring peptide strands. In the regular secondary structures all amide protons are involved in hydrogen bonds, with the following exceptions: the first four residues in an α helix; the first three residues in a 3_{10} helix; every second residue in the peripheral strands of β sheets.

The two main methods developed for calculation of protein structures are:

Distance Geometry:

DISGEO: (DIStance GEOmetry) a program that works initially purely in distance space, calculating a consistent matrix of distance bounds between all atoms, started from the limited set of distances (NOEs and covalent distances) input to it. It then embeds a subset of these distances into Cartesian space and refines the resultant structure to the distance matrix.

DYANA: (Dynamic Algorithm for NMR Applications) it works in angle space. Starting from an initial structure, e. g. an extended chain, it folds the peptide so that it satisfies the torsion angles. It uses only he information that comes from NMR, plus

torsion angles. (DIANA: is the previous program, based on the same conceptual features).

CYANA: is the evolution of DYANA program.

Restrained Molecular Dynamics (RMD): in which the standard forces are supplemented by others representing NOE constraints, angle restraints, etc. Thus for avoiding the local minima, in which the peptide chain is tangled up incorrectly. RMD insert not only the information coming from NMR but also a host of other information, much of it empirical.

2.3 In *Silico* approach

Computational techniques provide transformation of peptide ligands into small molecule ligands. Three starting situations are conceivable:

- detailed information on the active complex comprising the protein target and its peptidic ligand are available;
- the structure of the target protein and the sequence of one or more active peptidic ligands are known;
- ligand sequence and detailed structure-activity data for these ligands are known.

The SAR of constrained analogues together with the information obtained from biophysical studies (X-ray, NMR) and computational methods can be used, in an iterative process, to provide information about the receptor-bound and/or biologically active conformation. Since SRIF was object of investigation by researcher, nobody found detailed information on the active complex sst-ligand.

Energetically favoured peptide conformations can also be calculated using different computational methods and both, NMR and computational methods, have been used to estimate binding conformations of peptides. The solution structure or a calculated low-energy structure does not necessarily reflect the bound conformation of the active peptide and may be a misleading starting point for pharmacophore generation. Moreover, the binding conformation of active ligands is often not a low-energy conformation. This factor is one of the reasons why computational assessment of binding conformations, using straightforward techniques of simulated annealing or molecular dynamics, is critical. When sampling the conformational space, the most important parameter for the simulation is the energy of the conformations and, normally, low energy conformations are selected. Moreover, due to the huge conformational space of peptides, a complete conformational sampling of this space for an oligo-peptide is often not feasible. The primary goal is to identify only consensus conformations that represent a common spatial arrangement of shared binding features.

Technically, this goal is achieved by a dynamics simulation of a collection of molecules, which are tethered together at their corresponding binding features, while ignoring non-bonded interactions between the molecules. This procedure only generates conformations from the entire conformational space where the constrained binding

features, within all peptides of an *ensemble*, occupy a similar location in space. As a result, the conformational space of each peptide is considerably reduced by limiting it to the part, which overlaps with the corresponding conformational space of all peptides in the *ensemble*. The resulting structures do not represent low energy structures for a single peptide but for the entire *ensemble*, since the behaviour of one peptide constraints that of each other. The appropriate choice of tethering features requires a rigorous structure-activity analysis.[84]

2.3.1 On the question of GPCR

The G protein coupled receptors GPCRs are a large and widely distributed super-family of membrane-bound protein that are involved in signal transduction in many physiological and pathological processes. GPCRs are one of the most relevant targets for small molecules, representing the site of action of ca. 40% of the marketed drugs (Figure 17.).

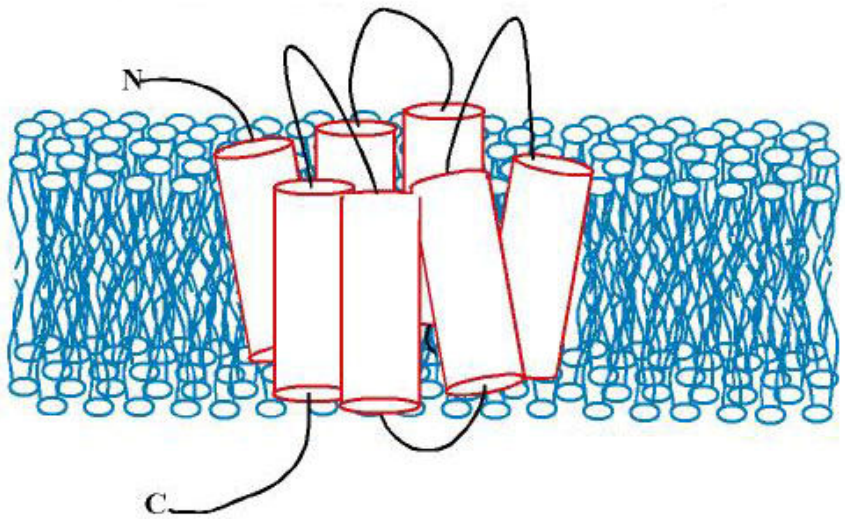

Figure 17. Trans-membrane domains of GPCR.

Even considering their relevance and popularity as targets for drug discovery, GPCRs can still be challenging targets. Because they are integral membrane proteins, little structural information are available. Because of the difficulty in crystallizing GPCRs, attempts to elucidate the structural and functional domains of these molecules have resorted to indirect methods such as site-directed mutagenesis and receptor chimeras. Based on such studies, the ligand binding site of GPCRs has been postulated

[84] Hummel G.; Reineke U.; Reimer U. Exploiting drug diversity for drug discovery. 184, RSC Publishing.

to consist of a number of non-contiguous amino acid residues which form a binding pocket within the folded receptor structure.[85,86]

By exploiting the differential ability of SRIF to bind to sst_2 but not sst_1, Kaupmann et al., systematically mutated sst_1 to resemble sst_2 [87], they found two crucial residues, Gln^{291} and Ser^{305}, in TMs VI and VII respectively of sst1, substitution of which to the corresponding residues Asn^{276} and Phe^{294} in sst_2 increased the affinity of sst_1 for SRIF and other octapeptide analogues 1000 fold. By molecular modelling using these identified residues, as well as the known structure of SRIF, Kaupman et al. have postulated a binding cavity for SMS involving hydrophobic and charged residues located exclusively within TMs III-VII. Their findings predict that the core residues Phe^7, D-Trp^8, Lys^9, Thr^{10} of SRIF interact with Asn^{276} and Phe^{294} located at the outer end of TMs VI and VII respectively (present in sst_2 but not in sst_1) which provide a hydrophobic environment for lipophilic interactions with Phe^7, D-Trp^8, Thr^{10} and Asp^{137} in TM III which anchors the ligand by an electrostatic interaction with Lys^9. SRIF binds poorly to sst_1 because of the presence of residues Gln^{291} and Ser^{305} located close to the extracellular rims of TM helices VI and VII which prevent the short peptide from reaching deep within the pocket, whereas the corresponding residues Asn^{276} and Phe^{294} in sst_2 provide for a stable interaction with the disulphide bridge of SRIF. Because of their greater length and flexibility, the natural ligands SRIF-14 and SRIF-28 can presumably adopt a conformation that allows their entry into the binding pocket of all five ssts. Such a model is consistent with mutational studies of the Asp residue in TM III which abolishes ligand binding although it is not known whether this is due to a direct interaction of the residue with sst ligands or to a secondary alteration in receptor structure.[88, 89] Due to the absence of homology modelling receptor and other featuring knowledge on sst receptors, the only available strategy in SRIF peptide design was the ligand based design.

[85] Baldwin J. M. Structure and function of receptors coupled to G proteins. *Curr. Opin. Cell Biol.* **1994**, *6*, 180.
[86] Strader C. D.; Fong T. M.; Graziano M. P.; Tota M. R. The family of G protein coupled receptors. *FASEB J* **1995**, *9*, 745.
[87] Kaupman K.; Bruns C.; Raulf F.; weber H. P.; Mattes H.; Lubbert H.; Two aminoacids, located in trnsmembrane domains VI and VII, determine the selectivity of the petide agonist SMS201-995 for the SSTR2 somatostatin receptor. *EMBO J.* **1995**, *14*, 727.
[88] Nehring R. B.; Meyerhof W.; Richter D.; Aspartic acid residue 124 in the third transmembrane domain of the somatostatin receptor subtype 3 is essential for somatostatin 14 binding. *DNA and Cell Biol.* **1995**, *14*, 939.
[89] Strnad J.; Hadcock J. R. Identification of a critical aspartate residue in transmembrane domain three necessary for the binding of somatostatin to the somatostatin receptor SSTR2. *Biochem. Biophys. Res. Commun*. **1995**, *216*, 913.

2.3.2 The pharmacophore model

One of the ligand-based design approach is to take the functional groups of the peptide that interact with the target. The ligand structure can be translated into a pharmacophore model, which is a 3D representation of the ligand's functionalities or features important for the target-ligand interaction. Topographic information from the 3-D pharmacophore model is used to position the amino acid side chains in the correct spatial arrangement on selected non-peptidic scaffolds or templates, such as small (five-to-seven-membered) ring systems of defined stereochemistry. A pharmacophore is defined as the ensemble of steric and electronic features that ensure the optimal interactions with a specific biological target to modulate its biological response. A pharmacophore is not an actual molecule or collection of specific functional groups; rather, it is an abstract representation that summarizes what is known about the way a group of molecules interacts with the target. This pharmacophore can be used for the virtual screening or huge libraries of small molecules. Typical pharmacophore functionality include: hydrophobes, ring centres, hydrogen-bond donors and acceptors and positive and negative ionisable functional groups. Mapping these features in to the ligand structure results in a pharmacophore model that can be readily used for the design of new molecules.

AIM OF THE PROJECT

"... Non vogliate negar l'esperienza
di retro al sol, del mondo sanza gente.
Considerate la vostra semenza
fatti non foste a viver come bruti
ma per seguir virtute e conoscenza."

Dante Alighieri,
(1265-1321)
(Divina Commedia, Inferno
canto XXVI, 116-120

In the last thirty years, as described in the introduction many effort have been done to synthesize somatostatin analogues useful in the treatment and diagnosis of tumour. Nevertheless only few analogues of octreotide were accepted for clinical use in a small number of tumour types and for this reason somatostatin analogues not fully fulfil the old promises. The progress in SRIF biology and medical chemistry, induced by the discovery and intensive studies on sst, rekindled the interest on somatostatin analogues. Some authors move on broad spectrum analogues other to selective one to use in specific sst expressing tumour.

In this PhD thesis we tried to achieve both target trough the synthesis of conformationally restricted peptides. In mostly of the cases SRIF analogs maintained the disulphide bridge prone to be cleaved by endogenous reducing enzymes, like glutathione reductase and thioredoxin reductase, or by nucleophilic and basic agents, resulting in a diminished bio-stability of the molecule, moreover same types of labelling procedures were unable with the disulphide bridge. The substitution of the S-S bridge with a unsaturated carbon –carbon bond can be a way to obtain more stable analogues. Using the approach of Ring Closing Metathesis (RCM) on two Hag, replacing Cys in octreotide sequence, we obtained the first so called dicarba-analogue of octreotide.[90]

In order to obtain more stable and flexible analogues, we synthesized also the saturated dicarba-analogues of the compounds obtained from RCM procedure.

We also focus on the design of new molecules. The classical approach of synthesize lot of molecule was substitute by a rational approach supported by the *in silico* and the NMR studies. By the modelling approach we predicted virtual bioactive structure whereas NMR analysis supported us in understanding SAR. Finally accordingly to recent studies we modified the sequence of the dicarba–analogues and we enlarged the cycle size. Recent studies concerning the structure-activity relationships of SRIF's ligands, which paid attention to the role of the ring size, discovered that eight-mer cycles containing the disulfide bridge may have antagonist activity, that is more suitable for their use as radiolabeled drugs. This find prompted us to attempt to obtain the corresponding dicarba-analogues. [91]

[90] Carotenuto, A.; D'Addona, D.; Rivalta, E.; Chelli, M.; Papini, A. M.; Rovero, P.; Ginanneschi, M. Synthesis of a Dicarba-Analog of Octreotide Keeping the II' β-Turn of Pharmacophore in Water Solution. *Letters in Organic Chemistry*, **2005**, *2*, 274-279.

[91] Debora D'Addona, Carotenuto A., Novellino E., Piccand V., Reubi J.C., Alessandra Di Cianni, Francesca Gori, Anna Maria Papini and Mauro Ginanneschi. 'Novel sst5-selective Somatostatin Dicarba-analogues. Synthesis and Conformational-affinity Relationship' *Journal Medicinal Chemistry*, **2008**, *51*, 512-520.

In this PhD thesis we reported the procedure used for the realization of a data-base for the *in silico* predictions; the synthesis of twenty-six new dicarba-analogues of octreotide, optimizing this step in oil bath and then on a microwave instrument; 3D structures of nine peptides determined by ^{1}H NMR spectroscopy and a new pharmacophore model for sst_5 was proposed. [92]

The stability of the first dicarba-analogue in human *sera* was demonstrated. Now a day just thirteen analogues were subjected to binding essay towards all sst receptors and the most actives were conjugated with two different chelating agent and labelled with radio-nuclides. Bio-distribution essay on mice, using the radio-labelled peptides, internalisation and cellular retention, concerns on cell lines expressing ssts, were performed. Here below four tables describe the final target compounds synthesized in this PhD thesis (Table 3A. 3B. 3C. 3D). In order to facilitate the reader we report here the explanation of the abbreviation contained in the table below: dhDsa-C, dehydrodiaminosuberic acid C-terminus; dhDsa-N, dehydrodiaminosuberic acid N-terminus; Dsa-N, diaminosuberic acid N-terminus; Dsa-C, diaminosuberic acid C-terminus

3A. D-Phe^{2}-*c*[Xaa^{3}-Yaa^{7}-D-Trp^{8}-Lys^{9}-Zaa^{10}-Kaa^{14}]-Thr(ol)^{15}-OH

Peptides	Xaa	Yaa	Zaa	Kaa
27	dh-Dsa-N	L-Phe	L-Phe	dh-Dsa-C
28	dh-Dsa-N	L-Phe	L-Thr	dh-Dsa-C
45	Dsa-N	L-Phe	L-Thr	Dsa-C
29	dh-Dsa-N	L-Phe	L-Tyr(Bzl)	dh-Dsa-C
48	Dsa-N	L-Phe	L-Tyr(Bzl)	Dsa-C
30	dh-Dsa-N	L-1-Nal	L-Thr	dh-Dsa-C
46	Dsa-N	L-1-Nal	L-Thr	Dsa-C
31	dh-Dsa-N	L-1-Nal	L-Tyr(Bzl)	dh-Dsa-C
32	dh-Dsa-N	L-Phe	L-Tyr	dh-Dsa-C
33	dh-Dsa-N	L-Tyr	L-1-Nal	dh-Dsa-C
34	dh-Dsa-N	L-Phe	L-Tyr(Me)	dh-Dsa-C

[92] Saveanu, A.; Gunz, G.; Dufour, H.; Caron, P.; Fina, F.; Ouafik, L.; Culler, M. D.; Moreau, J. P.; Enjalbert A.; Jaquet P. BIM-23244, a Somatostatin Receptor Subtype 2 and 5 Selective Along with Enhanced Efficiency in Suppressing Growth Hormone (GH) from Octreotide-Resistant Human GH-Secreting Adenomas. *The Journal of Clinical Endocrinology & Metabolis.* **2001**, *86*, 140-145.

3B. NH_2-L-Gly-[Xaa^3-Kaa^6-Yaa^7-Jaa^8-Lys^9-Thr^{10}- Zaa^{11}- dhDsa-C^{14}]-COOH

Peptides	Xaa	Kaa	Yaa	Jaa	Zaa
36	L-dh-Dsa-N	D-Phe	L-Phe	D-2-Nal	D-Phe

3C. NH_2-[Xaa^3-Kaa^6-Yaa^7-Jaa^8-Lys^9-Phe^{10}- Zaa^{11}- dhDsa-C^{14}]-$CONH_2$

Peptides	Xaa	Kaa	Yaa	Jaa	Zaa
37	dh-Dsa-N	D-Phe	L-Phe	D-Trp	D-Phe
47	Dsa-N	D-Phe	L-Phe	D-Trp	D-Phe

3D. NH_2-[Xaa^3-Kaa^6-Yaa^7-Jaa^8-Lys^9-Thr^{10}-Zaa^{11}-dhDsa-C^{14}]-$CONH_2$

Peptides	Xaa	Kaa	Yaa	Jaa	Zaa
38	L-dh-Dsa-N	D-Phe	L-Phe	D-Trp	D-Phe
39	L-dh-Dsa-N	L-Phe	L-Phe	D-Trp	L-Phe
40	D-dh-Dsa-N	L-Phe	L-Phe	D-Trp	L-Phe
41	L-dh-Dsa-N	L-Phe	L-Phe	D-2-Nal	L-Phe
42	D-dh-Dsa-N	L-Phe	L-Phe	D-2-Nal	L-Phe
43	D-dh-Dsa-N	L-Phe	L-Tyr	D-2-Nal	L-Phe

3D. (CA)-Peptide

Compounds	Chelating Agents	Unsaturated-Peptide
49	DOTA	29
50	DOTA	30
51	DOTA	31
52	DOTA	32
53	PN_2S	28
54	PN_2S	30

Table 6. Target compounds synthesized in this work.

Formulas of all compounds were given in supplementary information (figures S27-54).

RESULTS AND DISCUSSION

" When a multistep process,
such as the preparation
of a long polypeptide or protein
is contemplated, the saving in time
and effort and materials could be very large.
The fact that all of the steps
just described are heterogeneous reactions
between a soluble reagent in the liquid phase
and the growing peptide chain in the
insoluble solid phase
led to the introduction of the name
"solid phase peptide synthesis".

Robert Bruce Merrifield

(1921 – 2006)

Nobel Prize in Chemistry, December 8th 1984

Drug discovery in the pharmaceutical industry have changed dramatically in the last two decades. By the late 1980s, a strong belief had emerged that drug development is purely a number game, with anticipated drop-out rates at each stage of the process such that only one compound out of 10,000 synthesised would survive to make it to the market. Stimulated by the automation of peptide synthesis on solid support, the concepts now embodied in combinatorial chemistry have completely changed the way in which compound collections are assembled and SARs are explored. Reactions are accelerated by microwaves and other non-traditional techniques; reaction workups are streamlined with solid-phase reagents and parallel or mix-and-split formats enable chemists to make hundreds of analogues in the time they used to synthesize one or two.[93] Early attempts at high-throughput chemistry utilised this strategy, exploiting the advantages of solid-chemistry, which facilitates reaction work-up and rapid sample processing. These changes have not only altered the operational aspects of organic synthesis, but also given rise to entirely new strategies in synthetic planning.[94]

[93] R. B. Merrifield; J. M. Stewart. Automated peptide Synthesis. *Nature* **1965**, *207*, 522-523.
[94] M. R. Spaller; M. T. Burger; M. Fardis; P. A. Bartlett. Synthetic strategies in combinatorial chemistry. *Curr. Opin. Chem. Biol.* **1997**, *1*, 47-53.

4.1 Chemical Synthesis

Chemical steps to obtain the target compounds:

- Choice of the solid support.
- SPPS of linear peptide.
- On resin RCM.
- Optimization of oil-bath RCM.
- Microwave assisted RCM.
- Hydrogenation of the unsaturated analogues.
- Conjugation with chelating agents: DOTA and PN_2S.

4.1.1 Linear peptides synthesis

The synthesis of the linear peptides was performed at first in a manual than in a semiautomatic instrument by solid phase peptide synthesis (SPPS). Three resins were used for the synthesis of peptides:

- H–L-Thr(*t*-Bu)–ol–2-chlorotrityl resin
- Wang [p-Benzyloxibenzylalchool resin (HMP resin)]
- Rink amide AM [4-(2',4'-Dimethoxyphenyl-Fmoc-aminomethyl-phenoxy-acetamido-norleucylaminomethyl resin]

In this technique the compounds are bounded to an insoluble support, at the end of any synthetic step, each unreacted reagent can be removed by a simple washing procedure. In this PhD thesis we used the Fmoc/*t*-Bu strategy which has as orthogonally protecting group the Fmoc, removable with basic solution, for the amino group; *t*-Bu or Boc groups and Trt group, for amino acids side chains, removable with acid treatment. The steps of SPPS are well described in the figure (Scheme 3) and can be summarized as follow:

- Anchoring of the first amino acid (or linker or building block) to an insoluble support via the *C*-terminal carboxyl group.
- Colorimetric test revealing the non reacted free amino groups on the resin: Kaiser test.[95]
- Removal of Fmoc protecting the amino group: basic condition 20% piperidine in DMF.
- Washing of the resin.
- Activation of carboxylic group of the next N-protected amino acid.
- Elongation of peptide sequence.
- Cleavage of the peptide from the resin and removal of the amino acid side chains with acid condition by threefluoro-acetic acid and scavengers.

[95] Kaiser, E.; Colescott, R. L.; Bossinger, C. D.; Cook, P. I. Color test for detection of free terminal amino groups in the solid-phase synthesis of peptides. *Anal. Biochem*. **1970**, *34*, 595-598.

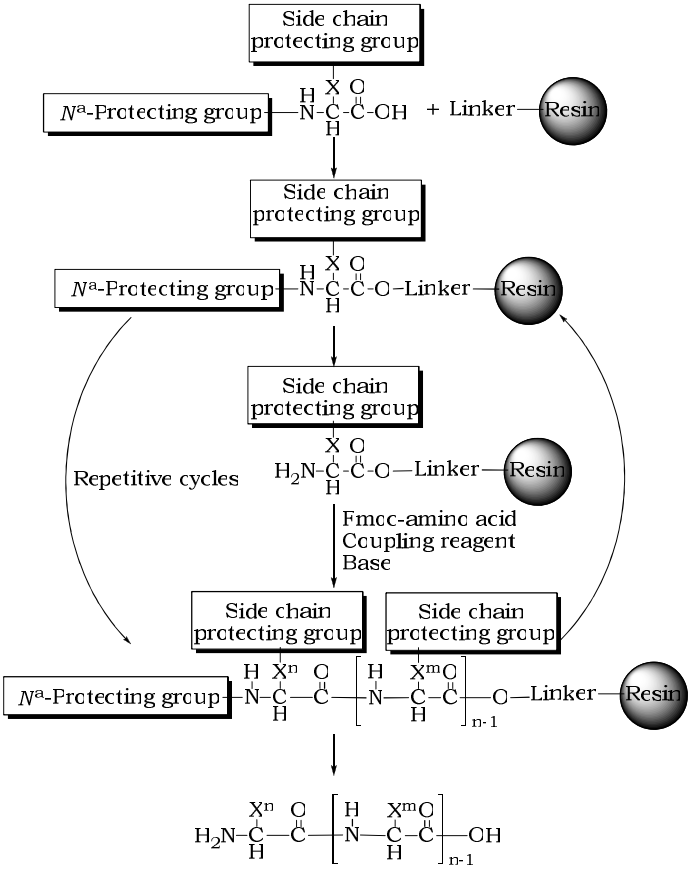

Scheme 3. Chemical steps of the SPPS.

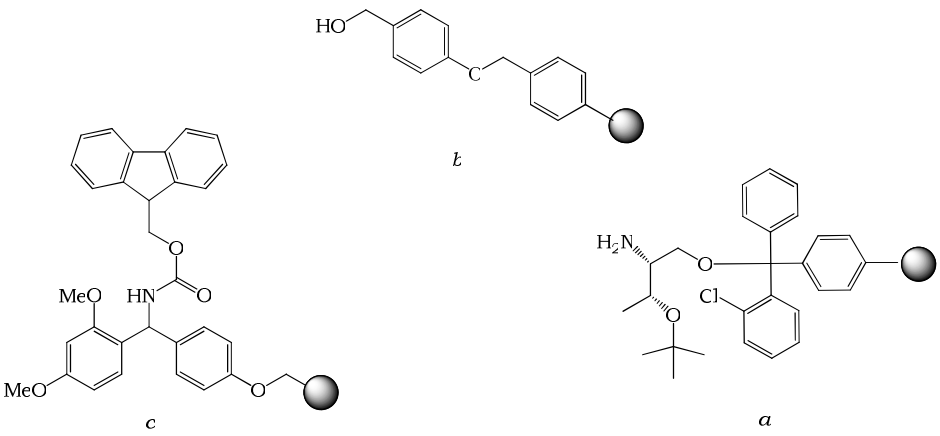

Figure 18. a: H–L-Thr(t-Bu)–ol–2-chlorotrityl resin; b: Wang Resin; c: Rink amide resin.

Depending on C-terminus function we needed to obtain, we employed respectively: H–L-Thr(*t*-Bu)–ol–2-chlorotrityl resin when a Thr(ol) was required at C-terminus; Wang resin when C- terminus bear a carboxy moiety; Rink amide AM resin for the amino group in C-terminus (Figure 18, a, b, c).

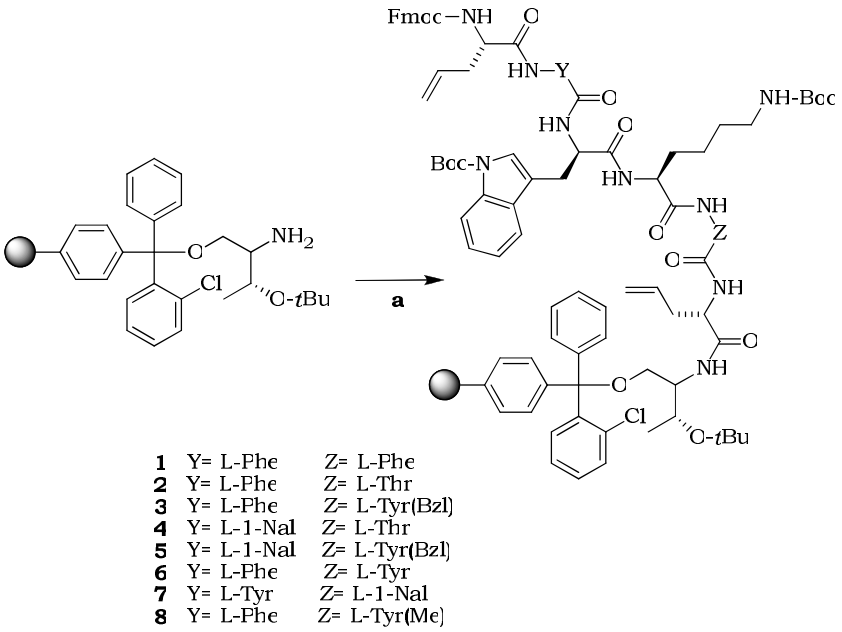

*Scheme 4. Synthesis of linear **1-8** peptides on H–l-Thr(t-Bu)–ol–2-chlorotrityl resin.*
a. (i) Fmoc- L-Hag, HATU/NMM, 40 min r.t.; (ii) 20% piperidine in DMF (2 x 10 min); (iii) Coupling with the amino acid.

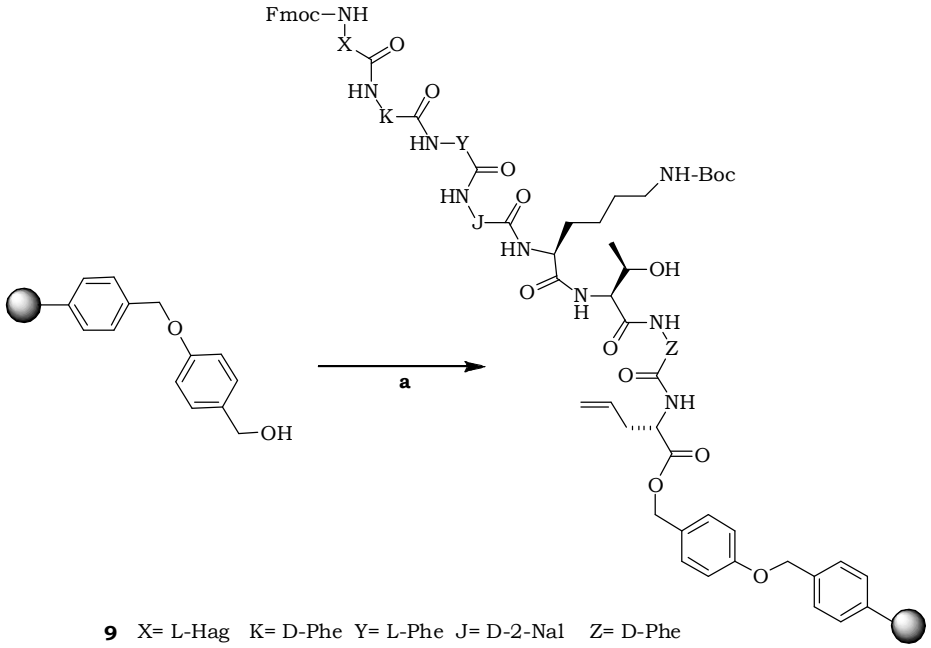

*Scheme 5. Synthesis of **9** on Wang resin.*
a.(i) Fmoc- L-Hag, HATU/NMM, 40 min r.t.; (ii) 20% piperidine in DMF (2 x 10 min); (iii) Coupling with the amino acid.

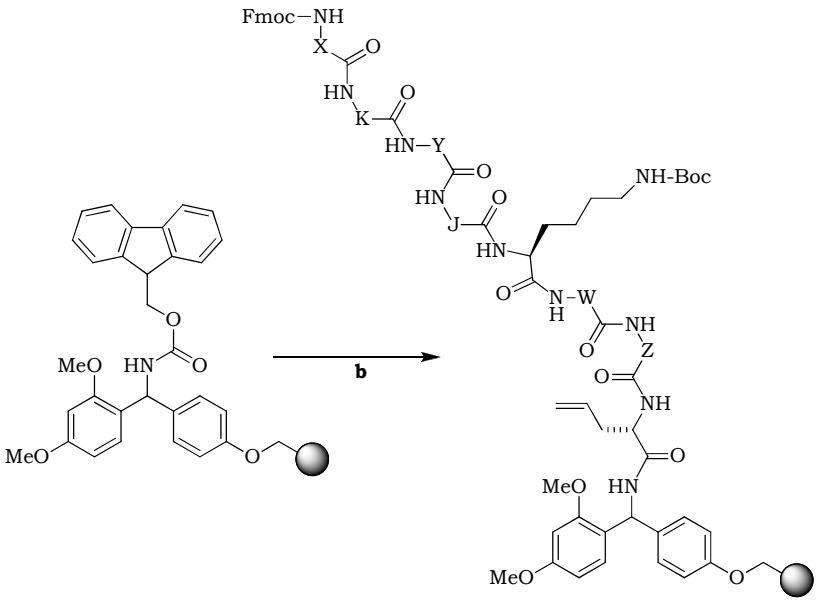

10	X= L-Hag	K= D-Phe	Y= L-Phe	J= D-Trp	W= L-Phe	Z= D-Phe
11	X= L-Hag	K= D-Phe	Y= L-Phe	J= D-Trp	W= L-Thr	Z= D-Phe
12	X= L-Hag	K= L-Phe	Y= L-Phe	J= D-Trp	W= L-Thr	Z= L-Phe
13	X= D-Hag	K= L-Phe	Y= L-Phe	J= D-Trp	W= L-Thr	Z= L-Phe
14	X= L-Hag	K= L-Phe	Y= L-Phe	J= D-2-Nal	W= L-Thr	Z= L-Phe
15	X= D-Hag	K= L-Phe	Y= L-Phe	J= D-2-Nal	W= L-Thr	Z= L-Phe
16	X= D-Hag	K= L-Phe	Y= L-Tyr	J= D-2-Nal	W= L-Thr	Z= L-Phe

*Scheme 6. Synthesis of linear **10-16** peptides on Rink amide resin.*
b. (i) 20% piperidine in DMF (2 x 10 min ; (ii) Coupling with the amino acid.

H–L-Thr(*t*-Bu)–ol–2-chlorotrityl resin (Scheme 4) already contains the first amino acid of the sequence. After the first coupling (Fmoc-Hag) the loading of the resin was measured through a spectrophotometric test. Piperidine was added to 3 mg resin, Fmoc group, as dibenzofulven, form a compound with piperidine (procedure was repeated three times). This compound absorbed at 301 nm. Through a mathematical formula (mmol/g = (A301/7800)x(10 mL/g resin) it is possible to determine the loading of the resin. This measurement demonstrated that the loading was 0.5 mmol/g for all the three resins, low enough to create the pseudo-dilution condition for the subsequent cyclization step. As described in the following paragraph, at the beginning of this work we synthesized the octa-peptides (N-terminus D-Phe was added before the cyclization) on H–L-Thr(*t*-Bu)–ol–2-chlorotrityl-resin, then we switch to the synthesis of hepta-peptide described in Scheme 4 due to the advantage in the yield of cyclization step. At the end of the linear peptide sequence a micro-scale cleavage was performed. All peptides were cleaved from the resin with 94% TFA, 2% dichloromethane (DCM), 2% Etanditiolo(EDT), 2% Phenol, but peptide **3** and **5**, which needed a low TFA percentage in order to retain the protecting Bzl group on Tyr^{10}. Those peptides were cleaved with

70%TFA, 26% DCM, 2% EDT and 2% Phenol.[91] The Fmoc protected peptides were analyzed by RP-HPLC, revealing a purity of about 97%.

Fmoc linear peptides synthesized in this work are summarized in the table below (Table 7).

Compound	Linear peptides sequences
1	Fmoc-Hag^{3}-L-Phe^{7}-D-Trp^{8}-Lys^{9}-L-Phe^{10}-Hag^{14}-Thr(ol)^{15}
2	Fmoc-Hag^{3}- L-Phe^{7}-D-Trp^{8}-Lys^{9}-Thr^{10}-Hag^{14}-Thr(ol)^{15}
3	Fmoc-Hag^{3}- L-Phe^{7}-D-Trp^{8}-Lys^{9}-Tyr(Bzl)^{10}-Hag^{14}-Thr(ol)^{15}
4	Fmoc-Hag^{3}-1-Nal^{7}-D-Trp^{8}-Lys^{9}-Thr^{10}-Hag^{14}-Thr(ol)^{15}
5	Fmoc-Hag^{3}-1-Nal^{7}-D-Trp^{8}-Lys^{9}-Tyr(Bzl)^{10}-Hag^{14}-Thr(ol)^{15}
6	Fmoc-Hag^{3}-L-Phe^{7}-D-Trp^{8}-Lys^{9}-L-Tyr^{10}-Hag^{14}-Thr(ol)^{15}
7	Fmoc-Hag^{3}-L-Tyr^{7}-D-Trp^{8}-Lys^{9}-L-1-Nal^{10}-Hag^{14}-Thr(ol)^{15}
8	Fmoc-Hag^{3}-L-Phe^{7}-D-Trp^{8}-Lys^{9}-L-Tyr(Me)^{10}-Hag^{14}-Thr(ol)^{15}
9	Fmoc-L-Hag^{3}-D-Phe^{6}-L-Phe^{7}-D-2-Nal^{8}-Lys^{9}-Thr^{10}-D-Phe^{11}-L-HagCOOH^{14}
10	Fmoc-L-Hag^{3}-D-Phe^{6}-Phe^{7}-D-Trp^{8}-Lys^{9}-L-Phe^{10}-D-Phe^{11}-L-Hag-NH$_2$^{14}
11	Fmoc-L-Hag^{3}-D-Phe^{6}-L-Phe^{7}-D-Trp^{8}-Lys^{9}-Thr^{10}-L-Phe^{11}-L-Hag-NH$_2$^{14}
12	Fmoc-L-Hag^{3}-L-Phe^{6}-L-Phe^{7}-D-Trp^{8}-Lys^{9}-Thr^{10}-L-Phe^{11}-L-Hag-NH$_2$^{14}
13	Fmoc-D-Hag^{3}-L-Phe^{6}-L-Phe^{7}-D-Trp^{8}-Lys^{9}-Thr^{10}-L-Phe^{11}-L-Hag-NH$_2$^{14}
14	Fmoc-L-Hag^{3}-L-Phe^{6}-L-Phe^{7}-D-2-Nal^{8}-Lys^{9}-Thr^{10}-L-Phe^{11}-L-Hag-NH$_2$^{14}
15	Fmoc-D-Hag^{3}-L-Phe^{6}-L-Phe^{7}-D-2-Nal^{8}-Lys^{9}-Thr^{10}-L-Phe^{11}-L-Hag-NH$_2$^{14}
16	Fmoc-D-Hag^{3}-L-Phe^{6}-L-Tyr^{7}-D-2-Nal^{8}-Lys^{9}-Thr^{10}-L-Phe^{11}-L-Hag-NH$_2$^{14}

*Table 7. Linear epta-peptides(**1-8**) and octa-peptides (**9-16**) synthesized in this work.*

4.1.2 Synthesis of unsaturated cyclic peptides

The key reaction to achieve the target compounds is an olefin metathesis reaction, among different types we chose RCM.

Olefin metathesis is a fundamental chemical reaction involving the rearrangement of carbon-carbon double bonds, and can be used to couple, cleave, ring-closure, ring-open, or polymerize olefin (Scheme 7).

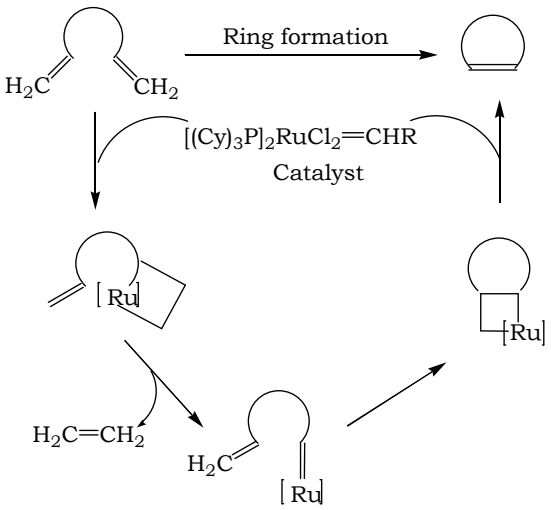

Scheme 7. Olefin metathesis.

The widely accepted view that olefin metathesis revolutionized the different fields of synthetic chemistry led to the awarding of the 2005 Nobel Prize in Chemistry to Yves Chauvin, Robert H. Grubbs and Richard R. Schrock "for the development of metathesis method in organic synthesis".[96,97,98] While Chauvin had proposed the 'carbene' mechanism to explain how the metathesis process function[99] and Schrock had prepared the first well-defined highly active metathesis catalysts,[100] Grubbs provided the synthetic chemistry with active catalysts that could be handled in air and were tolerant of various functional group, such as ester, amides, ketones, aldehydes and even protonic

[96] Chauvin, Y. Angew. Chem. Int. Ed. Olefin Metathesis: The Early Days (Nobel Lecture) **2006**, *45*, 3740.
[97] Schrock, R. R. Multiple Metal-Carbon Bonds for Catalytic Metathesis Reactions. *Angew. Chem. Int. Ed.* (Nobel Lecture). **2006**, *45*, 3748.
[98] Grubbs, H. R. Handbook of Metathesis. Wiely-VCH: Weinheim. **2003**, Vol. 1-3.
[99] Herisson, J. L.; Chauvin, Y. Catalysis of Olefin Transformations by Tungsten Complexes. II. Telomerization of Cyclic Olefins in the Presence of Acyclic Olefins, *Makromol. Chem.* **1971**, *141*, 161-176.
[100] Schrock, R. R.; DePue, R. T.; Feldman, J.; Schaverien, C. J.; Dewan, J. C.; Liu A. H. Preparation and reactivity of several alkylidene complexes of the type W(CHR')(N-2,6-C6H3-iso-Pr2)(OR)2 and related tungstacyclobutane complexes. Controlling metathesis activity through the choice of alkoxide ligand. *J. Am. Chem. Soc.* **1988**, *110*, 1423-1435.

functionalities like alcohol, water and acids.[101] The Grubbs catalysts are based on a ruthenium atom surrounded by five ligands: two neutral electron-donating entities (e.g. trialkylphosphines, N-heterocyclic carbenes), two mono-anionic groups (e.g. halides), and one alkylidene moiety (e.g. unsubstituted and substituted methylidenes). These catalysts are divided into two categories based on the nature of the neutral ligand: $L_2X_2Ru=CHR$ complexes (where L is a phosphine ligandan and X is Cl atom R is a phenyl group) were discovered first and are referred to as first generation Grubbs catalysts, and $(L)(L')X_2Ru=CHR$ complexes (where L is a phosphine ligand and L' is a N-heterocyclic carbene or NHC ligand and X is Cl atom R is a phenyl group) were subsequently developed and are referred to as the second-generation Grubbs catalysts. In the figure below two catalysts used in this work (Figure 19).

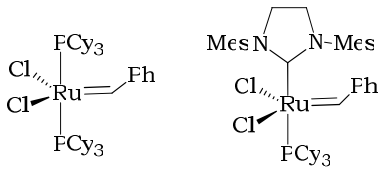

*Figure 19. 1st generation Grubbs catalyst (**17**). 2nd generation Grubbs catalyst (**18**).*

The 1st generation Grubbs catalyst **17** has demonstrated attractive functional group tolerance and handling properties. Nonetheless, the utility of **17** is somewhat limited, many of the limitation of **17** have been addressed through the development of the 2nd generation Grubbs catalysts, among them **18**, which posses excellent metathesis activity while retaining the handling characteristics.[102,103]

The RCM was applied directly on peptides bonded to one of the three resins used in this work (chlorotrityl resin, wang and rink amide AM). (Scheme 8, Scheme 9,

Scheme 10).[104]

[101] Nguyen, S. T.; Grubbs, R. H.; Ziller, J. W. Synthesis and activities of new single-component, ruthenium-based olefin metathesis catalysts. *J. Am. Chem. Soc.* **1993**, *115*, 9858-9859.
[102] Scholl, M.; Ding, S.; Lee, C. W.; Grubbs, R. H. Synthesis and Activity of a New Generation of Ruthenium-Based Olefin Metathesis Catalysts Coordinated with 1,3-Dimesityl-4,5-dihydroimidazol-2-ylidene Ligands. *Org. Lett*. **1999**, *1*, 953-956.
[103] Morgan, J. P.; Grubbs, R. H. In Situ Preparation of a Highly Active N-Heterocyclic Carbene-Coordinated Olefin Metathesis Catalyst. *Org. Lett*. **2000**, *2*, 3153-5155.
[104] Miller, S. J.; Blackwell, H. E.; Grubbs, R. H. Application of Ring-Closing Metathesis to the Synthesis of Rigidified Amino Acids and Peptides. *J. Am. Chem. Soc.* **1996**, *118*, 9606-9614.

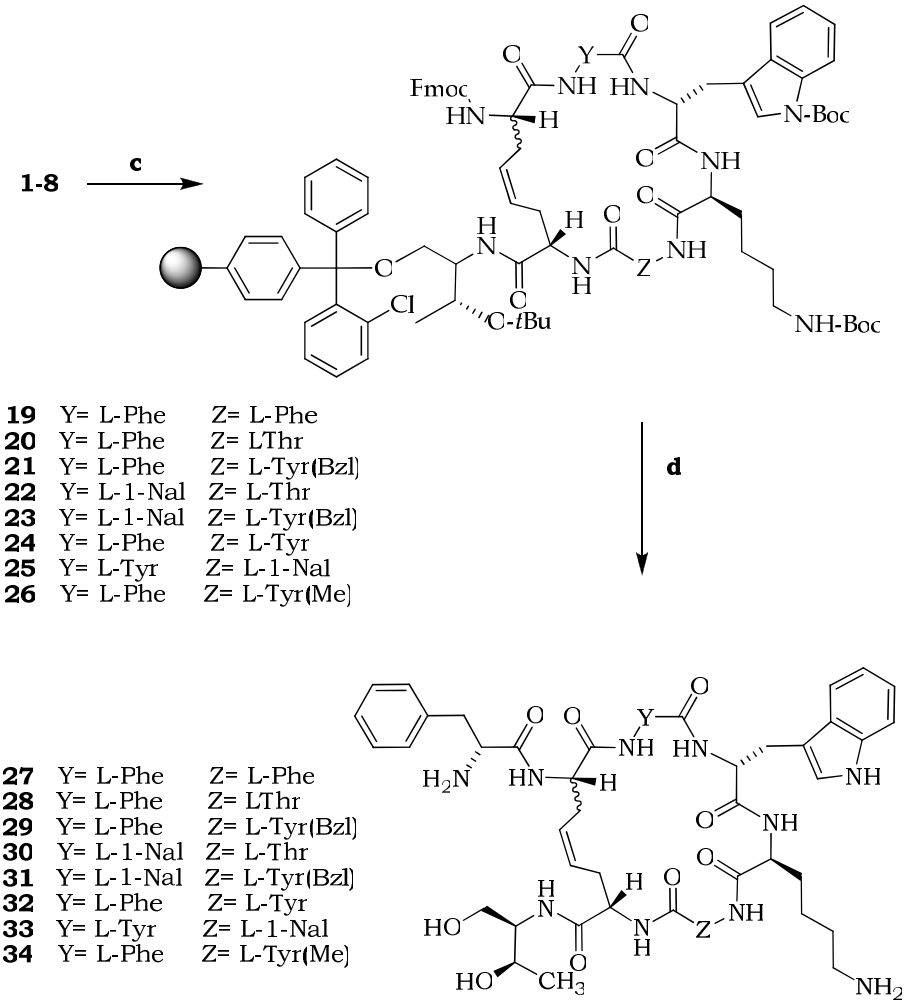

*Scheme 8. c. Catalyst **18**, 45°C, 24 h (**20-24**) and 48 h (**19**; **25-26**);*
(i) 20% piperidine in DMF, Fmoc-D-Phe/HATU/NMM 40 min, r.t.
*d.(ii) Cleavage of **19, 20, 22, 24, 25, 26** TFA/DCM/EDT/Phenol (94:2:2:2);*
***21** and **23** TFA/DCM/EDT/Phenol (70:26:2:2).*

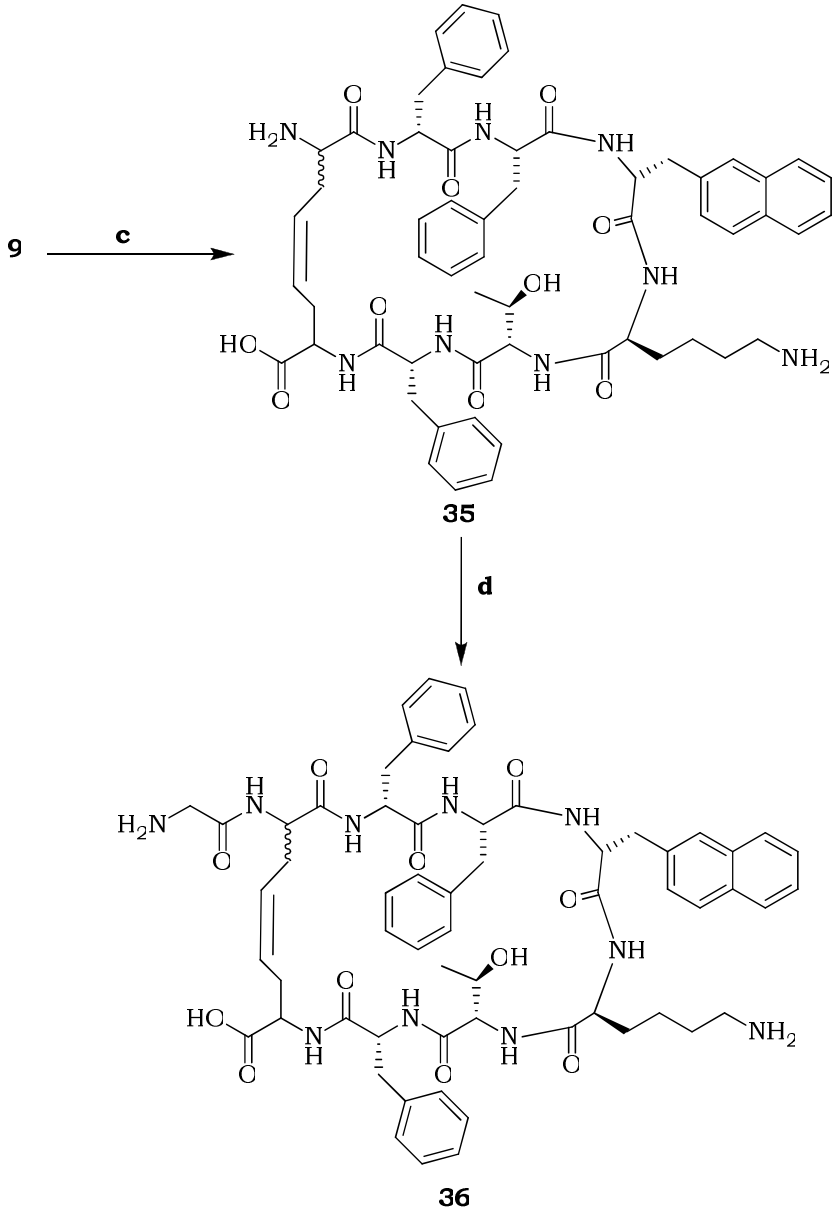

*Scheme 9. c. Catalyst **18,** 45 °C, 48h;*
d. (i) 20% piperidine in DMF, Fmoc-GLY/HATU/NMM 40 min, r.t.
*(ii). Cleavage of **36** TFA/DCM/EDT/Phenol (94:2:2:2).*

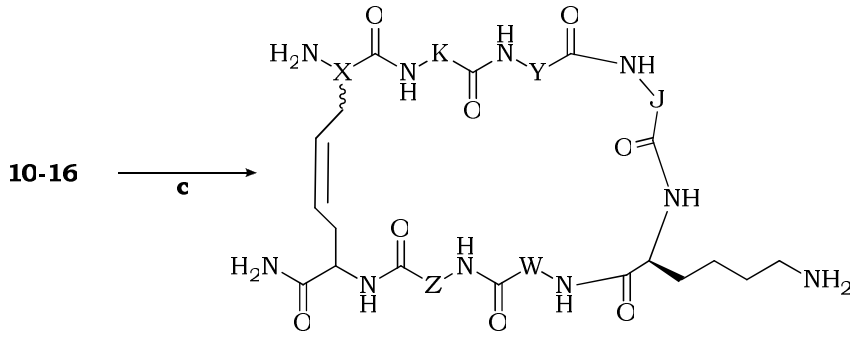

37	X= L-Hag	K= D-Phe	Y= L-Phe	J= D-Trp	W= L-Phe	Z= D-Phe
38	X= L-Hag	K= D-Phe	Y= L-Phe	J= D-Trp	W= L-Thr	Z= D-Phe
39	X= L-Hag	K= L-Phe	Y= L-Phe	J= D-Trp	W= L-Thr	Z= L-Phe
40	X= D-Hag	K= L-Phe	Y= L-Phe	J= D-Trp	W= L-Thr	Z= L-Phe
41	X= L-Hag	K= L-Phe	Y= L-Phe	J= D-2-Nal	W= L-Thr	Z= L-Phe
42	X= D-Hag	K= L-Phe	Y= L-Phe	J= D-2-Nal	W= L-Thr	Z= L-Phe
43	X= D-Hag	K= L-Phe	Y= L-Tyr	J= D-2-Nal	W= L-Thr	Z= L-Phe

*Scheme 10. c. Catalyst **18,** 45 °C, 48h; cleavage: TFA/DCM/EDT/Phenol (94:2:2:2).*

The factors that affect the success of the RCM on peptide cyclization are not yet fully understood. It is common opinion that inappropriate orientation of the alkilic side-chains may hamper the RCM. Not many papers concerning solid phase RCM on peptides have been reported so far but the cycles obtained in a smoothly way generally contain proline or *N*-alkyl residues in the sequence.[105,106] More recently, dicarba-analogues of oxytocin were prepared by RCM on solid phase of the parent linear peptides.[107] Consequently, we planned a more convenient synthetic approach to these cyclopeptides. The elongation of the peptide sequence was stopped after the coupling of Hag^3 residue (Scheme 8 and Scheme 9), with the aim of removing any possible interference of the aromatic ring of D-Phe^2 (**27-34**) or Gly^2 (**36**) on the correct orientation of the Hag side chains. It is worth of note that the presence of Phe^{10} (**27**) negatively affected the RCM, no matter what kind of catalyst was used. The Phe^2 residue close to Hag^3 hampered the RCM more than the bulky aromatic Tyr(Bzl)^{10} (**29**), suggesting that RCM is not affected by the size of the residues in position 10 but, probably, by the influence they have on the proper orientation of the allyl side-chains. To increase the yield of peptides we decided to perform RCM using **18**.[91]

[105] Harris, P. W. R.; Brimble, M. A.; Gluckman, P. D. Synthesis of Cyclic Proline-Containing Peptides via Ring-Closing Metathesis. *Org. Lett*. **2003**, *5*, 1847-1850.
[106] Schmiedberg, N.; Kessler, H. Reversibile Backbone protection Enables Combinatorial Solid-Phase Ring –Closing Metathesis Reaction (RCM) in Peptides. *Org. Lett*. **2002**, *4*, 59-62.
[107] Stymiest, J. L.; Mitchell, B. F; Wong, S.; Vederas, J. C. Synthesis of Oxytocyn Analogues with Replacement of Sulfur by Carbon Gives Potent Antagonists with Increased Stability. *J. Org. Chem.* **2005**, *70,* 7799–7809

Dicarba-analogues	Catalyst (hours of reflux)	% yield[a]	cyclic/linear ratio[b]
	Six-mer-ring peptides		
27	18 (48)	13	50:50
28	18 (24)	35	85:15
29	18 (24)	35	90:10
30	18 (24)	40	95:5
31	18 (24)	35	90:10
32	18 (24)	30	90:10
33	18 (48)	35	90:10
34	18 (48)	30	90:10
	Eight-mer-ring-peptides		
36	18 (48)	20	60:40
37	18 (48)	40	95:5
38	18 (48)	25	65:35
39	18 (48)	0	0/100
40	18 (48)	0	0/100
41	18 (48)	0	0/100
42	18 (48)	0	0/100
43	18 (48)	0	0/100

*Table 8. Cyclization of the linear six-mer-ring peptides (**27-34**) and eight-mer-ring peptides (**36-43**) with catalyst **18**. [a] Overall yield of isolated pure compounds(Z/E mixture), calculated on the basis of an average peptide loading of 0.5 mmol/g of resin. [b] Calculated on the basis of peaks area in analytical RP-HPLC.*

Surprisingly, conventional RCM doesn't work on peptides **39-43**. Changing the stereochemistry of Hag[3] did not had the expected effect. Because of D-Phe[6] and D-Phe[11] in compounds **36-38** were replaced by the corresponding L aminoacids in all the other peptides, we thought that L-Phe[6] and L-Phe[11] could disfavor the correct side-chains orientations prone to undergo RCM. Robinson et al., in fact, remarked the ability of Phe in peptide sequence to assist the cyclization *via* π-stacking interactions.[108] We decided

[108] Illesinghe J.; Guo C. X.; Garland R.; Ahmed A.; Van Lierop B.; Elaridi J.; Jackson R.; Robinson A. Metathesis assisted synthesis of cyclic peptides. *J. Chem Comm.* **2009**, 295-207.

to attempt RCM as before with Hoveyda-Grubbs 1st generation catalyst (**44**) (Figure 20.).

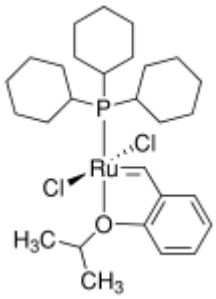

*Figure 20. Hoveyda-Grubbs 1st generation catalyst (**44**).*

We thought that a smaller catalyst like **44** could be more suitable for our sterically crowded peptides in increasing the catalytic efficiency. Unfortunately, also the use of **44** was unsuccessful and the linear precursors were the only products obtained. Peptides **39-43** were obtained only by MW-assisted RCM (see paragraph 4.1.3.2).

The isolation of peptides obtained on-resin by RCM is often complicated by the tendency of the organometallic molecules to bind the solid support. Several washing methods have been suggested to eliminate Ru contaminants.[109,110,111] However, no one of them gave satisfactory results in our hands. Notably, we found that centrifugation of the aqueous suspension after the cleavage and separation by SPE afforded compounds which were then easily purified from the residual catalyst contaminants by semi-preparative RP-HPLC. Analytical RP-HPLC and ESI-MS analysis of the crude compounds showed two chromatographic peaks with the same molar weight, probably corresponding to geometric isomers (ratio ≈ 90:10) and in compounds **29** and **32** with a ratio ≈ 70:30 (Z/E: see NMR analysis, paragraph 4.2). Following binding and conformational studies were performed only on the most abundant isomers, but in compounds **29** and **32**, whose isomers were analysed both. After purification all peptides were characterized by their MS (Table 9) and retention times (R_t) (Table 10).

[109] Stimyest, J. L.; Mitchell, B. F.; Wong, S.; Vederas, J. C. Synthesis of Biologically Active Dicarba Analogues of the Peptide Hormone Oxytocin Using Ring-Closing Metathesis. *Org. Lett.* **2003,** *5*, 47-49.
[110] Heather, D. M.; Grubbs, R. H. Purification Technique for the Removal of Ruthenium from Olefin Metathesis Reaction Products. *Tetrahedron Lett.* **1999**, *40*, 4137-4141.
[111] Paquette, L. A.; Schloss, J. D.; Efremov, I.; Fabris, F.; Gallou, F.; Méndez-Andino, J.; Yang, J. A Convenient Method for Remouving all Highly-Colored Byoproducts Generated During Olefin Metathesis Reaction. *Org. Lett.* **2000**, *2*, 1259-1261.

Compound	$[M+H]^+$ calcd.	$[M+H]^+$ found	$[M+2H]^{2+}$	$[M+Na]^+$
27	1026.53	1027.38	514.46	1049.58
28	980.10	981.45	491.87	1003.54
29 E	1132.57	1133.76	567.47	1156.66
29 Z	1132.57	1133.76	567.47	1156.66
30	1030.53	1032.0	516.0	1054.98
31	1182.59	1184.04	592.51	1206.94
32 E	1042.53	1043.76	522.35	1066.67
32 Z	1042.53	1043.76	522.35	1066.67
33	1092.54	1093.43	547.52	1115.51
34	1056.44	1057.43	529.51	1079.50
36	1080.54	1081.55	541.27	1104.45
37	1085.55	1087.0	544.1	1109.9
38	1039.53	1041.1	521.1	1064.0
39	1039.53	1040.63	521.1	1063.0
40	1039.53	1040.63	520.94	1063.0
41	1050.53	1051.99	526.46	1073.18
42	1050.53	1051.54	526.46	1074.18
43	1066.53	1067.27	534.5	1090.79

Table 9. Mass spectrometry data of pure unsaturated cyclic compounds.

Compound	HPLC method[a]	R_t (min)
27	30%-80% in 20 min	14.643
28	20%-60% in 20 min	10.502
29 E	45%-55% in 20 min	6.321
29 Z	45%-55% in 20 min	9.533
30	20%-60% in 20 min	13.273
31	40%-60% in 20 min	16.935
32 E	25%-35% in 10 min	5.968
32 Z	25%-35% in 10 min	6.323
33	30%-60% in 20 min	11.808
34	30%-60% in 20 min	11.689
36	30%-60% in 20 min	12.342
37	30%-80% in 20 min	14.674
38	30%-60% in 20 min	10.045
39	30%-60% in 20 min	10.735
40	35%-50%- in 20 min	10.266
41	35%-50%- in 20 min	12.664
42	35%-50%- in 20 min	16.266
43	30%-90%- in 20 min	16.225

Table 10. RP-HPLC analytical data of the pure cyclic compounds with the alkenyl bridge. [a] *A: H_2O 0.1% TFA; B: CH_3CN 0.1% TFA.*

4.1.3 Microwave-assisted RCM

Microwaves heating is today an important and accepted method of heating in preparative chemistry.[112,113,114] The attractions of microwave-heated technologies are many. For example, reaction times can in numerous cases be shortened from hours or days to minutes or seconds. The microwave story in the drug-discovery area began in the late 1990s, although a number of pioneers had started using microwave irradiation

[112] P. Lidström; J. Tierney; b. Wathey; J. Westman. Microwaves assisted organic synthesis. *Tetrahedron,* **2001**, *57*, 9225.
[113] K. Olofsson; A. Hallberg; M. Larhed. Microwaves in Organic Synthesis. A. Loupy (ed), Wiley-VCH, Weinheim, **2002**, 379.
[114] C. O. Kappe. Controlled Microwave heating in modern organic synthesis. *Angew. Chem. Int. Ed.* **2004**, *43*, 6250.

for organic synthesis much earlier.[115] In terms of personal dynamics in the integration of microwave technology with medicinal chemistry, important contributions were made by Anders Hallberg,[116] who early emphasized the potential of combining microwave heating and transition metal catalysis in the development of sophisticated lead molecules. When the benefits of combining microwave heating with solid-phase chemistry was recognised, this concept was investigated in detail by especially Oliver Kappe.[117] Microwaves are electromagnetic waves with wavelengths approximately in the range of 30 cm (frequency 1 GHz) to 1 mm (300 GHz) (Figure 21). However, the boundaries between far infrared light, terahertz radiation, microwaves, and ultra-high-frequency radio waves are fairly arbitrary and are used variously between different fields of study. The term microwave generally refers to "alternating current signals with frequencies between 300 MHz (3×10^8 Hz) and 300 GHz (3×10^{11} Hz)".[118]

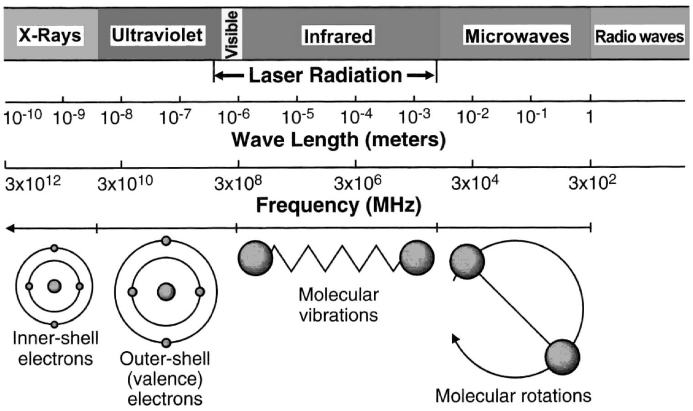

Figure 21. Electromagnetic spectrum.

A microwave oven works by passing microwave radiation, usually at a frequency of 2450 MHz (a wavelength of 12.24 cm), through the solids. When the microwaves enter a cavity, they are reflected by the walls. The reflections of the waves eventually generate a three dimensional stationary pattern of standing waves within the cavity, called modes. Most early microwave-enhanced synthesis works were done in multi-mode systems. Multi-mode reactors present larger cavities with a microwave field that contains multiple modes of energy of different intensity, so called hot and cold spots.

[115] a) D. M. P. Mingos; D. R. Baghurst. Chem. Soc. Rev. 1991, 20, 1. b) S. Caddick. *Tetrahedron*. **1995**, *51*, 10403
[116] M. Larhed; A. Hallberg. *Drug Discov. Today*. **2001**, *6*, 406.
[117] C. O. Kappe. *Curr. Opin. Chem. Biol.* **2002**, **6**, 314.
[118] Pozar, D. M. *Microwave Engineering* **1993** Addison-Wesley Publishing Company. ISBN 0-201-50418-9

As a consequence, this non uniform microwave irradiation inside the reactor is compensate, as possible, by rotation of samples through the field. While multi-mode strategy is particularly suitable for parallel synthesis, the small individual samples characteristic of drug discovery are problematic in multi-mode systems, due to the hot and cold spots intrinsic in the cavity design. Moreover, the power density in the cavity is low, making it difficult to heat small individual samples. Recently, in order to obtain a well-defined heating pattern for small loads, single-mode cavities with good uniform energy distribution and the ability to couple with small samples more efficiently have become available. These cavities are better suited for drug discovery work, because the higher power density allows the energy to be more focused. Because of this type of cavity allows only one single mode to be present. Much higher field strengths can be obtained, giving rise to more rapid heating. A suitably designed cavity also prevents the formation of 'hot and cold spots' within the sample, resulting in a uniform heating pattern. This is very important when microwave technology is used in organic chemistry, since the heating pattern for small samples can be well controlled. This allows for higher reproducibility and predictability of results as well as optimization of yields, which are usually more difficult when using a domestic microwave oven.

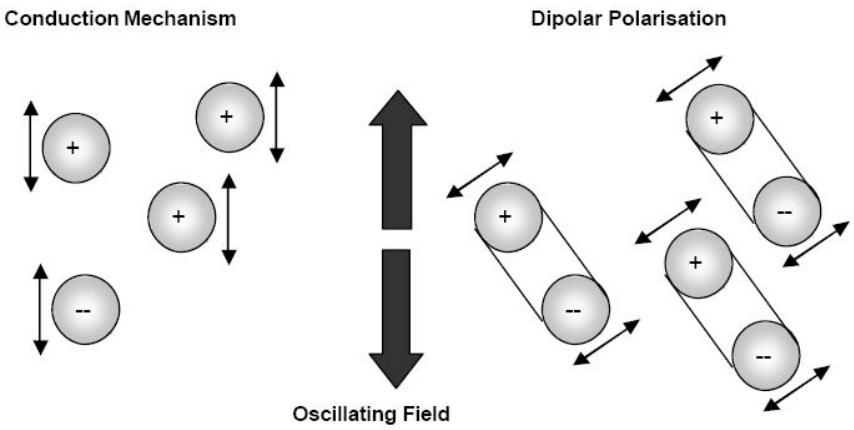

Figure 22. Heating by microwave irradiation.

Microwave-enhanced chemistry is based on different efficient heating of material by "microwave dielectric heating" effects. This phenomenon is dependent on the ability of a specific material (solvent or reagent) to absorb microwave energy and convert it into heat. The electric component of electromagnetic field causes heating by two main mechanisms: dipolar polarization and ionic conduction (Figure 22).

On the other hand, conventional heating transfers energy to reaction *via* conduction or convection. Irradiation of the sample at microwave frequencies results in the dipoles or ion aligning in the applied electric field. As the applied field oscillates, the dipole or ion field attempts to realign itself with the alternating electric field and, in the process, energy is lost in the form of heat through molecular friction and dielectric loss. The amount of heat generated by this process is directly related to the ability of the matrix to align itself with the frequency of the applied field. If the dipole does not have enough time to realign, or reorients too quickly with the applied field, no heating occurs. The allocated frequency of 2.45 GHz used in all commercial system lies between these two extremes and gives the molecular dipole time to align in the field, but not to follow the alternating field precisely. The heating characteristics of a particular material under microwave irradiation conditions are dependent on its dielectric properties. The ability of a specific substance to convert electromagnetic energy into heat at a given frequency and temperature is determined by the so-called loss factor. A reaction medium with a high tan δ value is required for efficient absorption and, consequently, for rapid heating. Traditionally, organic synthesis is carried out by conductive heating with an external heat source. The heating depends on the thermal conductivity of the various materials that must be penetrated, and results in the temperature of the reaction vessel being higher than of the reaction mixture. In contrast, microwave irradiation produce efficient internal heating (in-core volumetric heating) by direct coupling of microwave energy with the molecules (solvent, reagent, catalyst) that are present in the reaction mixture. Since the reaction vessel employed are typically made out of microwave-transparent materials, such as borosilicate glass, quartz or Teflon, an inverted temperature gradient results compared to conventional thermal heating (Figure 23).[119] The very efficient internal heat transfer results in minimized wall effects which may lead to the observation of so-called specific microwave effect, for example in the context of diminished catalyst deactivation. Since the early days of microwave synthesis, the observed rate acceleration and sometimes altered products distribution compared to oil-bath experiments have led to speculation on the existence of so-called “specific” or “non-thermal” microwave effects.

[119] Kappe, C. O. Controlled Microwave Heating in Modern Organic Synthesis. *Angew Chem Int Ed Engl.* **2004**, *43*, 6250-6284.

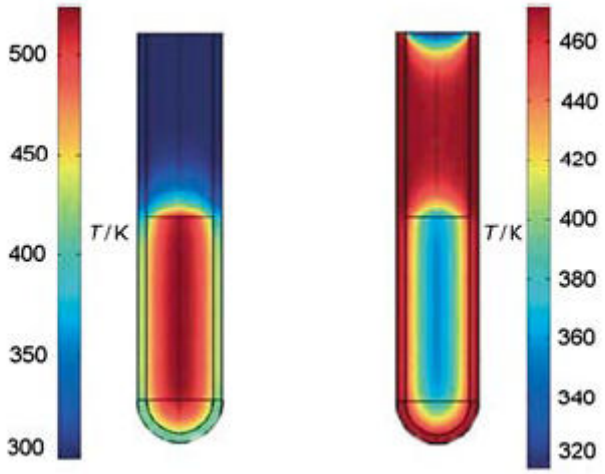

Figure 23. Inverted temperature gradients in microwave versus oil-bath heating: Difference in the temperature profile: after 1 min of microwave irradiation (left) and treatment in oil-bath (right).

Most of scientists agree that in the majority of cases the reason for the observed rate enhancement is the purely thermal/kinetic effect, that is, a consequence of the high reaction temperature that can rapidly be obtained when irradiating polar materials in a microwave field. Some authors have suggested the possibility of 'non-thermal microwave effects'. These should be classified as accelerations that cannot be rationalized by either purely thermal/kinetic or specific microwave effects. Non thermal effect essentially results from a direct interaction of the electric field with specific molecules in the reaction medium. Considering the Arrhenius equation ($k = Ae^{(-Ea/RT)}$), it has been argued that the presence of an electric field lead to orientation effects of dipolar molecules and hence changes the pre-exponential factor A or the activation energy (entropy term). Microwave effects are the subject of considerable current debate and controversy, and it is evident that extensive research efforts will be necessary to truly understand these and related phenomena.

Many academic and industrial research group are already using microwave-assisted organic synthesis as a forefront technology for rapid optimization of reaction and the efficient synthesis of new chemical entities, and for discovery and probing new reactivity. Microwave assisted chemistry is applied to many types of reaction and many articles were so far written on microwave assisted RCM.[120,121,122,123]

[120] Chapman, R. N.; Arora, P. S. Optimized Synthesis of Hydrogen-Bond Surrogate Helices: Surprising Effects of Microwave Heating on the Activity of Grubbs Catalysts. *Org. Lett.* **2006**, *8*, 5825-5828.
[121] Robinson, A. J.; Elaridi, J; Van Lierop, B. J.; Mujcinovic, S.; Jackson, W. R. Microwave-assisted RCM for the Synthesis of Carbocyclic Peptides. *J. Pept. Sci.* **2007**, *13*, 280-285.

4.1.3.1 Six-mer-ring peptides

Recently in our laboratory it has been available a microwave instrument, CEM Discover. In order to obtain shorter time of RCM, we applied a microwave assisted RCM to achieve peptide **27-32** and hereafter on compounds **33-34**.

Resin bounded peptides **1-6** were suspended in DCM in a appropriated microwave vessel, **18** was added and microwave instrument methods were started. Table 11 reports methods used for each compound and the analytical HPLC conversion linear to cyclic peptides.

Notably, comparing these data with those obtained with external heating we must remark that these high yields were obtained without the use of anhydrous conditions neither for solvent nor for the inert atmosphere. Due to the limited duration of the reaction, catalyst did not decompose therefore it not need argon atmosphere as in oil-bath. We started from 10 minute at 100 °C and for each peptide micro-scale cleavage was performed after the coupling whit D-Phe[2]. After the cleavage cyclic linear ratio were calculated. 10 minutes were enough to obtain a small amount of desired peptide but an additional time was required for improving yield. Moreover, a specific power and temperature value was necessary in order to obtain a selective MW effect on each peptide (Table 11). MW-assisted RCM conditions was specific for each sequence. We like to underline that oil-bath cyclization of **27** gave very low yield, on the contrary, MW-assisted RCM gave good conversion rates. Analyzing the chromatogram we noticed, for peptide **29**, a low intense peak before the cyclic one that, by ESI-MS, had m/z ratio of **29** without benzyl moiety (15 %).

[122] (a) *Microwaves in Organic Synthesis*, 2nd ed.; Loupy, A., Ed.; Wiley-VCH: Weinheim, Germany, **2006**. (b) Microwaves-Assisted Organic Synthesis; Lindström, P.; Tierney, J. P., Eds.; Blackwell Publishing: Oxford. U. K., **2005**. (c) Kappe, C. O., Stadler, A. *Microwaves in organic and Medicinal Chemistry*; Wiley-VCH: Weinheim, Germany, **2005**.

[123] (a) Chen, J. J.; Deshpande, S. V. *Tetrahedron Lett*. **2003**, 44, 8873. (b) Matthew, F.; Jayaprakash, K. N.; Fraser-Reid, B.; Mathew, J.; Scicinski, J. *Tetrahedron Lett.* **2003**, 44, 9051. (c) Leadbeater, N. E.; Pillsbury, S. J.; Shanahan, E.; Williams, V. A.; Tetrahedron **2005**, 61, 3565. (d) Arvela, R. K.; Leadbeater, N. E. Org. Lett.**2005**, 7, 2101. (e) JAchuck, R. J. J.; Selvaraj, D. K.; Varma, R. S.; Green Che. **2006**, 8, 29. (f) Singh, B. K.; Appukkuttan, P.; Claerhout, S.; Parmar, V. S:; Van der Eucken, E. Org Lett. **2006**, 8, 1863. (g) Baxendale, I. R.; Griffiths-Jones, C. M.; Ley, S. V.; Tranmer, G. T.; Chem-Eur. J. **2006**, 12, 4407.

Compounds	Microwaves methods	Cyclic/linear ratio[a]
27	300 W, 100 °C, 1 hour Dynamic	95:5
28	150 W, 100 °C, 30 minutes SPS	85:15
29	300 W, 100 °C, 50 minutes Power Cycling	90:10[b]
30	150 W, 100 °C, 30 minutes SPS	90:10
31	100 W, 80 °C, 30 minutes Dynamic	80:20
32	300 W, 100 °C, 50 minutes Power Cycling	85:15

*Table 11. Microwave-assisted RCM on peptides **27-32**;*
[a] Calculated on the basis of peaks area in analytical RP-HPLC.
*b. 75% of **29** and 15% of **29** without benzyl moiety.*

4.1.3.2 Eight-mer-ring peptides

As mentioned in paragraph 4.1.2, conventional RCM didn't work on peptides **39-43,** neither with catalyst **44**. Aimed by the results obtained with six-mer-ring peptides, we performed the MW-assisted RCM on eight-mer-ring peptides. It is noteworthy that MW is useful in reducing peptide aggregation, leading to proper peptide construction.[108]

Differences among the five methods of irradiation available in our CEM apparatus are due to the possibility of setting temperature or power as a function one of each other, while pressure has a fixed upper limit threshold. Its value is correlated to temperature and power (see experimental part). Compounds **12-16** were treated with all the five methods**,** but the fixed power one; this method, in fact, was discarded because once the temperature has reached the set value, the instrument stopped to provide MW radiations. Power cycling and SPS methods maintain the required conditions (100 °C

and 300 W)[124], while a lower MW power is granted in Standard and Dynamic methods. All the parameters were monitored during the whole reaction and for each compound.

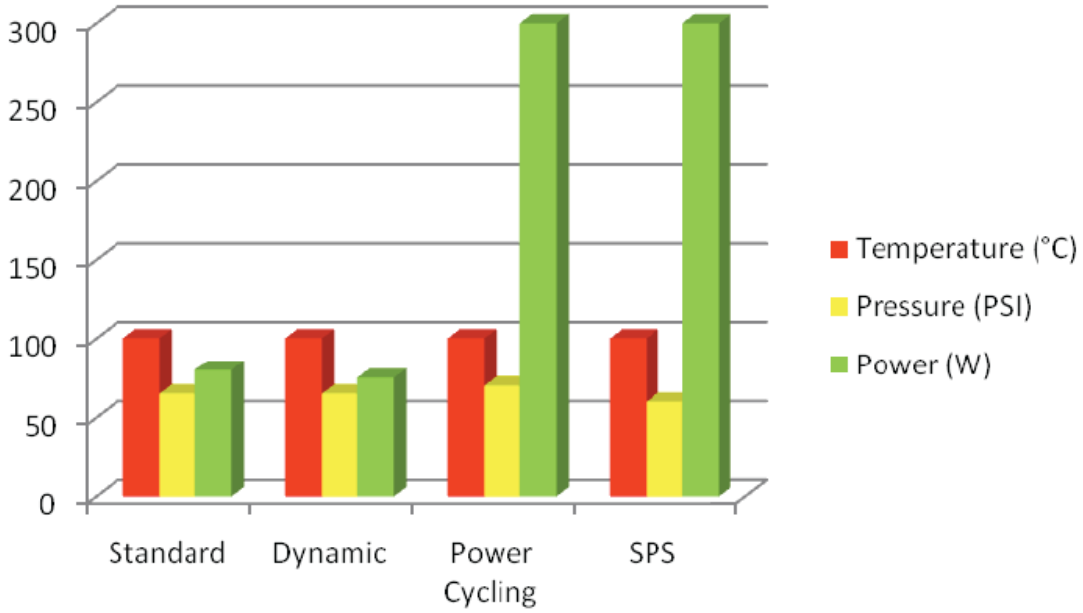

Graphic 1. Temperature, pressure and power for each of the four employed methods. Mean values monitored during 30 minutes of reaction.

On resin linear peptides **12-16** were suspended in DCM and, after one hour swelling, a fresh solution of **18** (10 % mol) was added. Reaction mixture was kept under 100 °C and 300 W for 30 minutes. A micro-cleavage of the resin bound peptides was performed. HPLC chromatograms of crude compounds revealed the presence of the cyclic derivatives (**39-43**) in good yields (Graphic 2). No other by-products were observed, but still a small amount of the starting liner peptides.

Notably, using one strategy instead of another had not the same effect (see previous paragraph). Power cycling and SPS methods were the best in order to perform RCM, although it can be possible achieving the cyclic compounds **39-43** even when MW power is kept under 100 watt (Standard and Dynamic methods). Regardless of the relatively large body of published work on microwave chemistry, the exact reasons why microwave heating enhance chemical processes are still unknown.[115] MW decreases activation energy and hence promote the cyclization of peptides otherwise impossible to obtain. Considerations could be made on the effects of temperature and power. Thermal

[124] Robinson, A. J.; Elaridi, J.; Van Lierop, B. J.; Mujcinovic S.; Jackson, W. R.; Microwaves-asisted RCM for the synthesis of carbocyclic peptides. *J. Pept. Sci*. **2007**, *13*, 280-285.

effects, which are due to temperature, are still now the main features that rule MW process: in general a higher temperature favours reaction process by thermal/kinetic factors due to a macroscopic effect, involved in reaction process.[125]

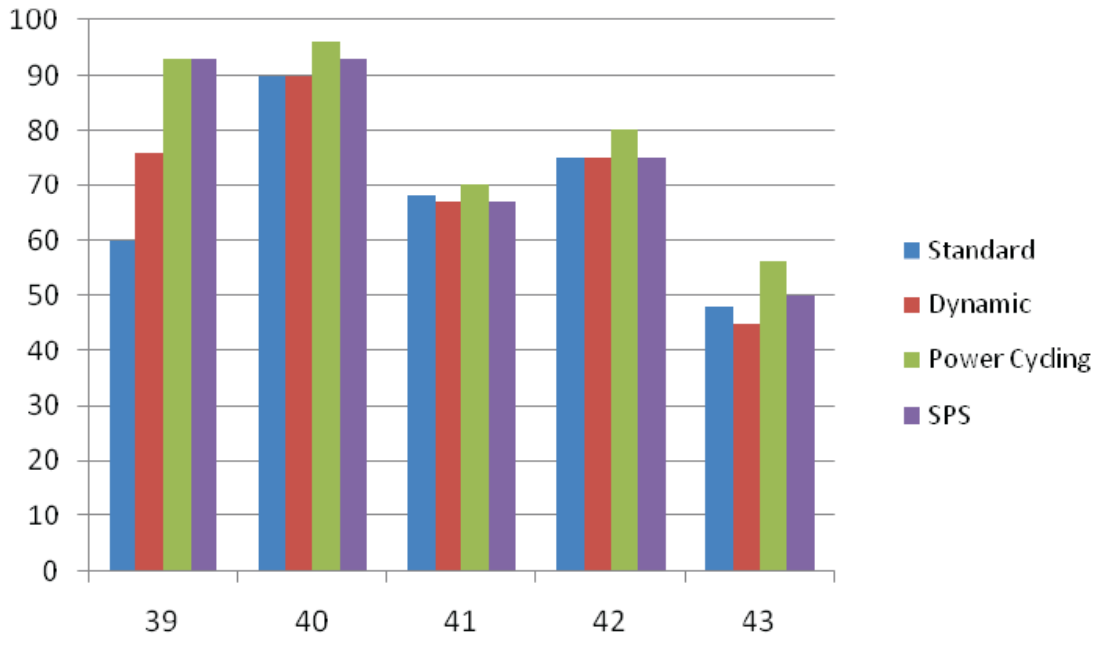

*Graphic 2. Cyclic peptides (**39-43**) yields after 30 minutes of MW-assisted RCM performed with four different methods.*

Concerning the influence of the power level, it is evident that lower or higher electric field is important in the reaction yield. The continuous external gas cooling (Power Cycling and SPS methods) provide a higher level of microwaves power to be directly administered on the reaction mixture, thereby potentially enhancing any aspecific or "non thermal" microwaves effects. Nevertheless, it is not easy to understand the reason behind the so called "non-thermal" effects. Surely, the success of MW-assisted RCM is due to a decrease of activation energy barrier rather than to decrease steric constraints. This deduction is supported by the evident failure of **44**. It was worth of note that also inappropriate orientation of the Hag[3] side chains in MW-assisted cyclization may influence in some extent the RCM . In fact, changes from L-Hag[3] to D-Hag[3] stereochemistry had effect on the yields of the cyclic dicarba-analogues. The D-Hag[3] containing cyclic compounds **40** and **42** were obtained in higher yields than their parents L-Hag[3] peptides **39** and **41**, still remarking the importance of the allyl side chain orientation.

[125] Garbacia, S.; Desai, B.; Lavastre, O.; Kappe, O. J. Org. Chem. *Microwaves-assisted ring-closing Metathesis revisited. On the question of non thermal effect*. **2003**, *68*, 9136-9139.

Many papers have been written about the ability of MW to spread the side chains and hence enhance the reactivity. We can suppose that a different alkenyl side chains orientation can favor or strongly disfavor the RCM in peptides. Valuable differences are also found between peptides bearing D-Trp^{8} or D-2-Nal^{8}.

Graphic 2 shows a higher yields for **39** and **40**, which bear D-Trp^{8} than for compounds **41** and **42** (D-2-Nal^{8}). In accordance with the results achieved by Chapman and colleagues,[120] we supposed that some sequences display structural motives which cannot favorably interact with catalysts. This hypothesis is supported by the loss of the helical motif[91] when Trp^{8} is substituted with D-2-Nal^{8} and hence by the difficulty of the alkenyl side chains to assume a favorable orientation. MW get a great contribute in lowering activation energy and in the correct arrangement of the allylic side-chain respect to the Ru-catalysts. This matter of facts was confirmed by the failure of the conventional heating during RCM in obtaining compounds with different stereochemical substitutions. None speculation was possible about **43**. This compound bear contemporary substitution D-2-Nal^{8}, the D-Hag^{3} and a Tyr^{7}. Hence any speculation was difficult to rationalize.

Due to the possibility of increase the yields of the analogues **39-43**, we also evaluated the influence of time on MW-assisted RCM (

Graphic 3). Each method was applied for three times (3 x 30 minutes) on each starting linear compound (**12-16**). Increasing time reaction had as a consequence the enhancement of the cyclic dicarba-analogues yields. Both in the Standard and Dynamic method, an additional time of 30 minutes was useful for increase the yield of **39**. Compounds **14** needed of a further 60 minutes for obtaining **41** in 75 % yield of and 90 minutes for a conversion of 90% with the Standard methods while Dynamic method seems not so prone to favor cyclization, even after 120 minutes. This matter of fact suggested a different kinetic profile for the five different compounds.

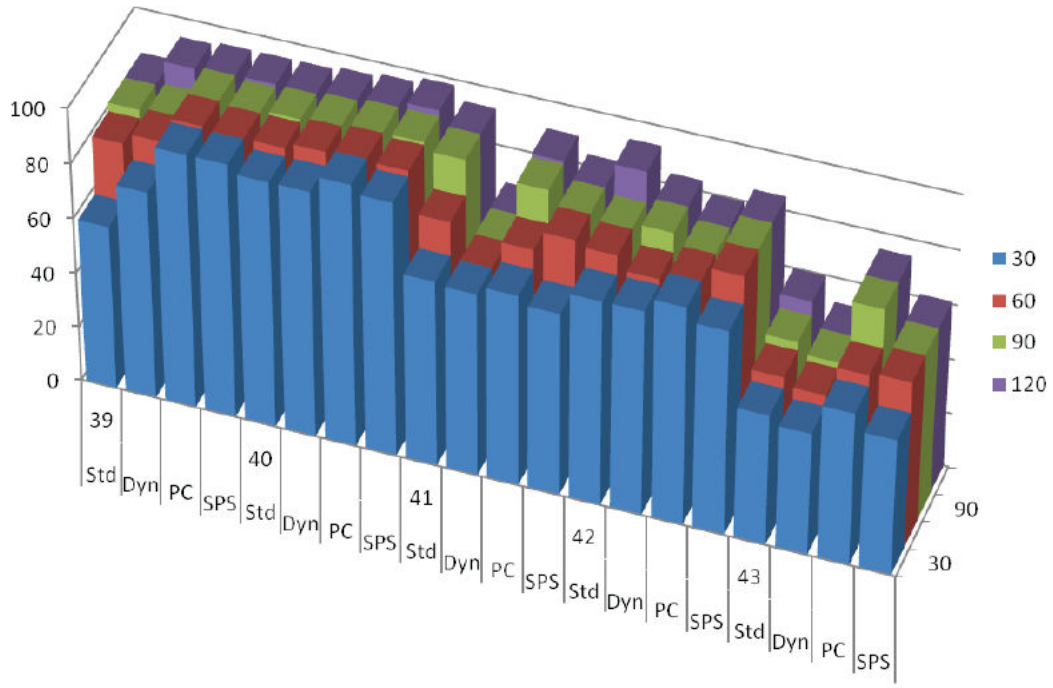

Graphic 3. Time-dependent yield.
Values are referred as a HPLC cyclic/linear ratio of the E/Z isomers mixture.

4.1.4 Synthesis of saturated cyclic peptides

The olefin bridge of the analogues **28**, **29**, **30** and **37** was hydrogenated in order to study the effect of the higher flexibility of the $-CH_2-CH_2-$ group on the conformational behaviour. Hydrogenation was accomplished using two different methods because of the different substitution in position 10. The Pd/C catalyst, that is the most used tool to reduce olefinic bridges obtained by RCM on peptides, did not work well for the reduction of **29**. [90,91] Therefore, the saturated analog **45-47** was obtained by using H_2 fluxing in the presence of $Pd(OH)_2/C$. However, heating at 30 °C of the reaction mixture was needed to obtain the saturated compound in good yield (Scheme 1).

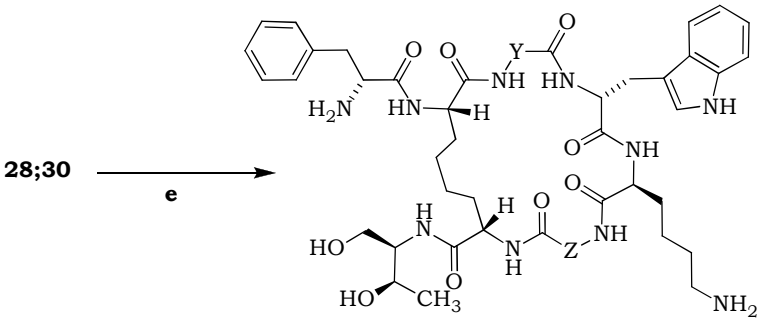

45 Y= Phe Z= Thr
46 Y= 1-Nal Z= Thr

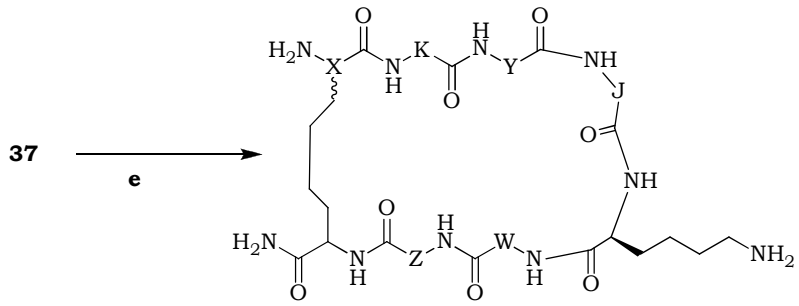

47 X= L-Hag K= D-Phe Y= L-Phe J= D-Trp W= L-Phe Z= D-Phe

*Scheme 11. Synthesis of saturated dicarba-analogues **45-47**.*
e: 20% $Pd(OH)_2$/C, H_2, 24 h, 30 °C.

Unsaturated peptide **29** cannot be reduced by $Pd(OH)_2$/C because it was cleaved the Bzl moiety in the reaction medium; therefore analog **48** was achieved using Wilkinson's catalyst $Rh(PPh_3)_3Cl_6$.[126,127] On resin peptide **29** was suspended in DCM/MeOH and inserted in an appropriated vessel for autoclave reaction, which was performed under 60 psi for 24 hours (Scheme 12).[128]

All saturated compounds were purified by RP-HPLC and the isolated compounds were characterized by their MS (Table 12) and retention times (R_t) (Table 13).

[126] Jourdant, A.; Gonzalez-Zamora, E.; Zhu, J. Wilkinson's Catalyst Catalyzed Selective Hydrogenation of Olefin in Presence of Aromatic Nitro Function: a Remarcable Solvent Effect. *J. Org. Chem*. **2002**, *67*, 3163-3164.
[127] Burgess, K.; Van der Donk, W. A. In Encyclopedia of reagent for organic synthesis. Paquette LA, Ed. Wiley: New York. **1995**, *2*, pp 1253-1261.
[128] Wheland, A. N.; Elaridi, J.; Mulder, R. J.; Smith, S. V.; Robinson, A. J; Jackson, W. R. Metal-Catalyzed Tandem Metathesis-Hydrogenation Reactions for the Synthesis of Cyclic Peptides. *Can. J. Chem.* **2005**, *83*, 875-881.

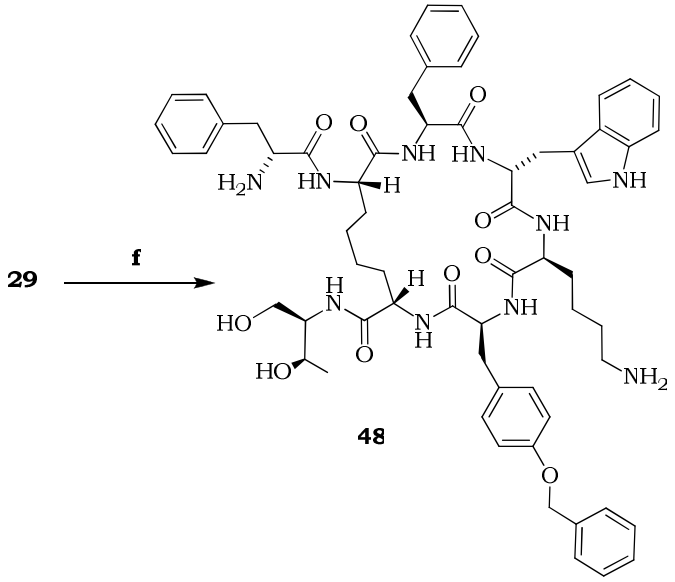

*Scheme 12. Synthesis of the saturated analog **48**;*
f. (i) MeOH/DCM, Wilkinson's catalyst 2.5%, H_2 (60 psi); (ii) 20% piperidine in DMF, Fmoc-D-Phe/HATU/NMM, 40 min, r.t.;
(iii) 20% piperidine in DMF, cleavage.

Compounds	[M+H]+ calcd.	[M+H]+ found	[M+2H]2+	[M+Na]+
45	982.53	983.44	492.60	1005.52
46	1032.22	1033.9	517.90	1055.23
47	1087.3	1089.0	545.5	1111.1
48	1134.35	1135.50	568.42	1157.54

Table 12. Mass spectrometry data of pure saturated cyclic compounds.

Compound	HPLC method[a]	Rt (min)
45	20%-60% in 20 min	10.134
46	20%-60% in 20 min	12.935
47	30%-80% in 20 min	14.561
48	20%-60% in 20 min	8.662

Table 13. RP-HPLC analytical data of pure saturated cyclic compounds.
[a] A: H_2O 0.1% TFA; B: CH_3CN 0.1% TFA.

4.1.5 Synthesis of radiolabeled unsaturated peptides

It is not the scope of the this PhD thesis to give an extensive description of the various labelling methods and radiopharmaceutical, used in clinical oncology. Nevertheless we considered the opportunity to spend a few words on this subject.[129]

Radiopharmaceuticals are drugs containing atoms of some radioactive elements. They are designed for diagnostic or therapeutic purposes, to deliver small doses of ionizing radiation to the disease sites in the body. Radiopharmaceuticals, unlike classical chemotherapeutics, act against malignant cells with high specificity. Radiopharmaceuticals are mostly small organic molecules, such as peptides or peptidomimetics. Bio-distribution of radiopharmaceuticals can be determined either by their chemical and physical properties or by their biological interactions. Radiopharmaceuticals, which act through receptor binding, are called targets-specific, as the cases described in this PhD thesis. Ideally, these radiopharmaceuticals are designed to locate with high specificity at cancerous tumours, even if their location in the body is unknown, while producing minimal radiation damage to normal tissues.[130,131] In the past decade significant progress has been made in the development of peptide-based target-specific radiopharmaceuticals, which have become an important class of imaging agents for the detection of various diseases.

Direct labelling methods are mostly based on the binding of a radionuclide to thiol groups in the targeting molecule. However, such a labeling process is difficult to control; consequently the detailed chemistry is unknown and may lead to unplanned changes in the structure, stability, and pharmacokinetic properties of the labeled molecule. The direct labelling approach is rather unsuitable for small peptides, which either do not possess disulfide linkage or are unable to maintain their activity after reduction. For example Thakur has reported,[132] the alteration of the receptor binding properties of the radiolabeled somatostatin analogues, when the disulfide bridge was reduced to free thiol groups and subsequently radiolabeled with ^{99m}Tc. It is one of the reason we synthesized dicarba-analogues, that without disulphide linkage could be radiolabeled directly with ^{99m}Tc.

[129] Verbruggen, A. M. Radiopharmaceuticals: state of the art. Eur. *J. Nucl. Med.* **1990**, *17*, 346-364.
[130] Hoefnagel, C. A. Anticancer radiopharmaceuticals. *Anticancer Drugs* **1991**, *2*, 107-132.
[131] Pauwels, E. K.; McCready, V. R.; Stoot, J. H. M. B.; van Deurzen, D. F. P. The mechanism of accumulation of tumour-localising radiopharmaceuticals. *Eur. J. Nucl. Med.* **1998**, *25*, 277-305.
[132] Thakur, M. L. Tc-99m labeled sandostatin: preparation and preliminary evaluation. *J. Labeled Cmpd. Radiopharm.* **1993**, *32*, 365-367.

On the other hand in the chelate methods a radionuclide is bound to the targeting molecule indirectly, through a BFCA as described in the introduction of this thesis for somatostatin radiopharmaceutical analogues. In general, a radiopharmaceutical containing a BFCA consists of the following parts: a targeting molecule, BFCA, radionuclide, and a linker. The targeting molecule is a carrier of a radionuclide to the receptor site *in vivo*. A radionuclide serves as a radiation source. A BFCA, covalently attached to the targeting molecule, functions as the coordinator of the radionuclide. A linker, not always necessary, is a spacer residue, which separates a targeting molecule from a chelating agent. Functional groups, naturally present in the peptide or introduced synthetically, are responsible for covalent attachment of BFCA.

This approach is the one used in the synthesis of unsaturated radiolabeled peptides. Peptide **29**, **31** and **32** were conjugated with DOTA and compounds **28** and **30** with DOTA and PN_2S both, in order to radiolabelled the dicarba-analogues respectively with ^{111}In and ^{99m}Tc.

4.1.5.1 Synthesis of DOTA conjugated peptides

Peptides **29-32** synthesized as described in paragraph 4.1.2 were deprotected on the N-terminus amino group of D-Phe[2] and conjugated with DOTAtri(*t*-Bu)-ester.

The obtained peptides were then cleaved from the resin by cleavage mixture described in 4.1.1, but for compounds **49** and **51** and with a new mixture (TFA,TES, DCM 70%:20%:10% 4h) for keeping the benzyl moiety and cleaving the t-Bu group. Deprotected peptides were obtained as showed in Figure 24 after purification by RP-HPLC (Table 15). Complete formulas were given in the supplementary information (figures S21-S24).

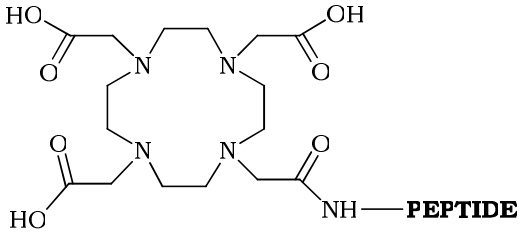

Peptides	DOTA-Peptides
29	49
30	50
31	51
32	52

*Figure 24. General formula of unsaturated DOTA-dicarba-analogues **49-52**.*

All DOTA conjugated peptides were dispatched to the Regional Centre of Nuclear Medicine of the University of Pisa for the radiolabelling.

Compound	$[M+H]^+$ calcd.	$[M+H]^+$ found	$[M+2H]^{2+}$	$[M+Na]^+$
49	1518.75	1519.46	760.54	1541.0
50	1416.71	1417.72	709.7	1440.62
51	1568.77	1569.44	785.56	1591.49
52	1428.71	1429.39	715.58	1452.44

Table 14. Mass spectrometry data of the pure conjugated peptides.

Compound	HPLC method[a]	R_t (min)
49	45%-55%-in 20 min	10.284
50	20%-60%-in 20 min	14.050
51	50%-60% in 20 min	9.693
52	30%-40% in 20 min	12.790

Table 15. RP-HPLC analytical data of the pure conjugated peptides.
[a] A: H_2O 0.1% TFA;B: CH_3CN 0.1% TFA.

4.1.5.2 Synthesis of PN_2S peptide conjugates

N-[N-(3-Diphenylphosphinopropionyl)glycyl]cysteine (PN_2S) is a chelating agent synthesized at the Department of Pharmaceutical Chemistry of the university of Padova.[133] PN_2S is able to chelate ^{99m}Tc and $^{186/188}Re$ and as the carboxyl function of cysteine for the anchoring to peptides. Due to the experience of SPPS we have in our laboratory we decided not to couple directly the pseudo-tripeptide, but to proceed the synthesis on resin peptides step by step.

Peptides **28** and **30**, synthesized as described in paragraph 4.1.2 were deprotected on the N-terminus amino group of D-Phe[2] and coupled with L-Cys-(Trt), than with L-Gly and finally with 3-diphenylphosphinopropionic acid succinimidic ester. Because of the thiol and phosphinic groups are easily oxidized, the cleavage procedures were performed under argon and cleavage mixtures were degassed affording the PN_2S-peptides **53** and **54** (Scheme 13).

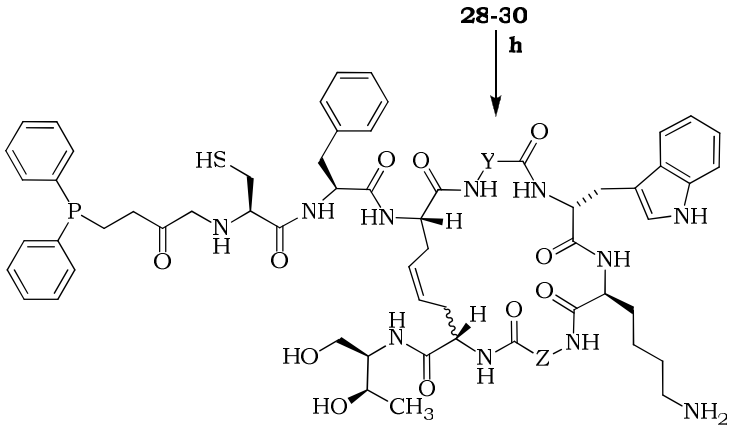

53 Y= 1 Phe Z = Thr
54 Y= 1 Nal Z = Thr

*Scheme 13. Synthesis of PN_2S conjugated peptides **53** and **54**. h: (i) 20% piperidine in DMF; (ii) coupling with L-Cys-(Trt), L-Gly/HATU/NMM 40 min, r.t.; 3-diphenylphosphinopropionic acid succinimidic ester/NMM 40 min, r.t.(iii) Cleavage TFA/DCM/EDT/Phenol (94:2:2:2).*

The purification of the crude peptide was performed in degassed solvent and the collected fractions were quickly frozen and lyophilized to avoid degradation of oxidable groups.

[133] Visentin, R.; Rossin, R.; Giron, M. C.; Dolmella, A.; Bandoli, G.; Mazzi U. Synthesis and Characterization of Rhenium(V) Oxo Complexes with N-[N-(3-Diphenylphosphinopropionyl)glycyl]cysteine Methyl Ester. X-ray Crystal Structure of {ReO[Ph2P(CH2)2C(O)-Gly-Cys-OMe(P,N,N,S)]}. *Inorg. Chem.* **2003**, *42*, 950-959.

In the tables below a summary was given of the mass spectrometry data (Table 16) and of the methods used for analytical HPLC Table 17).

Compounds	**$[M+H]^+$ calcd.**	**$[M+H]^+$ found**	**$[M+2H]^{2+}$**	**$[M+Na]^+$**
53	1381.58	1382.1	691.9	
54	1430.64	1432.41	717.0	

Table 16. Mass spectrometry data of the pure conjugated peptides.

Compounds	**HPLC method[a]**	**R_t (min)**
53	30%-100% in 20 min	12.55
54	40%-70% in 20 min	16.514

Table 17. RP-HPLC analytical data of the pure conjugated peptides.
[a] A: H_2O 0.1% TFA;B: CH_3CN 0.1% TFA.

4.2 NMR Analysis

Nuclear magnetic resonance is the most useful tool to carry out conformational studies of peptidic molecules in solution. Obtaining the structure of peptides is generally not easy, because they assume multiple flexible conformations in solution. Determination of the dominant conformers and evaluation of their populations is the aim of peptide conformation studies, in which theoretical and experimental methods play complementary roles. Numerous biological experiments strongly support the results of conformational investigations, clearly indicating that peptide activity is determined not only by the presence of functionally active groups that bind to a target protein but also depends dramatically on the conformational properties of the whole peptide.[134,135]

Many groups of researchers tried to understand the requirements for the binding to one of more sst receptors. Recently studies of Grace, Reubi and Rivier achieved to propose the consensus structure for sst_2 and sst_4.[136,137] The goal we tried to achieved, trough peptide conformations investigation, is to determine the relationship between conformation and activity of peptides synthesized in this work and propose finally a pharmacophore models.[91]

NMR analysis were performed using 1D and 2D proton homonuclear experiments at the Department of Pharmaceutical Chemistry and Toxicology, University of Napoli. NMR analysis of peptides **28**, **45**, **29 E** (*trans* geometric isomers) and **48** were recorded in water/DMSO-d_6 8:2 solution and in SDS solution for compounds **29 Z**, **30**, **31**, **32 E** and **32 Z**. All the analysis were performed at 2 mM (277.1 K) concentration on a Varian Inova-Unity 700 MHz spectrometer.

NMR derived constraints obtained for all the analyzed peptides were used as the input data for a simulated annealing structure calculation as implemented within the standard protocol of DYANA program.[138] NOEs were translated into interprotonic distances and used as upper limit constraints in subsequent annealing procedures to

[134] Williamson, M. P.; Waltho, J. P. Peptide Structure from NMR. *Chem. Soc. Rev.* **1992**, *21*, 227-236.
[135] Bierzyñski, A. Methods of peptides conformational studies. *Acta Biochimica Polonica*. **2001**, *48*, 191-1099.
[136] Grace, C. R. R.; Erchegyi, J.; Koerber, S. C.; Reubi, J. C.; Rivier, J. E.; Riek, R. Novel sst_2-Selective Somatostatin Agonists. Three-Dimensional Consensus Structure by NMR. *J. Med. Chem.* **2006**, *49*, 4487-4496.
[137] Grace, C. R. R.; Koerber, S. C.; Erchegyi, J.; Reubi, J. C.; Rivier, J. E.; Riek, R. Novel sst_4-Selective Somatostatin (SRIF) Agonists. 4. Three-Dimensional Consensus Structure by NMR. *J. Med. Chem*. **2003**, *46*, 5606-5618.
[138] Güntert, P.; Mumenthaler, C.; Wüthrich, K. Torsion Angle Dynamics for NMR Structure Calculation with the New Program DYANA. *J. Mol. Biol.* **1997**, *273*, 283-298.

produce 200 conformations from which 50 structures were chosen, whose interprotonic distances best fitted NOE derived distances, and then refined through successive steps of restrained and unrestrained energy minimization calculations using the program Discover (Biosym, San Diego). A family of 20 structures, satisfying the NMR derived constraints (violations smaller than 0.40 Å), was chosen for further analysis. The PROMOTIF program was used to extract details of the location and types of structural secondary motives.[139]

4.2.1 Water/DMSO NMR spectra

Solvent mixture water/DMSO-d_6 8:2 solution was chosen since it allowed a better dispersion of the amide proton signals of some of the studied peptides compared to the water solution.[91]

*4.2.1.1 NMR analysis of **28***

Compound **28** is the first dicarba-analog of octreotide, substituting disulphide bridge with a C-C double bond (Scheme 8). Almost complete ^{1}H chemical shift assignments were effectively achieved according to the Wüthrich procedure,[63] only HN-2 was not observable (Table 18).

Coupling constant value ($^3J_{CH=CH}$ = 8.1 Hz) between the two olefinic protons of the bridge and a relatively strong NOE between the same protons established the *Z* geometry about the double bond. No signal attributable to the *E* isomer could be detected in the spectra, indicating a unique configurational structure. Compound **28** showed spectral features with some tendency to the helical structure. For instance, its NOESY spectra showed, at the same time, both strong H_α-9/NH-10, H_α-10/NH-14, and H_α-14/NH-15 NOE contacts, consistent with a β-sheet structural cluster and $d_{\alpha N}$(i, i+2) diagnostic connectivities between H_α-8/NH-10, H_α-9/NH-14, and H_α-10/NH-15, characteristic of folded structures for the C-terminal residues. These data could be explained only hypothesizing an equilibrium between extended and folded conformational states, as already proposed for octreotide.[140]

[139] Hutchinson, E. G.; Thornton, J. M. PROMOTIF- A Program to Identify and Analyze Structural Motifs in Proteins. *Protein Sci.* **1996**, *5*, 212-220.
[140] Melacini, G.; Zhu, Q.; Goodman, M. Multiconformational NMR Analysis of Sandostatin (Octreotide): Equilibrium between β-Sheet and Partially Helical Structures. *Biochemistry* **1997**, *36*, 1233-1241.

Residue	NH ($^3J_{\alpha N}$, -$\Delta\delta/\Delta T$)[b]	$C^{\alpha}H$	$C^{\beta}H$ ($^3J_{\alpha\beta}$)	Others
D-Phe[2]		4.19	3.08, 3.18 (6.4-9.0)	7.24 (δ); 7.39 (ε)
dhDsa-N[c]	8.55 (7.6, 6.8)	4.15	2.29, 2.33 (overl.)[c]	5.06 (γ)
Phe[7]	8.44 (7.8, 6.1)	4.62	3.09, 2.91 (7.2-9.8)	7.24 (δ); 7.41 (ε)
D-Trp[8]	8.59 (4.4, 6.5)	4.16	2.98, 2.76 (7.7–9.4)	7.11(δ); 10.37, 7.53(ε); 7.48, 7.23(ζ); 7.30(η)
Lys[9]	8.60 (4.3, 3.7)	4.05	1.55, 1.15 (11.5-5.6)	0.46, 0.24 (δ); 1.28 (ε); 2.55 (ε)
Thr[10]	8.19 (5.6, 2.8)	3.99	4.25 (5.4)	1.28 (γ)
dhDsa-C[c]	8.10 (7.1, 5.8)	4.44	2.48, 2.25 (7.3-9.7)	5.44 (γ)
Thr(ol)[15]	7.35 (6.8, 5.4)	3.80	3.91 (5.9)	1.12 (γ); 3.66, 3.58 (ω)

*Table 18. NMR Data[a] of Peptide **28** in Water/DMSO 8:2 solution.*
[a] Obtained at 277.1 K, with TSP (δ 0.00 ppm) as reference shift. Chemical shifts are accurate to ±0.02 resonances. [b] $^3J_{\alpha N}$ and $^3J_{\alpha\beta}$ coupling constants are in Hz. -Δδ/ΔT = temperature coefficients (ppb/K). [c] Overlapped signals.

Notably, calculated structures (Figure 25) are characterized by an antiparallel *β*-platelet sheet with a type II' *β*-turn at residues D-Trp[8]/Lys[9], but several violations (NH-10/NH-14, H_{α}-10/NH-15, and NH-14/NH-15, H_{β}-14/NH-15) were observed consistently with the hypothesized *β*-sheet/helical equilibrium. The analysis of the secondary structure showed the existence of a distorted *β*II'-type turn conformation about residues Phe[7]-D-Trp[8]-Lys[9]-Thr[10]. This well-conserved region is stabilized by a hydrogen bond between Phe[7] CO and Thr[10] HN.

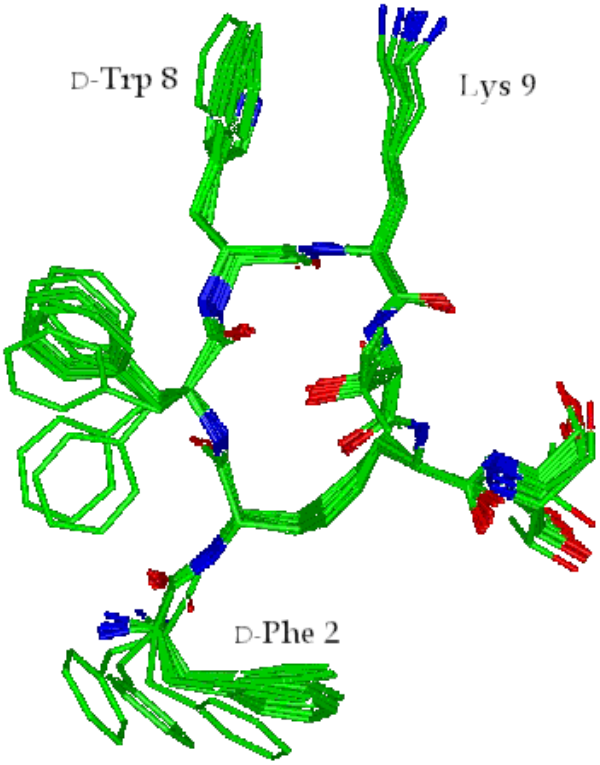

*Figure 25. Superposition of the 10 lowest energy conformers of **28**. Structures were superimposed using the backbone heavy atoms of residues 3-14. Heavy atoms are shown with different colours (carbon, green; nitrogen, blue; oxygen, red). Hydrogen atoms are not shown for clarity.*

Figure 26 shows the superposition of the structure of **28** with that of octreotide (Protein Data Bank entry 1SOC). It can be observed the almost perfect overlapping of the backbone heavy atoms of the turn region.

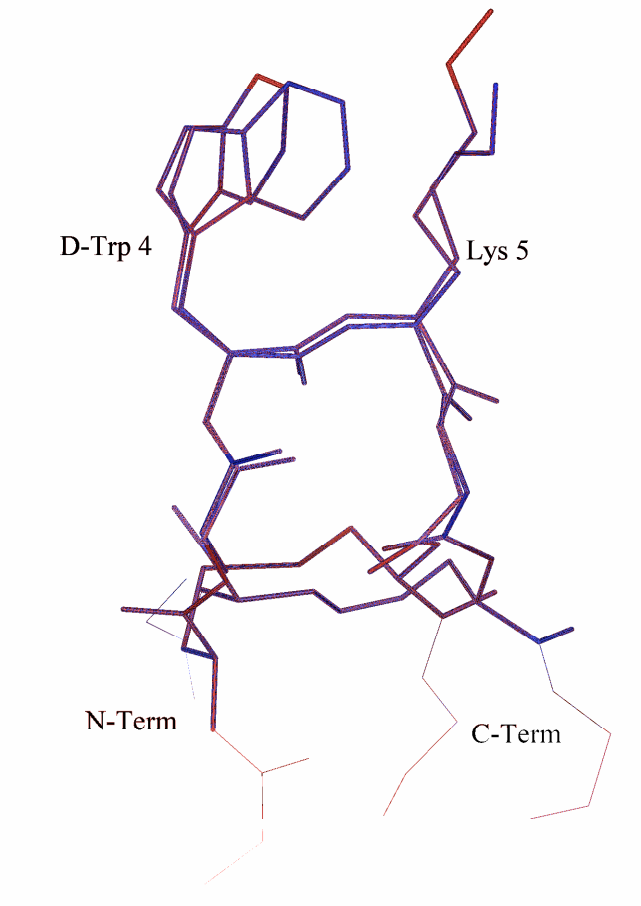

*Figure 26. Superposition of the most representative structure of **28** (blue) with octreotide structure (PDB entry 1SOC, red). Structures were superimposed using the backbone heavy atoms of residues 3-14. Hydrogen atoms are not shown for clarity.*

*4.2.1.2 NMR analysis of **45***

Compound **45** is a carbocyclic analogue of octreotide with the disulfide group replaced by a CH_2–CH_2 bridge derived from the unsaturated parent compound **28** (Scheme 11). A qualitative analysis of short and medium-range NOEs, $^3J_{NH\text{-}H\alpha}$ coupling constants, and temperature coefficients for exchanging NH was used to characterize the secondary structure of **45** (Table 19). Spectra analysis supported the presence of a β-turn about residues 3-6. Interestingly, the up-field shift observed for H_γ's of Lys^9 (δ = 0.51, and δ =0.30 ppm) has been used for decades as diagnostic for biological activity.[141,142]

[141] Arison, B. H.; Hirschmann, R.; Veber, D. F. Inferences About the Conformation of Somatostatin at a Biologic Receptor Based on NMR Studies. *Bioorg. Chem.* **1978**, *7*, 447-451.
[142] Wynants, C.; Van Blist, G.; Loosli, H. R. SMS 201-995, an Octapeptide Somatostatin Analogue. *Int. J. Pept. Prot. Res.* **1985**, *25,* 615-621.

Residue	NH ($^3J_{\alpha N}$, -$\Delta\delta/\Delta T$)[b]	$C^{\alpha}H$	$C^{\beta}H$ ($^3J_{\alpha\beta}$)	Others
D-Phe[2]		4.17	3.07, 3.23 (6.8–9.8)	7.26(δ); 7.40(ε); 7.37 (ζ)
Dsa-N[c]	8.51 (7.9, 6.9)	4.08	1.44, 1.40 (overl.)[c]	0.79, 0.94 (γ)
Phe[7]	8.44 (8.2, 6.2)	4.60	3.10, 2.92 (6.0–9.8)	7.25(δ); 7.42(ε)
D-Trp[8]	8.53 (4.5 6.5)	4.11	3.00, 2.79 (11.1–5.5)	7.11(δ); 10.37, 7.50 (ε); 7.49, 7.19(ζ); 7.25(η)
Lys[9]	8.53 (4.4, 3.7)	4.08	1.57, 1.17 (4.5-11.0)	0.51, 0.30(γ); 1.32 (δ); 2.67, 2.59 (ε)
Thr[10]	8.17 (7.8, 2.6)	4.07	4.30 (5.7)	1.33, 5.92 (γ)
Dsa-C[c]	7.98 (8.1, 7.3)	4.38	1.93, 1.37 (6.8–8.8)	1.08, 1.34 (γ)
Thr(ol)[15]	7.38 (8.8, 6.9)	3.82	3.95 (5.7)	1.12 (γ); 3.70, 3.60 (ω)

*Table 19. NMR Data[a] of Peptide **45** in Water/DMSO 8:2 solution.*
[a] Obtained at 277.1 K, with TSP (δ 0.00 ppm) as reference shift. Chemical shifts are accurate to ±0.02 resonances. [b] $^3J_{\alpha N}$ and $^3J_{\alpha\beta}$ coupling constants are in Hz. -Δδ/ΔT = temperature coefficients (ppb/K). [c] Overlapped signals.

Surprisingly, hydroxyl proton signal of Thr[10], which usually exchanges too quickly to be observed in water solution, was detected in the NMR spectra of **45**. This feature indicates that it can be engaged in a H-bond. Backbone arrangement of **45** was well defined, possessing an average root mean square deviation (RMSD) of the heavy atoms equal to 0.32 Å(Figure 27). The analysis of the secondary structure showed the existence of a distorted type II' β-turn conformation about residues Phe[7]–D-Trp[8]–Lys[9]–Thr[10]. The turn structure is stabilized by hydrogen bonds between Phe[7] CO and Thr[10] NH, and between Phe[7] CO and Thr[10] OH.

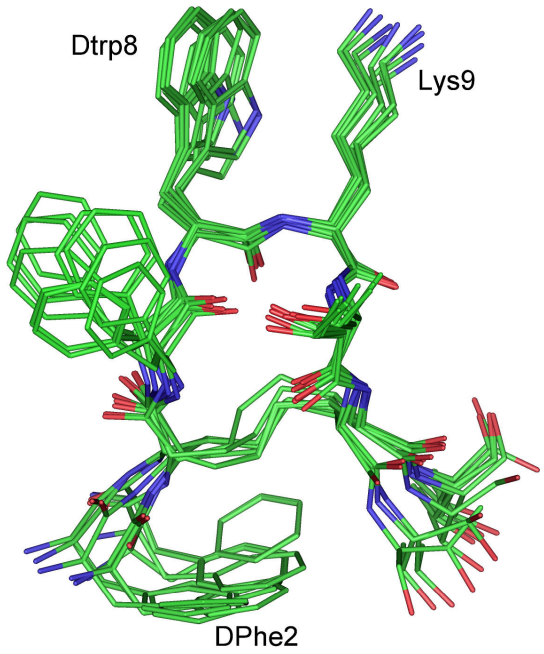

*Figure 27. Superposition of the 10 lowest energy conformers of **45**.*
Structures were superimposed using the backbone heavy atoms of residues 3-14. Heavy atoms are shown with different colours (carbon, green; nitrogen, blue; oxygen, red). Hydrogen atoms are not shown for clarity.

The turn is flanked by two short extended regions defining an antiparallel β-sheet. Also, the side chain have defined orientations (RMSD of all the heavy atoms equal to 0.88 Å). These orientations allowed a close spatial proximity between D-Phe^{2}–Dsa-N^{3}, Phe^{7}–Thr^{10}, and D-Trp^{8}–Lys^{9} side chains. Finally, the sequential Thr^{10} NH–Dsa-C^{14} NH and Dsa-C^{14} NH–Thr(ol)^{15} NH NOEs indicative of folded structures are consistently violated by the β-sheet conformations (violations of about 0.30 Å). Melacini et al. found similar inconsistencies studying octreotide in DMSO solution.[140] The authors hypothesized the existence of a conformational equilibrium between the β-sheet structural cluster and a second conformational ensemble involving folded structures for the C-terminal residues where the inconsistencies were observed. Therefore, a similar equilibrium should hold also for **45**. Superposition of the structure of **45** with that of octreotide showed very similar structures in the active region (Figure 28). In contrast, the structure of the N-terminal D-Phe^{2} and C-terminal Thr(ol)^{15} residues are significantly different in the two peptides.

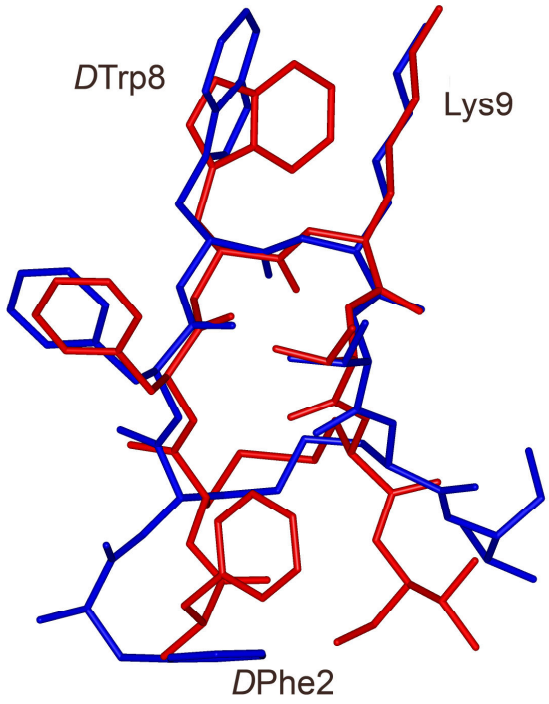

*Figure 28. Superposition of the most representative structure of **45** (blue) with octreotide structure (PDB entry 1SOC, red). Structures were superimposed using the backbone heavy atoms of residues 3-14. Hydrogen atoms are not shown for clarity.*

*4.2.1.3 NMR analysis of **29E***

Compound **29 E** is an unsaturated analogs with Tyr(Bzl)[10] (Scheme 8). Coupling constant value ($^3J_{CH=CH}$ = 15.1 Hz) between the two olefinic protons of the bridge and NOE contacts between the same olefinic H_γ of residue 3 (14) and H_β's of residue 14 (3) established the *E* geometry about the double bond. No signal attributable to the *Z* isomer could be detected in the spectra, indicating a unique configurational structure. 3D structures of **29 E** were calculated as described above. The quality of the structure was reflected by the small RMSD (backbone heavy atoms RMSD = 0.40 Å), which can also be visually depicted from Figure 29 showing the bundle of 10 conformers representing the 3D structure. A *β*-turn about residues D-Trp[8]-Lys[9] followed by a short 3_{10}-helix along residues Tyr(Bzl)[10]- Dsa-C14-Thr(ol)[15] were the main backbone features. An overall enhancement of the backbone conformational rigidity is observed for **29 E** (backbone RMSD = 0.40 Å vs 0.48 Å).

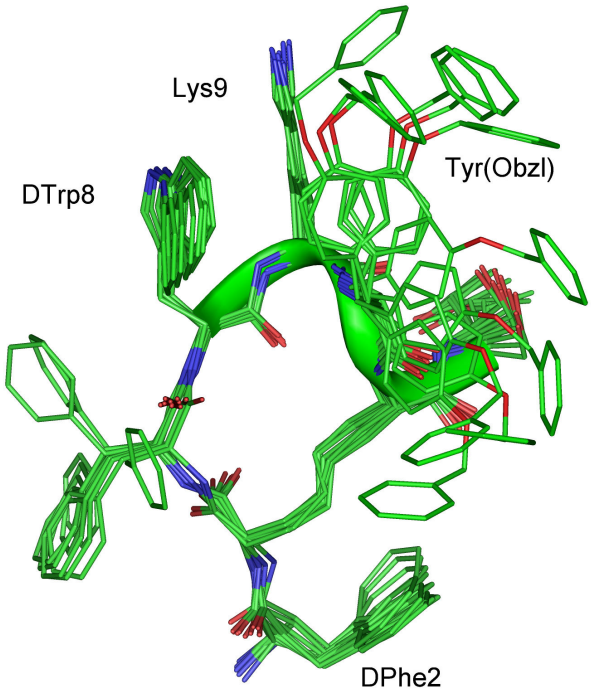

*Figure 29. Superposition of the 10 lowest energy conformers of **29 E**.*
Structures were superimposed using the backbone heavy atoms of residues 3-14. Heavy atoms are shown with different colours (carbon, green; nitrogen, blue; oxygen, red). Hydrogen atoms are not shown for clarity.

Reduced entities of the NOE violations for the proton couples Hα-9/NH-10, Hα-10/NH-14, and Hα-14/NH-15 (about 0.3 Å), and lower values of the temperature coefficients observed for NH-14 and NH-15 (Table 20), indicated that the conformational equilibrium between the extended and the helical structures was shifted towards the helical conformation in **29 E**.

Residue	NH ($^3J_{\alpha N}$, -$\Delta\delta/\Delta T$)[b]	$C^{\alpha}H$	$C^{\beta}H$ ($^3J_{\alpha\beta}$)	Others
D-Phe[2]		4.21	3.07, 3.19 (6.5-10.3)	7.24(δ); 7.40 (ε)
dhDsa-N[c]	8.36 (7.6, 6.7)	4.11	2.10, 2.22 (5.6-5.5)	4.95 (γ)
Phe[7]	8.26 (7.7, 6.6)	4.66	3.05, 2.92 (5.9-10.9)	7.16 (δ); 7.38 (ε)
D-Trp[8]	8.22 (4.5, 6.5)	4.13	2.92, 2.84 (10.6-6.4)	7.06(δ); 10.39, 7.46(ε); 7.45, 7.15(ζ); 7.23(η)
Lys[9]	8.29 (4.2, 3.7)	3.88	1.41, 1.10 (5.8-10.8)	0.49, 0.34 (γ); 1.30 (δ); 2.63 (ε)
Tyr(Bzl)[10]	8.15 (4.4, 2.8)	4.25	3.05 (overl.)[c]	7.17(δ); 7.01(ε); 7.48, 7.17, 7.01 (ω)
dhDsa-C[c]	7.37 (4.6, 3.0)	4.36	2.51, 2.24 (5.5-11.4)	5.32 (γ)
Thr(ol)[15]	7.43 (4.9, 3.4)	3.81	3.97 (5.6)	1.18 (γ); 3.68, 3.62 (ω)

*Table 20. NMR Data[a] of Peptide **29 E** in Water/DMSO 8:2 solution.*
[a] Obtained at 277.1 K, with TSP (δ 0.00 ppm) as reference shift. Chemical shifts are accurate to ±0.02 resonances. [b] $^3J_{\alpha N}$ and $^3J_{\alpha\beta}$ coupling constants are in Hz. -$\Delta\delta/\Delta T$ = temperature coefficients (ppb/K). [c] Overlapped signals.

Finally, also the side chain orientations of **29 E** of Tyr(Bzl)[10] was very flexible showing an equilibrium between *trans* and *gauche*$^-$ orientations.

*4.2.1.4 NMR analysis of **48***

In compound **48**, as in **45**, the disulfide group of octreotide was replaced by a CH_2–CH_2 bridge.[91] Compound **48** differs from **45** since Thr[10] residue is replaced by the Tyr(Bzl)[10] residue. Similar substitution into a cyclohexapeptide somatostatin mimic led

to the discovery of a potent sst_{1-5} ligand.[54] NMR data clearly indicated the presence of a nascent helix, or consecutive β-turn structures along residues 8-15. NMR derived constraints obtained for **48** were used as the input data for a simulated annealing structure calculation as described above.

Residue	NH ($^3J_{\alpha N}$, -$\Delta\delta/\Delta T$)[b]	$C^{\alpha}H$	$C^{\beta}H$ ($^3J_{\alpha\beta}$)	Others
D-Phe[2]		4.15	3.06, 3.22 (6.4-10.5)	7.24 (δ); 7.39 (ε); 7.35 (ζ)
Dsa-N[c]	8.46 (7.6, 6.7)	4.09	1.42, 1.34 (5.4-5.6)	0.95, 0.84 (γ)
Phe[7]	8.43 (7.7, 6.6)	4.70	2.96 (overl.)[c]	7.13 (δ); 7.30 (ε)
D-Trp[8]	8.32 (4.7, 6.5)	4.20	2.98, 2.84 (10.5-6.6)	7.10(δ); 10.34, 7.51(ε); 7.47, 7.15(ζ); 7.24(η)
Lys[9]	8.02 (4.2, 3.8)	3.84	1.22, 0.98 (6.0-10.7)	0.46, 0.35(γ); 2.11(δ); 2.65(ε)
Tyr(Bzl)[10]	8.13 (4.6, 3.1)	4.38	3.10, 3.02 (5.2-10.9)	7.17(δ); 6.98(ε); 7.48, 7.17, 6.97(ω)
Dsa-C[c]	7.81 (4.8, 3.4)	4.31	1.77, 1.45 (5.7-10.8)	1.18, 1.10 (γ)
Thr(ol)[15]	7.54 (5.2, 3.9)	3.81	3.97 (5.8)	1.11(γ); 3.69, 3.57 (ω)

*Table 21. NMR Data of Peptide **48** in Water/DMSO 8:2 solution.*
[a] Obtained at 277.1 K, with TSP (δ 0.00 ppm) as reference shift. Chemical shifts are accurate to ±0.02 resonances. [b] $^3J_{\alpha N}$ and $^3J_{\alpha\beta}$ coupling constants are in Hz. -$\Delta\delta/\Delta T$ = temperature coefficients (ppb/K). [c] Overlapped signals.

The quality of the structure was reflected by the small RMSD (backbone heavy atoms RMSD = 0.48 Å), which can also be visually depicted from Figure 30 showing the bundle of 10 conformers representing the 3D structure.

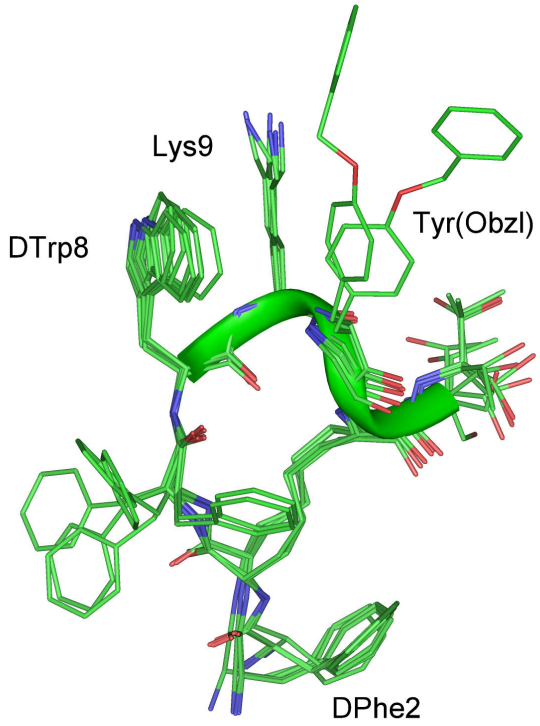

*Figure 30. Superpositionof the 10 lowest energy conformers of **48**.*
Structures were superimposed using the backbone heavy atoms of residues 3-14. Heavy atoms are shown with different colours (carbon, green; nitrogen, blue; oxygen, red). Hydrogen atoms are not shown for clarity.

From the backbone torsion angles a distorted type II' β-turn about residues D-Trp^{8}-Lys^{9} followed by a short 3_{10}-helix along residues Tyr(Bzl)^{10}-Dsa-C^{14}-Thr(ol)^{15} could be identified (Figure 30). The helical structure was stabilized by H-bonds between D-Trp^{8} CO and Dsa-C^{14} NH and between Lys^{9} CO and Thr(ol)^{15} NH. Helical structure is in conformational equilibrium with more extended conformations. In fact, violations of the NOE derived distances H_{α}-9/NH-10, H_{α}-10/NH-14, and H_{α}-14/NH-15 (about 0.5 Å), together with relatively high temperature coefficients observed for NH-10, NH-14 and NH-15 ($-\Delta\delta/\Delta T$ > 3.0 ppb/K) indicated that the helical structure was quite flexible. Finally, side chains of D-Phe^{2}, Dsa-N^{3}, D-Trp^{8}, Lys^{9}, Tyr(Bzl)^{10}, and Dsa-C^{14} showed well defined χ_1 values (i.e. *trans*, *gauche*$^{+}$, *trans*, *gauche*$^{-}$, *gauche*$^{-}$, and *gauche*$^{-}$ orientations, respectively). χ_1 values obtained by MD calculations were in accordance with the experimental $^{3}J_{H\alpha H\beta}$ coupling constants (Table 21). These orientations allowed a

close spatial proximity between D-Phe^2/Dsa-N^3, and D-Trp^8/Lys^9 side chains; moreover, tyrosyl group of the residue 10 pointed towards Lys^9 side-chain. In contrast, Phe^7 side chain showed almost free rotation about χ_1 angle. Also, the benzyl group of residue 10 was highly flexible.

4.2.2 SDS NMR spectra

Later we decided to perform NMR analysis in SDS micelles solution. The use of SDS micelles to study the conformational properties of hU-II analogues was motivated on the basis of their interaction with a membrane receptor. For peptides acting as ligands of membrane receptors (such as GPCR), the use of membrane mimetic media was suggested, hypothesizing a membrane-assisted mechanism of interactions between the peptides and their receptors. According to this model, the membrane surface plays a key role in facilitating the transition of the peptide from a random coil conformation adopted in the extracellular environment to a conformation that is recognized by the receptor. The increase of the local concentration of the peptide and the reduction of the rotational and translational freedom of the neuropeptide are membrane-mediated events acting as determinant steps for the conformational transition of the peptide. Actually SDS NMR analysis are still in progress. Here below we report just preliminary conclusions.

*4.2.2.1 NMR analysis of **29 E***

We have already analyzed **29 E** in water/DMSO mixture.[91] The geometry of the double bond was confirmed as *trans* (*E*) from the coupling constant ($^3J_{CH=CH}$ = 15.1 Hz) between the two olefinic protons of the bridge and NOE contacts between the same olefinic and the Hβs of residue 14 (3). Spectra analysis supported the presence of a β-turn about residues 3–6. Interestingly, the upfield shift observed for Hγs of Lys^9 (δ = 0.52, 0.43 ppm) (Table 22) has been used for decades as diagnostic for biological activity.[40,41] Backbone arrangement of **29 E** was well-defined, possessing an average root mean square deviation (rmsd) of the heavy atoms equal to 0.15 Å. Main backbone features were a type II' β-turn about residues D-Trp^8-Lys^9, followed by a short 3_{10}-helix along residues Tyr(Bzl)^{10}-dhDsa-C^{14}-Thr(ol)^{15}. The helical structure is stabilized by H-bonds between D-Trp^8 CO and dhDsa-C^{14} NH and between Lys^9 CO and Thr(ol)^{15} NH. These bonds are typical of 3_{10}-helix structure (i, i+3). The analysis of the backbone

dihedral angles showed the existence of a distorted type II' β-turn conformation about residues Phe[7]-D-Trp[8]-Lys[9]-Tyr(Bzl)[10].

Residue	$C^{\alpha}H$	$C^{\beta}H$	Others
D-Phe[2]	4.225	3.097; 3.228	7.263(δ) 7.309(ε)
dhDsa-N[c]	3.812	2.224	5.159(γ)
Phe[7]	4.744	2.977	7.027(δ); 7.161(ε)
D-Trp[8]	4.381	3.087, 3.210	7.205(δ); 7.678, 10.053(ε); 7.138, 7.491(ζ); 7.138(η)
Lys[9]	4.086	1.254, 1.435	0.426, 0.523(γ); 1.385(δ); 2.755(ε)
Tyr(Bzl)[10]	4.252	2.874, 3.126	7.086(δ); 6.894(ε);
dhDsa-C[c]	4.387	2.231, 2.515	5.269 (δ)
Thr(ol)[15]	3.798	3.945	1.147 (γ);

*Table 22. NMR Data of Peptide **29 E** in SDS solution.*
Obtained at 277.1 K, with TSP (δ 0.00 ppm) as reference shift. Chemical shifts are accurate to ±0.02 resonances.

The turn structure was stabilized by hydrogen bonds between Phe[7] CO and Thr[10] NH. Finally, side chains of dhDsa-N[3], D-Trp[8], Lys[9], Tyr(Bzl)[10], and dhDsa-C[14] showed well-defined χ1 values (i.e., *trans*, *trans*, *gauche*-, *gauche*-, and *gauche*+ orientations, respectively). These orientations allowed a close spatial proximity between D-Trp[8]/Lys[9] side chains; moreover, the tyrosyl group of the residue 10 points toward the Lys[9] side chain. In contrast, D-Phe[2] and Phe[7] side chain showed almost free rotation about χ1 angle. Also, the Bzl group of residue 10 was highly flexible.

Finally, the sequential dhDsa-C[14] H_{α}-Thr(ol)[15] NH NOEs, indicative of folded structures, is consistently violated by the helical conformations (violations of about 0.30 Å) indicating conformational equilibrium at the C-terminus.

*4.2.2.2 NMR analysis of **29 Z***

The analogue **29 Z** is the geometric (*Z*) isomer of **29 E** as established by the coupling constant ($^3J_{CH=CH}$ = 8.1 Hz) between the two olefinic protons of the bridge and the relative strong NOE between the same olefinic Hγs. This analogue showed spectral features similar to those found in **29 E** (Table 23) but with some higher tendency to an equilibrium between two families of structures: the impossibility of resume all the data in a unique structure suggested us to propose two conformational families.

It's noteworthy that the NMR data of the cognate molecule octreotide, using a single average conformation, revealed several important inconsistencies including severe violations of mutually exclusive backbone-to-backbone NOE's.[140]

The first family obtained by a first run of MD calculation had similar conformation to compound **29 E**, with a type II' *β*-turn about residues D-Trp^8-Lys^9, followed by a short 3_{10}-helix along residues Tyr(Bzl)^{10}-dhDsa-C^{14}-Thr(ol)^{15}.

For these structure a number of consistent violations were observed. In a second MD run, these violated upper limit constraints were upweighted for the contribution to the target function (Experimental Section). Hence, we obtained a second conformational family which differed from the first mainly because C-terminal residues were in extended conformation. Furthermore, side chain orientation of Tyr(Bzl)^{10} was *trans*. Hence, Benzyl nucleus was farer from the Lys^9 side chain. This is in accordance with the down-field shift of the Hγ's resonances of Lys^9 (δ = 0.68, 0.64 ppm) compared to the corresponding observed for compound **29 E**.

Residue	$C^{\alpha}H$	$C^{\beta}H$	Others
D-Phe[2]	4.214	3.081; 3.288	7.253(δ) 7.316(ε)
dhDsa-N[c]	3.792	2.129, 2.320	5.113(γ)
Phe[7]	4.731	2.898, 2.945	6.835(δ); 7.015(ε)
D-Trp[8]	4.611	3.044, 3.335	7.278(δ); 7.838, 10.027(ε); 7.163, 7.504(ζ); 7.146(η)
Lys[9]	4.071	1.367, 1.505	0.632, 0.677(γ); 1.452(δ); 2.823(ε); 7.368(ζ)
Tyr(Bzl)[10]	4.414	2.964, 3.087	7.145(δ); 6.891(ε);
dhDsa-C[c]	4.268	2.116, 2.443	5.197(δ)
Thr(ol)[15]	3.838	3.946	1.137(γ);

*Table 23. NMR Data of Peptide **29 Z** in SDS solution.*
Obtained at 277.1 K, with TSP (δ 0.00 ppm) as reference shift. Chemical shifts are accurate to ±0.02 resonances.

*4.2.2.3 NMR analysis of **30***

Compound **30** maintains the same octreotide scaffold, but position 7, which bears 1-L-Nal. The coupling constant ($^3J_{CH=CH}$ = 8.1 Hz) between the two olefinic protons of the bridge and the relative strong NOE between the same olefinic Hγs established (Z) configuration (Table 24). NMR-based structure calculation gave two conformational families, as for compound **29 Z**. The first family obtained by a first run of MD calculation showed a type II' *β*-turn about residues D-Trp[8]-Lys[9], followed by a short 3_{10}-helix along residues Thr[10]-dhDsa-C[14]-Thr(ol)[15]. Compared to the structures of the analogues **29 E** and **29 Z**, residue 7 showed a well defined trans orientation which forces naphthyl[7] moiety close to D-Trp[8] residue.

Residue	$C^{\alpha}H$	$C^{\beta}H$	Others
D-Phe[2]	4.243	3.137, 3.239	7.305 (δ)
dhDsa-N[c]	4.227	2.289, 2.449	5.286 (γ)
1-Nal[7]	4.732	3.418, 3.542	7.689(ζ) 7.424, 8.176(δ); 7.450 (ε)
D-Trp[8]	4.040	2.280, 2.592	6.881 (δ); 7.073, 9.860(ε); 6.976, 7.428(ζ); 7.109(η)
Lys[9]	3.881	1.251, 1.498	0.324, 0.581(γ); 1.328(δ); 2.651, 2.687(ε); 7.237(ζ)
Thr[10]	4.035	4.217	1.250(γ)
dhDsa-C[c]	4.364	2.217, 2.410	5.391 (δ)
Thr(ol)[15]	3.770	3.825	1.052 (γ);

*Table 24. NMR Data of Peptide **30** in SDS solution. Obtained at 277.1 K, with TSP (δ 0.00 ppm) as reference shift. Chemical shifts are accurate to ±0.02 resonances.*

This orientation was in accordance with the intense up-field shift observed for many D-Trp[8] proton resonances. As for compound **29 Z**, a number of consistent violations were observed. In a second MD run, we obtained a second conformational family which differed from the first mainly because C-terminal residues were in extended conformations.

*4.2.2.4 NMR analysis of **31***

The analogue **31** was rationalized starting from the previous compounds **29 Z** and **30**; in fact it bears 1-Nal[7] and (Bzl)Tyr[10]. For compound **31** a (Z) configuration was established from NOE's and coupling constant ($^3J_{CH=CH}$ = 8.1 Hz) between the two

olefinic protons (Table 25). NMR-based structure calculation gave two conformational families, as for compounds **29 Z**, showing a short 3_{10}-helix along residues Thr[10]-dhDsa-C[14]-Thr(ol)[15] and **30**, bearing an extended conformation along the same residues. In both families, D-Trp[8], Lys[9] and Tyr(Bzl)[10] side chain were spatially close and this was in accordance with the increased up-field shift of the H_γ and H_β resonances of Lys[9]. Differently from compound **30**, Nal[7] residue could not adopt a *trans* conformation, due to steric hindrance with Tyr(Bzl)[10]. In fact, Nal[7] side chain was preferentially in a *gauche*- conformation.

Residue	$C^\alpha H$	$C^\beta H$	Others
D-Phe[2]	4.256	3.171, 3.297	7.308(δ); 7.373(ε)
dhDsa-N[c]	4.198	2.335	5.187(γ)
1-Nal[7]	4.928	3.526, 3.640	7.670(ζ) 7.310, 8.222(δ); 7.795 (ε)
D-Trp[8]	4.103	2.716, 3.034	7.116(δ); 7.462, 10.004(ε); 7.150, 7.509(ζ); 7.144(η)
Lys[9]	4.000	0.931, 1.293	0.077, 0.223(γ); 1.270(δ); 2.693, (ε);
Tyr(Bzl)[10]	4.433	2.911, 3.061	7.087(δ); 6.870 (ε);
dhDsa-C[c]	4.435	2.349,2.455	5.366 (δ)
Thr(ol)[15]	3.849	3.968	1.147 (γ);

*Table 25. NMR Dat[a] of Peptide **31** in SDS solution.*
Obtained at 277.1 K, with TSP (δ 0.00 ppm) as reference shift. Chemical shifts are accurate to ±0.02 resonances.

*4.2.2.5 NMR analysis of **32 E***

The analogue **32 E** differ from compound **29** (**E** and **Z**), **30** and **31** since Tyr(Bzl)[10] residue is replaced by a Tyr. Following the same arguments as for **29**, an E configuration was assigned to compound **32 E** (Table 26).

Many potential diagnostic NOE's could not be observed in the NOESY spectra of this analogue due to signal overlapping and this precluded structure calculations. For instance, Hα of residues 5 and 8 resonated at the same chemical shift for both peptides. Actually, NMR parameters of **32 E** (Hα shifts, coupling constants, and temperature coefficients) are very similar to those of compound **29 E**. Therefore, it could be hypothesized that its 3D structures should be similar as well.

Residue	$C^{\alpha}H$	$C^{\beta}H$	Others
D-Phe[2]	4.213	3.070,3.235	7.261(δ); 7.314(ε)
dhDsa-N[c]	3.959	2.183	5.212(γ)
Phe[7]	4.667	2.920	6.983(δ); 7.157(ε)
D-Trp[8]	4.430	2.974, 3.066	7.111(δ); 7.579, 10.013(ε); 7.082, 7.440(ζ); 7.147(η)
Lys[9]	3.954	1.244, 1.305	0.365, 0.537(γ); 1.341(δ); 2.714(ε); 7.305(ζ)
Tyr[10]	4.220	2.856,3.037	6.770(ε); 7.027(γ)
dhDsa-C[c]	4.314	2.297, 2.488	5.326 (δ)
Thr(ol)[15]	3.785	3.942	1.139 (γ);

*Table 26. NMR Data of Peptide **32 E** in SDS solution.*
Obtained at 277.1 K, with TSP (δ 0.00 ppm) as reference shift. Chemical shifts are accurate to ±0.02 resonances.

*4.2.2.6 NMR analysis of **32 Z***

For compound **32 Z** we can follow the same arguments as for **29 Z** and the same conclusion as for compound **32 E** (Table 27). NMR parameters of **32 Z** (Hα shifts, coupling constants, and temperature coefficients) are very similar to those of compound **29 Z**. Therefore, it could be hypothesized that 3D structures should be similar as well.

Residue	$C^{\alpha}H$	$C^{\beta}H$	Others
D-Phe[2]	4.231	3.097, 3.292	7.278(δ); 7.337(ε)
dhDsa-N[c]	3.798	2.107, 2.420	5.291(γ)
Phe[7]	4.732	2.764, 2.893	6.672(δ); 7.033(ζ) 6.951(ε)
D-Trp[8]	4.735	3.002, 3.335	7.292 (δ); 7.888, 9.985(ε); 7.176, 7.448(ζ); 7.211(η)
Lys[9]	3.938	1.409	0.611, 0.744(γ); 1.458(δ); 2.812(ε); 7.333(ζ)
Tyr[10]	4.409	2.880, 3.139	7.118(δ); 6.789(ε)
dhDsa-C[c]	4.286	1.926, 2.490	5.432(δ)
Thr(ol)[15]	3.828	3.959	1.151(γ);

*Table 27. NMR Data of Peptide **32 Z** in SDS solution.*
Obtained at 277.1 K, with TSP (δ 0.00 ppm) as reference shift. Chemical shifts are accurate to ±0.02 resonances.

4.3 Molecular Modeling

The use of structure-based design to transform an amino acid epitope in to a non-peptide lead compound remains one of the fundamental challenges of modern medicinal chemistry. In principle, combining the functional information obtained by protein mutagenesis or peptide synthesis with the structural information obtained by NMR, crystallography and molecular modeling should enable the *de novo* design of biologically active compounds with improved bioavailability. This Approach requires as a first step the elucidation of a bioactive conformation of potent ligands.

Because it is often impossible to directly determine the bound state conformations of biologically active peptides, conformational analysis procedure are frequently used to map energetically accessible conformations of flexible molecules interacting with a common site. Given a collection of such molecules, the primary goal of these procedures is to identify consensus conformations that present a common spatial arrangement of shared binding determinants.

In this PhD thesis we describe a complimentary exploration of peptide molecules, in particular SRIF analogues, using molecular dynamics studies to identify consensus conformations of bioactive cyclic peptides.

4.3.1 Peptide library realization

Peptides collection was featured of active peptides that were found in literature [56,143,144,145,146,147] and synthesized in our laboratory both.[91] Selection of an *ensemble* of peptide SRIF analogues necessitate of a family of molecule that were characterized by the same binding assay. We, in fact, come out a new algorithm able to correlate the

[143] Hocart Simon J.; Reddy Vik; Murphy William A.; Coy David H. Three-Dimensional Quantitative Structure-Activity Relationships of Somatostatin Analogues. 1. Comparative Molecular Field Analysis of Growth Hormone Release-Inhibiting Potencies. *J. Med. Chem.* **1996**, *38*, 1974-1989.
[144] Simona Golic Grdadolnik; Dale F. Mierke; Gerard Byk; Irena Zeltser; Chaim Gilon; Horst Kessler. Comparison of the Conformation of Active and Nonactive Backbone Cyclic Analogsof Substance P as a Tool To Elucidate Features of the Bioactive Conformation:NMR and Molecular Dynamics in DMSO and Water. *J. Med. Chem.* **1994**,*37,* 2145-2152.
[145] Jean Rivier; Judit Erchegyi; Carl Hoeger; Charleen Miller; William Low; Sandra Wenger; Beatrice Waser; Jean-Claude Schaer; Jean Claude Reubi. Novel sst4-Selective Somatostatin (SRIF) Agonists. 1. Lead Identification Using a Betide Scan. *J. Med. Chem.* **2003**, *46,* 5579-5586.
[146] Judit Erchegyi; Christy Rani R. Grace; Manoj Samant; Renzo Cescato; Veronique Piccand; Roland Riek; Jean Claude Reubi; Jean E. Rivier. Ring Size of Somatostatin Analogues (ODT-8)Modulates Receptor Selectivity and Binding Affinity. *J. Med. Chem.* **2008**, *51,* 2668–2675.
[147] Jean Claude Reubi; Jean-Claude Schaer; Sandra Wenger; Carl Hoeger; Judit Erchegyi; Beatrice Waser; Jean Rivier. SST_3-selective potent peptidic somatostatin receptor antagonists. *Proc. Nat. Am. Sci* **2000**, *97*, 25, 13973–13978.

affinity of all proposed peptides with their structure. The selection of all required structures followed the scheme below:

- A relevant number of SRIF analogues were chosen with different activity and selectivity among sst receptors. An overall of 37 peptides were employed.
- All compounds were assayed by the same binding test (see paragraph 4.4.2).[167]
- Binding affinity values were expressed in IC_{50}.
- All the molecules were designed using the Octreotide scaffold (PDB entry 1 SOC).
- The designed structures were minimized by the conjugated gradient algorithm.
- All the 37 minimized structures were subjected to a simulated annealing analysis by the module Discover of the INSIGHT II program. For each compound 100 conformations were collected.

4.3.2 PPS: the algorithm

This method was developed as part of a strategy in which peptide analogues were used to explore potential bioactive conformation(s) of the SRIF analogues sequence. This sequence is critical recognition feature and hence, in order to obtain other information, the modeling approach was employed. The previous 100 conformations, obtained from simulated annealing, were clustered by an RMS value. Those which posses a RMS value lower than 1.5 Å were ranked together. RMS value was employed as a measure of the similarity, among the overall structures, of the distance from a pharmacophore reference.

The Pharmacophore reference was constructed using the algorithm Parmacophore Posistion System (PPS), from Professor Melani, Pharmaceutical Science Department, Florence University.[148] PPS was employed to statistically correlate the binding affinity of all the listed peptides and their structures, on the base of a similarity trough the position of the pharmacophore areas (aromatic, lypophilic area, H donor, H acceptor were used) involved in the biological activity. Here below we list the procedure behind the PPS algorithm:

[148] F. Melani. Personal communication. **2008**

- 6 reference points were chosen and described as Cartesian coordinate on the backbone of the molecules (Cα backbone).
- Each ensemble of 100 minimized conformations for each compound was subjected to an iterative procedure and the final selected structures were ranked by an RMS value (less than 1.5 Å) as described above. Each cluster was representative of at least 30% of the overall structures; hence each structure could be represented by more than one cluster.
- Distances between the reference points and the pharmacophore areas mentioned above were calculated for all the 37 structures on the mean of the ensemble.
- The clustered molecules were aligned on the pharmacophore areas by the SIMPLEX algorithm.
- From the aligned structures the pharmacophoric areas (aromatic, lypophilic area, H donor, H acceptor) were positioned on the octreotide scaffold.

4.3.3 Pharmacophore model for SRIF receptors

For each receptor a qualitative pharmacophore model was proposed. Modeling qualitatively guided us through the design of new compounds featured of allowed and disallowed aminoacid substitution, prone for the biological activity among the five SRIF receptors. The following paragraphs just give a qualitative description of pharmacophore model for each SRIF receptor.

4.3.3.1 SST1 model

Position 2 is preferably occupied by a lypophilic bulky moiety. Ring are accepted while methyl groups or whatever alkyl moiety are discarded. In the *β*-turn region it seems that a Trp^8 could be substitute by a Naphtyl moiety and a bulky residue is requested while a H donor group is not necessary. Position 10 seems more sst_1 active when it bears a H acceptor group (for example, OH, NH). Aromatic residues are completely discarded in position 15, where a Thr-ol moiety is preferable.

4.3.3.2 SST2 model

Position 2 is preferably occupied by a bulky moiety and in particular an aromatic ring, unlike sst_1 pharmacophore model, is preferable. None consideration came out on the *β*-turn region: it seems that a D-Trp[8] is the best group in maintaining the sst_2 activity, as confirmed by our dicarba-analogues. Position 10 should bear a H-acceptor group (for example, OH, NH). Still a Thr-ol moiety is preferable at position 15.

4.3.3.3 SST3 model

Position 2 is preferably occupied by a bulky moiety, which should have the shape of a ring (aromatic or aliphatic), or a cycle, or even a branched alkyl chain. Even a H-donor is accepted near this position. *β*-turn region could bear the usual D-Trp but also a D-2-Naphtyl moiety is accepted (compunds **36**, **41**, **42** and **43**). Those peptides were designed with the aim to obtain sst_3 selective dicarba-analogues.[147] Position 10 could be featured by a H-donor next to a bulky moiety and in particular an Aromatic ring in position 11. Peptides **36**, **41**, **42** and **43** bear a Thr[10] residue and a Phe[11]. However a bulky area in position 10 which bear a H-donor is accepted. Thr-ol is not requested in position 15, where the OH group could be replaced by NH.

4.3.3.4 SST4 model

Still a bulky and lypophilic moiety should be insert in position 2. *β*-turn maintain its original substitution (D-Trp[8] and Lys[9]): hence other aminoacid replacement are avoided. Position 10 and 11 has the same features of sst_3 pharmacophore model. Still a H-acceptor, like Thr, is remarked in position 10 and a Phe in position 11. Just for sst_4, Thr-ol[15] or other H-donor groups seems to be harmful for the activity.

4.3.3.5 SST5 model

Conclusions obtained for sst_2 are acceptable for sst_5 too. It is not easy to have a different selectivity between these two receptors and octreotide affinity still remarks this fact. Just position 10 seems involved in a poor specificity: when a bulky residue occupies this area a major sst_5 affinity is showed.

4.4 Biological Part

4.4.1 Stability essays in human serum

The aim of our project was to synthesized, replacing disulphide bridge with carbon bond, more biologically stable octreotide analogues. Obviously a C-C bond is more chemically stable than a disulphide bridge. In order to investigate the stability of compound to the enzymes the first biological essay we made was the stability in human *serum*. We tested compounds **27**, **28** and **29**; the first (**27** and **28**) to demonstrate the stability of the backbone of the first dicarba-analogs of octreotide,[90] the second one (**29**) to investigate the stability of the amino acid in position 10 (Tyr(Bzl)). We used a standard procedure reported in the literature that use as analytical method RP-HPLC.[58] Human sera was divided in aliquots, a water solution of peptide **27**, **28** or **29** was added and each aliquots was incubated at 37 °C for 8h, 24h and 50h tests were performed in triplicate for each time and tree aliquots without peptides were used for the blank. At each time of incubation CH_3CN was added to tree aliquots and sera proteins were precipitated. The precipitates were centrifuged off and the surnatants were analyzed by RP-HPLC 10%-90% B in 20 minutes (A: H_2O 0.1% TFA;B: CH_3CN 0.1% TFA.). After each sample two analytical HPLC with method 5%-100% B were ran in order to clean from residues of the sample or serum the chromatographic column. For each compound, **27**, **28** and **29**, the intensity of the chromatographic peak is not diminished after 50h and no new peaks were detected in the chromatogram.

We demonstrate with this method that compounds **27**, **28** and **29** were stable in human sera even after 50h at 37 °C.

4.4.2 Binding affinity to $sstr_{1-5}$

Compounds **27**-**32**, **37**, **45**-**48** were dispatched to the Division of Cell Biology and Experimental Cancer Research, Institute of Pathology, University of Berne. The group of Professor Reubi tested all compounds for their ability to bind to the five human sst_{1-5}

receptors subtypes, in complete displacement experiments using the universal somatostatin radioligand [^{125}I]-[Leu^{8},D-Trp^{22},Tyr^{25}]-somatostatin-28.

	IC_{50} (nM)[a]				
Compound	**$sstr_1$**	**$sstr_2$**	**$sstr_3$**	**$sstr_4$**	**$sstr_5$**
SRIF-28	2.3 ± 0.4 (7)	3.0 ± 0.2 (7)	3.6 ± 0.5 (7)	1.6 ± 0.3 (7)	2.1 ± 0.2 (7)
27	961±294	>1000	>1000	141 ± 27	206 ± 97
28	>1000	44 ± 1	>1000	412 ± 68	28 ± 2
29 E	>1000	>1000	892 ± 245	>1000	29 ± 1
29 Z	25 ± 1	46 ± 3	25 ± 4	346 ± 23	12.3 ± 0.3
30	>1000	9.6 ±0.9	>1000	249± 51	16.5 ± 4.5
31	57.5 ± 12.5	101 ± 9	92.5 ± 0.5	> 1000	4.9 ± 1
32 E	1000	355.5± 45.5	1000	1000	418 ± 56
32 Z	>1000	87 ± 18	>1000	>1000	12.5 ± 27
37	>1000	>1000	>1000	>1000	>1000
45	>1000	49 ± 12	>1000	214 ± 9	203± 106
46	>1000	1.7 ±3.2	>1000	270± 99	81± 26
47	432±105	>1000	927±320	210± 50	788± 604
48	593 ± 39	393 ± 20	277 ± 123	846 ± 400	12 ± 2

Table 28. Receptor affinities of the somatostatin analogues.
[a]The number of independent repetitions to obtain the mean values ± SEM are indicated between brackets.
SRIF-28 is used as internal control.

SRIF- 28 was run in parallel as control. IC_{50} values were calculated after quantification of the data using a computer-assisted image processing system. Binding data (Table 28) indicated that **29 Z** showed nM binding affinities towards the sst_2, sst_4, and sst_5.

Peptide **45** shows similar binding affinity profiles towards the sst's, compared to **28**. The affinity towards sst_5 significantly decreased (203 *vs* 28 nM). Peptides **27**, **37** and **47** have no affinity to any sst receptors.

Most interestingly, binding data indicate that **28**, **29 E** and **48** were ligands less potent than SRIF (IC_{50} = 12 nM) but by far more selective (at least thirty fold) for the sst_5 subtype. Peptide **29 E** shows an enhanced selectivity towards the sst_5 compared to

29 Z while its affinity appears only slightly reduced. **29 Z** almost has a Pan-SRIF activity. Compound **30** is potent on sst_2 and sst_5 and **46** has the same affinity profile with minor activity, but for sst_2 (1.7 nm IC_{50}). Gilon et al. developed a backbone-cyclic somatostatin analogue (PTR 3046) with high selectivity towards sst_5.[149] The IC_{50} value for the binding of PTR 3046 to sst_5 was 67 nM, more than double compared to our compounds **28** and **29 E** and more than triple compared to our compounds **29 Z**, **30**, **31, 32 Z** and **48**. Some sst_5 selective non-peptide peptidomimetics have been also reported. One of them, named L-817,818 with some selectivity to sst_5 has been obtained at the Merck laboratories through combinatorial chemistry approach.[150] L-817,818 showed sub-nM affinity towards sst_5 (IC_{50} = 0.4 nM), but it was only eightfold more selective for sst_5 as compared to sst_1. The synthesis and screening of a focused library of β-turn mimetics based upon the crucial D-Trp-Lys motif, found in the turn region of SRIF, resulted in the identification of a small molecule ligand selective toward sst_5.[151] Its affinity towards sst_5 (IC_{50} = 87 nM) was lower compared to our selective compounds. Finally, two highly potent sst_4/sst_5 peptidomimetics have been recently described by Feytens et al.[152] Their structure is based on a constrained tryptophan scaffold and the most potent analogue has an IC_{50} value of 1.2 nM for the sst_5. These compounds showed also high affinity towards sst_4 being only three and ninefold more selective for sst_5 as compared to sst_4. Hence, peptides **29 Z**, **30**, **31, 32 Z** and **48** are among our dicarba-analogues the most potent and sst_5-selective compounds reported to date. The potential therapeutic utility of selective agonists for sst_5, which is expressed in the lymphoid system, in pancreatic beta cells, and in corticotrophe adenoma cells has been reported.

[149] Gilon, C.; Huenges, M.; Mathä, B.; Gellerman, G.; Hornik, V.; Afargan, M.; Amitay, O.; Ziv, O.; Feller, E.; Gamliel, A.; Shohat, D.; Wanger, M.; Arad, O.; Kessler, H. A Backbone-Cyclic, Receptor 5-Selective Somatostatin Analogue: Synthesis, Bioactivity, and Nuclear Magnetic Resonance Conformational Analysis. *J. Med. Chem.* **1998**, *41*, 919-929.

[150] Rohrer, S. P.; Birzin, E. T.; Mosley, R. T.; Berk, S. C.; Hutchins, S. M.; Shen, D. M.; Xiong, Y. S.; Hayes, E. C.; Parmar, R. M.; Foor, F.; Mitra, S. W.; Degrado, S. J.; Shu, M.; Klopp, J. M.; Cai, S. J.; Blake, A.; Chan, W. W. S.; Pasternak, A.; Yang, L. H.; Patchett, A. A.; Smith, R. G.; Chapman, K. T.; Schaeffer, J. M. Rapid Identification of Subtype-Selective Agonists of the Somatostatin Receptor Through Combinatorial Chemistry. *Science* **1998**, *282*, 737-740.

[151] Souers, A. J.; Virgilio, A. A.; Rosenquist, A.; Fenuik, W.; Ellman, J. A. Identification of a Potent Heterocyclic Ligand to Somatostatin Receptor Subtype 5 by the Synthesis and Screening of Beta-Turn Mimetic Libraries. J. *Am. Chem. Soc.* **1999**, *121*, 1817-1825.

[152] Feytens, D.; Cescato, R.; Reubi, J.C.; Tourwe´, D. New $sst_{4/5}$-Selective Somatostatin Peptidomimetics Based on a Constrained Tryptophan Scaffold. *J. Med. Chem.* **2007**, *50*, 3397-3401.

4.4.3 Radiolabeling of peptides with radioactive metals

*4.4.3.1 Radiolabeling of **49**, **50**, **51** and **52** with ^{111}In*

Peptide **49-52** were send to the Regional Centre of Nuclear Medicine of Pisa, group of Professor Mariani, where compounds were radiolabeled by Dr. Paola Erba.

Peptides **49-52** were radiolabeled with ^{111}In adding to a solution of peptides in H_2O MilliQ a sodium acetate buffer 1 M (pH = 5) and then a solution of the radioisotope in the form of chloride (MCl_3, with M = ^{111}In). The mixture was incubated at 95 °C for 30 min. Quality control was obtained with the use of a Sep-Pak C18 cartridge and RP-HPLC, resulting in highly pure radioligands.

Biodistribution and binding studies are in progress at the Pharmaceutical Department of the University of Pisa.

*4.4.3.2 Radioalbeling of **53** and **54** with ^{99m}Tc*

Peptide **53** and **54** were dispatched to the Department of Pharmaceutical Science of the University of Padova, group of Professor Mazzi, where compounds were radiolabeled by Dr. Elena Zangoni.

Peptides **53** and **54** were radiolabeled with ^{99m}Tc using two different methods in order to compare its efficiency and decide which will be the best in radiolabeling yield and stability.

Method A: Peptide **53** dithiocarbamate (DTCM) in ethanol was added $[^{99m}Tc(CO)_3(H_2O)_3]^+$ solution previousy prepared starting fom Isolink, the solutions were heated to 50 °C for 30 minutes. Reaction mixture was analyzed by RP-HPLC; radiochromatogram displayed the increasing of a peak attributed to $[^{99m}Tc(CO)_3]$(PN2S-peptide)(DTCM) complex up to 58 % yields. The labelling reaction mixture analyzed after 24 h at room temperature demonstrated the stability of the complex because the radiochromatograms remained unchanged.

Method B: **53** and **54** were dissolved in degassed ethanol, sodium gluconate, $SnCl_2$ in HCl and ^{99m} TcO_4^- in saline solution was added, the solution was heated at 70 °C for 30 minutes. Solution of $SnCl_2$ in HCl was prepared immediately before the labeling procedure. RP-HPLC of the reaction mixture revealed the presence of the

^{99m}TcO(PN2S-peptide) complex up to 60% yields, stable after 24h at room temperature and 1.5 h at 70 °C.

Comparing the two methods, the yield of radiolabeling were the same in our hand our peptides could be radiolabeled with both methods with ^{99m}Tc.

CONCLUSIONS

" In ogni attività
la passione toglie gran parte della difficoltà "

Erasmo Da Rotterdam
(1466-1536)

5.1 Peptide Design

In this PhD thesis a new algorithm (PPS) was developed for suggesting new selective and potent SRIF dicarba-peptide sequences.

NMR analysis provided, together with the modeling calculations, new peptides structures (**31**, **32**, **33** and **34**).

The most active compounds **29 Z**, **31** and **32 Z** were conjugated with DOTA and **30** with DOTA and PN_2S both.

5.2 Synthesis

In this PhD thesis we synthesized 26 new compounds. In particular the major studies were dedicated to the step of the RCM, the NMR conformational analysis and the realization of the peptides library to employ for the in *silico* prediction.

With the second generation Grubbs catalyst the yield of the pure compound were increased of about 10 % than ist generation catalyst. We were able to optimized for peptides **19-24** specific microwave that totally convert linear peptides into cyclic.

New methods for obtaining eight-mer ring dicarba-peptides (**39-43**) were presented, because in our hands MW technique afforded cyclic dicarba-compounds otherwise not achievable with standard method, in high yields and without side-products.

A critical analysis about the MW methods used was discussed: all the four methods were amenable to use, but the best results are obtained when the Power Cycling was applied and, in less extent, SPS method. Both allows a higher level of microwave power to be administered to the reaction mixture and, therefore, enhances any "non specific" microwave effects, reducing the activation energy. Among the specific reactivity of each compounds, there is evidence that differences in stereochemistry of the sequence could favour or disfavour the RCM, even when MW technique is employed.

5.3 Conformation-affinity relationships and pharmacophore model for sst_5 selective analogues

On the basis of the discussed results, we can draw some conformation-affinity relationships concerning the binding to the sst receptors. As most of the bioactive

analogues of SRIF reported so far,[153] the structures of the peptidomimetics presented here have a β-turn of type II' (paragraph 4.2) about residues D-Trp^8 and Lys^9. The side chain of D-Trp^8 is in the *trans* conformer, and the side chain of Lys^9 is in the *gauche*$^-$ conformer, bringing the two side chains adjacent to each other in close proximity. In compounds **28** and **45**, which retain affinity towards sst_2, the turn motif is part of a β-hairpin structure. This conformation is very similar to that observed for octreotide (Figure 26). A detailed comparison of the structures of **45** and **28** with octreotide showed a different spatial orientation of the D-Phe^2 aromatic cycle. Since, according to Grace et al,[136] this moiety belongs to the consensus structural motif of sst_2-selective analogues, the different orientation observed for D-Phe^2 aromatic cycle could explain the reduced affinities of **28** and **45** towards sst_2 compared to the parent octreotide. On this point, a direct involvement of the disulfide bridge in the interaction with the sst_2 have also been demonstrated.[140,154] In fact, a disulfide can replace an aromatic moiety in key somatostatin receptor-ligand interaction.

As for octreotide, a dynamical equilibrium between β-sheet and helical conformations was observed at the C-terminal residues of analogues **29 Z**. The increased helical character observed in compound **48** compared to **45** parallels its increased affinity towards sst_5 receptor. Actually, Grace et al. have reported that analogues should prefer the helical conformation to fit the sst_5 pharmacophore.[136] Accordingly, analogues **29 E** and **48**, which show high affinity and selectivity towards sst_5, feature a stable helical structure at the C-terminus. In these analogues, the β-turn motif is followed by a short 3_{10}-helix along residues Tyr(Bzl)^{10}-Dsa-C^{14}-Thr(ol)^{15}. The side chain of Tyr(Bzl)^{10}, that apparently stabilizes the helical structure, is in the *gauche*$^-$ conformer and it is located in close proximity to the D-Trp^8-Lys^9 pair. If this structure corresponds to the bound conformation of the analogue **48** (and **29 E**), then Tyr(Bzl) bulky side chain must accommodate in a suitable hydrophobic pocket within the sst_5 binding site. To explain sst_5 selectivity of analogues **29 E** and **48**, it can be hypothesized that this side chain is hardly accommodate into the $sst_{1\text{-}4}$ binding sites. Nonetheless, the Tyr(Bzl) residue replaced the Thr^{10} in other somatostatin analogues showing high-affinity binding towards all the sst receptors.[54] Hence, the selectivity of the new analogues **29 E** and **48** towards sst_5 should depend on the conformationally restricted

[153] Tyndall, J. D. A.; Pfeiffer, B.; Abbenante, G.; Fairlie, D. P: Over One Hundred Peptide-Activated G-Protein-Coupled Receptors Recognize Ligands with Turn Structure. *Chem. Rev.* **2005**, *105*, 793-826.
[154] Brady, S. F.; Paleveda, W. J.; Arison, B. H.; Saperstein, R.; Brady, E. J.; Raynor, K.; Reisine, T.; Veber, D. F.; Freidinger, R. M. Approaches to Peptidomimetics which Serve as Surrogates for the cis Amide Bond: Novel Disulfide-Constrained Bicyclic Hexapeptide Analogs of Somatostatin. *Tetrahedron* **1993**, *49*, 3449-3466.

helical structure which they adopt. Finally, considering our sst_5-selective analogues, the increased Tyr(Bzl) side chain flexibly observed in **29 E** compared to **48** can account for the reduced affinity towards the sst_5 observed in the first one.

Based on the results reported above, we proposed a pharmacophore model for sst_5-selective analogues.[91] The model involves the classical four side chains of the $sst_{2/3/5}$ pharmacophore,[140] namely those of residues D-Phe^2, Phe^7, D-Trp^8, and Lys^9, plus the Tyr(Bzl)^{10} side chain which enhanced sst_5 affinity for both compounds **29 E** and **48**. Since **31** is the most potent and selective sst_5 ligand among the analysed peptides, the relevant distances reported in the table below (Table 29) can be proposed as sst_5 pharmacophoric distances.

Compound	29 Z	31	48	$sst_{2/3/5}$[a]
Ar^2-Ar^7	9.9±0.5[b]	8.8±0.5	9.5±0.3	5-11
Ar^2-Ar^8	12.3±0.5	12.2±0.5	13.3±0.2	11-15
Ar^2-Lys^9	13.4±0.5	13.0±0.6	14.3±0.2	12-15
Ar^2-Ar^{10}	-	12.8±0.5	12.6±0.6	-
Ar^7-Ar^8	7.2±0.3	7.1±0.5	7.3±0.3	7-9
Ar^7-Lys^9	9.4±0.2	10.1±0.6	11.1±0.3	9-11
Ar^8-Lys^9	4.8±0.2	4.7±0.4	4.9±0.2	5
Ar^8-Ar^{10}	-	6.6±0.5	7.3±0.6	-
Lys^9-Ar^{10}	-	4.8±0.5	5.6±0.6	-

Table 29. Cγ-Cγ distances (Å) between putative pharmacophoric residues.
[a] Pharmacophore for the sst_2, sst_3, sst_5 selective SRIF analogues.[140] [b] Average distance and standard deviation calculated from the ensemble of ten structures.

In the same Table we also report the Cγ-Cγ distances found by Melacini and co. for the $sst_{2/3/5}$-selective SRIF analogues.[140] It can be observed that the distances found for **29 Z** and **31** agree with the $sst_{2/3/5}$ pharmacophore. Recently, the groups of J. Rivier and J.C. Reubi proposed pharmacophore models for sst_1-,[155] sst_2-,[136] sst_3-,[156] and sst_4-selective[137] analogues, by examining the NMR behaviour of a large number of cyclic

[155] Grace, C. R. R.; Durrer, L.; Koerber, S. C.; Erchegyi, J.; Reubi, J. C.; Rivier, J. E.; Riek, R. Somatostatin Receptor 1 Selective Analogues. 4. Three-Dimensional Consensus Structure by NMR. *J. Med. Chem.* **2005**, *48*, 523-523.
[156] Gairì, M.; Saiz, P.; Madurga, S.; Roig, X.; Erchegyi, J.; Koerber, S.C.; Reubi, J.C.; Rivier, J.E.; Giralt, E. Conformational Analysis of a Potent $SSTR_3$-Selective Somatostatin Analogue by NMR in Water Solution. *J. Pept. Sci.* **2006**, *12*: 82–91.

peptides containing the disulfide bridge. To the best of our knowledge, a model of the sst_5 pharmacophore has never been proposed so far.

Peptide **29 Z** showed a pan-SRIF-activity, but sst_4. To fit 4/5 receptor binding sites, it was expected an high degree of flexibility to this peptide. Actually, a dynamical equilibrium between β-sheet and helical conformations was observed at the C-terminal residues. Also, $Tyr(Bzl)^{10}$ side chain orientation was poorly defined. These conformational averages might account for low selectivity of **29 Z**.

Peptide **30** showed high affinity towards sst_2 and sst_5 among the tested compounds and a good affinity also towards sst_2. Here, the Nal^7 aromatic side chain, which is oriented in a *trans* conformation, adequately fit the binding pocket of both receptors.

Compound **31** is closely related to compound **29 Z**, sharing with it the configuration at the double bond and the amino acid sequence but Nal^7 which replaces Phe^7. Since the helical-extended conformational equilibrium is observable also in the case of **31**, the relatively low affinity towards sst_2 (about 10-fold reduction) compared to compound **31** is tentatively attributable to the different orientation of the Nal^7 side chain which could not adopt a *trans* conformation, due to steric hindrance with $Tyr(Bzl)^{10}$. *Gauche* orientations of naphtyl group is likely still suitable (or preferred) for sst_5 but not for sst_2 binding.

Analogue **32 E** showed a marked reduction of affinity towards sst_5 compared to the correlated compound **29 E**. Since NMR data of the two analogues pointed to similar conformational behavior, hence benzyl group of the Tyr(Bzl) residue must establish indispensable interactions with the receptor in the considered analogues. Similarly, comparing analogues **32 Z** and **29 Z**, it can be argued that the benzyl group, when adequately oriented (see above), is also important for sst_1 and sst_3 binding.

EXPERIMENTAL PART

6.1 Instruments and methods

Fmoc protected amino acids were purchased from Calbiochem-Novabiochem (Laufelfingen. Switzerland). 2nd generation Grubbs catalyst and Wilkinson's catalyst were obtained from Aldrich. Fmoc-Hag and Fmoc–O–benzyl-L-tyrosine and $Pd(OH)_2/C$ were purchased from Fluka. Rink amide resin [4-(2',4'-Dimethoxyphenyl-Fmoc-aminomethyl-phenoxy-acetamido-norleucylaminomethyl resin] and Wang [p-Benzyloxibenzylalchool resin (HMP resin)] were purchased from Novabiochem AG (Laufelfingen, Switzerland). H–L-Thr(*t*Bu)–ol–2–chlorotrityl resin, Fmoc-1-Naphtyl-L-alanine, Fmoc-O-Methyl-L-tyrosine and Fmoc-2-Naphtyl-D-alanine were purchased from Iris Biotech (Marktredwitz, Germany). HATU was obtained from Advanced Biotech Italia (Milan Italy). 3-diphenylphosphinopropionic acid succinimidic ester was provided from Argus Spechem S.a.s. (Prato, Italy). DOTA-tri(*t*-Bu) was purchased from Macrocyclics (Rich-ardson, Texas, USA). Peptide grade DMF was from Scharlau (Barcellona, Spain). All the other solvents and reagents used for SPPS were of analytical quality and used without further purification.

Linear peptides were synthesized at first in teflon reactor on a manual synthesizer PLS 4x4 (AdvancedChemTech) an than in Multi Synthec GmbH semiautomatic system peptides synthesizer SAP. SPE were performed on Spot liquid Cromatography flash (Armen instruments, Sant Ave, France), SiO_2 (SVF D22) with a flow of 12ml/min of increasing percentage of MeCN. HPLC-grade MeCN was purchased from Carlo Erba (Italy). Peptides were analyzed by analytical RP-HPLC (Alliance, model 2695 equipped with a diode array detector, Waters Corporation, Milford Massachusets) using a Jupiter C18 (5 μm, 250 x 4.6 mm) column (Phenomenex) at 1 mL/min at 32°C. The solvent systems used were A (0.1% TFA in H_2O) and B (0.1% TFA in CH_3CN). Peptides were purified by semi-preparative RP-HPLC (Alliance, model 2487 equipped with a diode array detector, Waters Corporation, Milford Massachusets) on a Jupiter C18 column (10 μm, 250 x 10 mm) at 4 mL/min by using the same solvent systems reported above. Peptides were characterized using Acquity UPLC (Waters Corporation, Milford Massachusets) coupled to a single quadrupole ESI-MS (Micromass ZQ) using Acquity BEH C18 at 40 °C column (2.1 x 50mm 1.6 μm), using a flow rate of 0.45 ml/min and the solvent system reported above. Radiolabeled peptides were analyzed with a C18 Agilent column (5 μm 250 x 4.6 mm) for HPLC on a Agilent 1100 series (Agilent Technologies United State) equipped with a diode array GABI star (Raytest Milan

Italy). Products were lyophilized with an Edwards Modulyo apparatus. Microwave assisted RCM was performed in a CEM single mode Discover with Explorer auto-sampler system, (CEM Corporation, Matthews, NC) using either custom-made high purity quartz or standard Pyrex vessels (capacity 10 ml; 30 ml).

Kaiser test:[95] to a small amount of peptide-resin placed in a test tube, three drops for each of the following solutions were added: ninhydrin (5 g) in ethanol (100 mL); phenol (80 g) in ethanol (20 mL); KCN (2 mL of 1 mM aqueous solution) in pyridine (98 mL). The tube is heated at 100 °C for 5 min. A positive test (resin beads and solution appear strongly blue-violet) states the presence of at least 5% free amino groups. UV measurement were performed on a spectrophotomer 1601 PC (Shimatzu Italy Milan).

Serum samples were centrifuged in a Heraeus Biofuge-pico (DJB Labcare Newport PagnellBuckinghamshire England).

Routine NMR spectra were acquired on a Varian Inova 700 apparatus. Deuterated solvents were purchased from Sigma Aldrich(Milwaukee, USA). SDS and TSP were purchased from Cambridge isotope (Andover, MA, USA).

TcO^{4-} is eluted from a generator $^{99}Mo/^{99m}Tc$ Drygen Sorin (Nycomed Amersham Sorin, Saluggia, Vercelli, Italy).

6.2 Synthesis

6.2.1 Synthesis of linear peptides

Peptides were synthesised in a Teflon reactor fitted with a polystyrene porous frit. Peptides were prepared using the general Fmoc-SPPS strategy on pre-swelled H–l-Thr(tBu)–ol–2–chlorotrityl resin, Wang [p-Benzyloxibenzylalchool resin (HMP resin)] and Rink amide AM [4-(2',4'-Dimethoxyphenyl-Fmoc-aminomethyl-phenoxy-acetamido-norleucylaminomethyl resin].

Couplings were performed by adding two equivalents of protected amino acids activated by HATU and six equivalents NMM in DMF, stirring for 40 minutes for each coupling and monitoring by the qualitative ninhydrin (Kaiser) test.[95] To a small amount of peptide-resin placed in a test tube, three drops for each of the following solutions were added: ninhydrin (5 g) in ethanol (100 mL); phenol (80 g) in ethanol (20 mL); KCN (2 mL of 1 mM aqueous solution) in pyridine (98 mL). The tube is heated at 100 °C for 5 min. A positive test (resin beads and solution appear strongly blue-violet) states the presence of at least 5% free amino groups.

At the end of the linear peptides synthesis a microscale cleavage was performed. All compounds were treated with TFA/DCM/EDT/phenol (94:2:2:2, 3 h) but compounds 3 and 5 (TFA/DCM/EDT/phenol 70:26:2:2, 2.30 h). The resin was filtered off, the solutions were concentrated, the peptide precipitated from Et_2O, centrifuged dissolved in water and lyophilized. RP-HPLC analysis of the crude products revealed the presence of the linear peptides in approximately 97% purity, without traces of isomers due to amino acids racemization.

6.2.2 Synthesis of unsaturated cyclic peptides

The resin aliquots containing the peptides 1-16 were swollen for 2 h in anhydrous DCM. The vessels were heated to 45 °C and an anhydrous DCM solution of catalyst 18 (0.5 mole equiv. calculated on the basis of 0.5 mmol/g of peptide) was added.[91,157,158]

[157] Gao, Y.; Lane-Bell, P.; Vederas, J. C. Stereoselective Synthesis of meso-2,6-Diaminopimelic Acid and Its Selectively Protected Derivatives. *J. Org. Chem.* **1998**, *63*, 2133-2143.
[158] Williams, R. M.; Liu, J. Asymmetric Synthesis of Differentially Protected 2,7-Diaminosuberic Acid, a Ring-Closure Metathesis Approach. *J. Org. Chem.* **1998**, *63*, 2130-2132.

The suspension was then stirred for 48 h at 45 °C for compounds 1, 5-16 and for 24 h for compound 2-4. Compounds 12-16 were also treated with 44 (0.5 mole equiv. calculated on the basis of 0.5 mmol/g of peptide) in order to obtain the respective cyclo-peptides. Compounds 39-43 will be obtained only by MW-assited RCM (see next paragraph). The resin aliquots of cyclic-peptides were washed with DCM (x3), MeOH (x3) and DMF (x3), then swelled for 45 min at room temperature in DMF. Fmoc–Hag was deprotected (2.5 mL of 20% piperidine in DMF for 10 min, 2 time repeated) and coupled with Fmoc–D-Phe as described in Scheme 8 or a Fmoc-L-Glycine as described in Scheme 9. Peptides 27-38 were deprotected and cleaved as previously described. The solutions were concentrated and treated with Et_2O giving crude dicarba-analogues 27-38 which were suspended in water and the precipitate centrifuged off. The aqueous solutions of the peptides obtained by RCM with 18, were pre-purified by SPE, eluting with an increased percentage of MeCN (from 0% to 90%). The fractions containing the desired peptides were collected, the solvent removed under reduced pressure and lyophilized, giving colourless powders. Due to the small amount of 27, obtained by RCM with 18, was not subjected to FCC and was directly purified by RP-HPLC. All compounds were then purified by semi-preparative RP-HPLC and the most abundant chromatographic peaks were collected. For all the products HPLC purity was >97%.

6.2.3 Microwaves-assisted RCM

6.2.3.1 Six-mer-ring peptides

The resin bound 27-32 (200 mg) was placed in a large wall glass vessels (CEM) and sealed with a cap and 4 ml of DCM was added and the resin was swelled and gentle stirred for 1 hour. An appropriate amount of catalyst 18 was added (10% mol loading of catalyst) and the reaction kept for the required time (Table 11) under gentle stirring. All reactions were carried out in a CEM single mode Discover with Explorer auto-sampler system, in custom-made high purity quartz or standard Pyrex vessels (capacity 30 ml) with the method described in Table 11. All microwave reactions were conducted in a sealed glass vessels; the pressure was monitored and did not exceed 95 psi, while the temperature was monitored by fiber-optic probes at the base of the reaction vessel. After the indicated time had elapsed, the solution was cooled rapidly by compressed air, and the resin washed with DMF (3x), MeOH (3x) and DCM (3x) and then dried. After each reaction the instruments was running with a cooling method, 10 minute compressed air,

in order to start the next experiment at the same temperature of the first one. In this way the ramp to reach the experiment temperature and the microwaves were approximately the same for all experiments.

Microwaves methods were build up as described below:

1. Pressure set point was given.
2. Maximum microwaves power was fixed (300 W).
3. Time of reaction was given.
4. Medium stirring was applied during the reaction.

Reaction time started when temperature set point was achieved.

Table 30 lists the five methods available in a CEM MW instruments. For each compounds (27-32) a specific method was applied (Table 11 and Table 30).

Method	Temperature (°C)	Power (W)	Pressure (Psi)
Standard	*Fixed*	*Variable*	*Variable*
Dynamic	*Variable*	*Variable*	*Variable*
Power Cycling	*Fixed*	*Fixed*	*Variable*
Fixed Power	*Variable*	*Fixed*	*Variable*
SPS	*Variable in a range*	*Fixed*	*Variable*

Table 30. MW-methods available in a CEM Discover MW instrument.

For the Power Cycling methods applied on 4-8 peptides reaction vessel were cooled from the outside by compressed air while being irradiated by microwaves.

6.2.3.2 Eight-mer-ring peptides

The resin aliquots containing peptides 12-16 were swollen for 2 h in anhydrous DCM and then were heated to 45°C and a DCM solution of 18 (0.5 mole equiv. calculated on the basis of 0.5 mmol/g of peptide) was added. The suspension was then stirred for 48h and kept under reflux at 45 °C. Fresh catalyst was added at the reaction mixture after the first 48 h. The resin aliquots were washed with DMF (3x), MeOH (3x)

and DCM (3x). The on-resin peptides were deprotected and a micro-cleavage was performed as previously described. The solutions were concentrated and treated with Et_2O giving crude dicarba-analogues, which were suspended in water and the precipitate centrifuged off. The aqueous solutions of the cyclic peptides 39-43 were analyzed by RP-HPLC. Chromatograms revealed the presence of still linear precursor 12-16. RCM was-re-performed on a new amount of compounds 12-16. 44 was added (0.5 mole equiv. calculated on the basis of 0.5 mmol/g of peptide). A micro-sample of peptides was obtained as described above. RP-HPLC chromatograms revealed still linear precursor 12-16.

MW-assited RCM was performed in the same manner of paragraph 6.2.3.1. The resin aliquots containing the peptides 12-16 were swollen for 1 h in DCM and a DCM solution of 18 (10% mol loading catalyst) was added and the vessels (capacity 10 ml) were heated to 100°C and 300 watt of MW and stirred for 20 minutes. The resin aliquots were washed with DMF (3x), MeOH (3x) and DCM (3x). The on-resin peptides 39-43 were cleaved as previously described. The solutions were concentrated and treated with Et_2O giving crude dicarba-analogues, which were suspended in water and the precipitate centrifuged off. Analytical RP-HPLC and ESI-MS analysis of the crude compounds showed two chromatographic peaks with the same MW, probably corresponding to geometric isomers (ratio ≈ 85:15). Peptides were obtained in a purity described in Graphic 2.

6.2.4 Synthesis of saturated cyclic peptides

Reduction Methods.

Method A. 10% w/w of 20% $Pd(OH)_2/C$ was added to the pure peptides 28, 30 and 37 and anhydrous MeOH were added to the mixture. The reaction vessel was purged with N_2 and then H_2 was flushed. The suspension was stirred at 30 °C for 24 h, filtered on celite, the solvent was evaporated under reduced pressure and the crude product was lyophilized. Analytical RP-HPLC still revealed the presence of the unsaturated peptides (20% by HPLC). The product was purified by semi-preparative RP-HPLC obtaining 45, 46 and 47 respectively in 35%, 35% an 47% yield.

Method B. To 29 suspended in a solution of 10% anhydrous MeOH in DCM, Wilkinson catalyst $Rh(PPh_3)_3Cl_6$ (2.5 mole %) was added. The reaction vessel was pressured with H_2 (60 psi) and left to stand under stirring at 30 °C for 30 h. The resin

was repeatedly washed with DCM (x2) and DMF (x3), then D-Phe was coupled to the resin-tethered reduced cyclopeptide 45. The saturated analogue 45 was cleaved from the resin as previously described and purified by semi-preparative RP-HPLC affording pure 48 in 13% yield.

6.2.5 Synthesis of radiolabeled unsaturated peptides

6.2.5.1 Synthesis of DOTA conjugated peptides

Resin bounded peptides 29-32 were deprotected on the amino terminal Hag and D-Phe was coupled. After washing and Kaiser tests[95] deprotection of D-Phe Fmoc group was performed, 2 equivalents of DOTA-tri-(t-Bu), 2 equivalent of HATU in DMF and 6 equivalent of NMM were added to the resin. Equivalent were calculated on the basis of the resin substitution of 0.5mmol/g. After 45 minutes resin was washed and peptides was cleaved from the resin.

Crude peptides 49-52 were dissolved in water and lyophilized, than purified by RP-HPLC. Pure compounds 49-52 were obtained in 10%, 20%, 25% and 30%.

6.2.5.2 Synthesis of PN_2S peptide conjugates

Resin bounded peptides 28 and 30 were deprotected on the amino terminal Hag and D-Phe was coupled. After washing and Kaiser tests[95] deprotection of D-Phe Fmoc group was performed. Cys-(Trt) 2 equivalent and Gly 2 equivalent activated by HATU 2 equivalent and NMM 4 equivalent were coupled. Teflon reactor was purge with N_2 and 2 equivalent of 3-diphenylphosphinopropionic acid succinimidic ester and 6 equivalent NMM were added to the resin and stand to reaction for 45 minute. Resin was washed under N_2. Cleavage mixture was degassed with N_2 and added to the resin in a vessel fritted with a cup and purged with Ar.

After cleavage the crude peptides were dissolved in milliQ degassed water and immediately fridge and lyophilized. Peptides were purified by RP-HPLC. CH_3CN was degassed with N_2 and He_2, H_2O was degassed and He_2 was gurgled in the bottle of HPLC for all the purification. Peptides 53 and 54 were obtained in 4% yield.

6.3 NMR Studies

6.3.1 NMR spectroscopy calculations

The samples for NMR spectroscopy were prepared by dissolving the appropriate amount of peptides in 0.40 ml of ^1H_2O (pH 5.0) and 0.10 ml of DMSO-d_6, obtaining 2 mM solutions or in the same amount of an SDS solution. TSP was used as internal chemical shift standard. The water signal was suppressed by the hard pulse WATERGATE scheme. NMR experiments were recorded on a Varian Inova-Unity 700 MHz at 277.1 K. Complete ^1H NMR chemical shift assignments were effectively achieved for all the analyzed peptides according to the Wüthrich procedure[63] via the usual systematic application of DQF-COSY[159,160], TOCSY[161] and NOESY[162] experiments recorded in the phase-sensitive mode using the method from States.[163]

Typical data block sizes were 2048 addresses in t2 and 512 equidistant t1 values. Before Fourier transformation, the time domain data matrices were multiplied by shifted sin_2 functions in both dimensions. A mixing time of 70 ms for ^1H_2O\DMSO-$d_6$was used for the TOCSY experiments, while a 100 ms mixing time for the experiment performed in SDS solutions. NOESY experiments were run with mixing times in the range of 150-300 ms. The qualitative and quantitative analyses of DQF-COSY, TOCSY, and NOESY spectra, were obtained with the support of the XEASY software package.[164] ^3J HN-Hα coupling constants were obtained from 1D ^1H NMR and 2D DQF-COSY spectra. ^3J Hα-Hβ coupling constants were obtained from 1D ^1H NMR and 2D PE-COSY spectra, the last performed with a β flip angle of 35°.[165]

[159] Piantini, U.; Sørensen, O. W.; Ernst, R. R. Multiple Quantum Filters for Elucidating NMR Coupling Network. *J. Am. Chem. Soc.* **1982**, *104*, 6800-6801.
[160] Marion, D.; Wüthrich, K. Application of Phase Sensitive Two-Dimensional Correlated Spectroscopy (COSY) for Measurements of ^1H-^1H Spin-Spin Coupling Constants in Proteins. *Biochem. Biophys. Res. Commun.* **1983**, *113*, 967-974.
[161] Braunschweiler, L.; Ernst, R. R. Coherence Transfer by Isotropic Mixing: Application to Proton Correlation Spectroscopy. *J. Magn. Reson.* **1983**, *53*, 521-528 .
[162] Jenner, J.; Meier, B. H.; Bachman, P.; Ernst, R. R. Investigation of Exchange Processes by Two-Dimensional NMR Spectroscopy. *J. Chem. Phys.* **1979**, *71*, 4546-4553.
[163] States, D. J.; Haberkorn, R. A.; Ruben, D. J. A Two-Dimensional Nuclear Overhauser Experiment with Pure Absorption Phase Four Quadrants. *J. Magn. Reson.* **1982**, *48*, 286-292.
[164] Bartels, C.; Xia, T.; Billeter, M.; Güntert, P.; Wüthrich, K. The Program XEASY for Computer-Supported NMR Spectral Analysis of Biological Macromolecules. *J. Biomol. NMR.* **1995**, *6*, 1-10.
[165] Mueller, L. P. E: COSY, a Simple Alternative to E. COSY. *J. Magn. Res.* **1987**, *72*, 191-196.

6.3.2 Structural determination and computational modeling

The NOE-based distance restraints were obtained from NOESY spectra collected with a mixing time of 150-300 ms. The NOE cross peaks were integrated with the XEASY program and were converted into upper distance bounds using the CALIBA program incorporated into the program package DYANA. 200 structures were chosen, whose interprotonic distances best fitted NOE derived distances, and then refined through successive steps of restrained and unrestrained energy minimization calculations using the Discover algorithm (Accelrys, San Diego, CA) and the consistent valence force field (CVFF).[166]

The minimization lowered the total energy of the structures. The final structures were analyzed using the Insight II program (Accelrys, San Diego, CA). Graphical representation were carried out with the Insight II program (Accelrys, San Diego, CA).

[166] Maple, J.; Dinur, U.; Hagler, A. T. Derivation of Force Fields for Molecular Mechanics and Dynamics from Ab Initio Energy Surface. *Proc. Natl. Acad. Sci.* U.S.A. **1988**, *85*, 5350-5354.

6.4 Molecular Modeling

6.4.1 Peptide virtual library construction

All the peptides employed in the library were undergone the same binding test.[91,144,145,146,147] CHO-K1 and CCL-39 cells stably expressing human sst_1-sst_5 receptors were emplyed. For each of the tested compounds, complete displacement experiments were done with the universal somatostatin radioligand [^{125}I]-[Leu^8,D-Trp^{22},Tyr^{25}]-somatostatin-28 using increasing concentrations of the unlabeled compounds ranging from 0.1 to 1,000 nmol/L. SRIF-28 was run in parallel as control using the same increasing concentrations. IC_{50} values were calculated after quantification of the data using a computer-assisted image processing system.

6.4.2 PPS algorithm

100 structures were chosen and refined through successive steps of energy minimization calculations using the Discover algorithm conjugated gradient (Accelrys, San Diego, CA) and the Amber force field.

A simulated annealing was performed on all the 37 structures (see paragraph 4.3.1) in order to explore to conformational space.

The pharmacophore areas described in paragraph 4.3.2 were featured as follow[148]:

Aromatic ring. It was described by the barycentre at the ring atoms.

Lypophilic area. It was described by the barycentre of neighbor lypophilic atoms (C sp^2, C sp^3, S and halydes).

H acceptor. It was described by the featured atom (O or N).

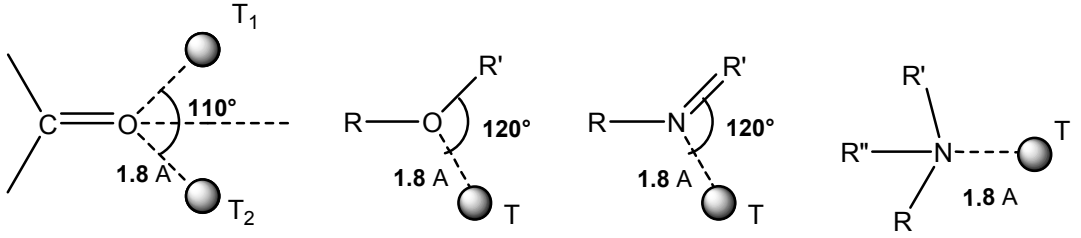

H donor. It corresponded to O or N atom.

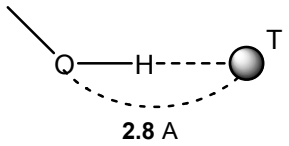

6.4.3 Pharmacophore model for SRIF receptors

As previously described in paragraph 4.3.3, the binding affinity of all 37 peptides was correlated to the position of the above described pharmacophore areas. The regression coefficient (R) described the quality of the model: the model is acceptable when a negative R value occurred; model was discarded when the R value was positive.[148] The probability of matching the right positions of the described areas along the peptide backbone was evaluated still by R: the highest was its value, the most was the probability of finding that area in the described position.

6.5 Biological Part

6.5.1 In serum stability

2.7 ml of human serum were divided in 27 aliquots of 100 µl each. An aqueous solution 8 mM of peptides 27, 28 and 29 was prepared. 20 µl of the aqueous solution of peptide was added to twenty-four serum aliquots, each aliquots were incubated at 37 °C. Three aliquots were used for the blank to perform an HPLC and identify the peaks of the serum. Each incubation time (time 0, 8h, 24h, 50h) were repeated in triplicate. Each aliquot was treated with 380 µl of CH_3CN, proteins were precipitated and centrifuged , the liquid was transferred in an eppendorf and 20 µl were injected in RP-HPLC and the sample run with method 10%-90% B (A: H2O 0.1% TFA; B: CH3CN 0.1% TFA). After each sample analysis two runs were performed with the injection of MeOH 20 µl.

The samples incubated for 50h for each peptide showed still the same intensity and retention time of the time zero analysis.

6.5.2 Binding essays

CHO-K1 and CCL39 cells stably expressing human sst_1-sst_5 receptors were grown as described previously.[167] Cell membrane pellets were prepared and receptor autoradiography was done on 20 µm thick pellet sections (mounted on microscope slides). For each of the tested compound, complete displacement experiments were done with the universal somatostatin radioligand [^{125}I]-[Leu^8,D-Trp^{22},Tyr^{25}]-somatostatin-28 using increasing concentrations of the unlabeled compounds ranging from 0.1 to 1,000 nmol/L. SRIF-28 was run in parallel as control using the same increasing concentrations. IC_{50} values were calculated after quantification of the data using a computer-assisted image processing system. Tissue standards containing known amounts of isotopes, cross-calibrated to tissue-equivalent ligand concentrations, were used for quantification.

[167] Reubi, J. C.; Schar, J. C.; Waser, B. Wenger, S.; Heppeler, A.; Schmitt, J. S.; Macke, H. R. Affinity Profiles for Human Somatostatin Receptor Subtypes SST1-SST5 of Somatostatin Radiotracers Selected for Scintigraphic and Radiotherapeutic Use. *Eur. J. Nucl. Med.* **2000**, *27*, 273-282

6.5.3 Radiolabeling procedure

The radiolabelling procedure with ^{111}In has been optimized as follow: 20 µg DOTA-peptide 49-52 was dissolved in 20 µl H_2O with about 150 µl gentisic buffer pH 5,5; after the addition of about 3 mCi $^{111}InCl3$ the solution was heated at 90° C for 30 min. Quality control was obtained with the use of a Sep-Pak C18 cartridge and RP-HPLC, resulting in highly pure radioligands (radiolabelling efficiency >88%).

Radiolabelling of 28 and 30 with ^{99m}Tc was achieved with two methods.

Method A. Solution A $[^{99m}Tc(CO)_3(H_2O)_3]+$: 1ml of $^{99m}TcO4-$ in degassed saline solution (~20mCi) were added to the vials with the kit Isolink™, this solution was placed in boiling H_2O for 20 minutes. The vials was cooled and the solution was neutralized with HCl 6N.

Solution B DTCM: solution of DTCM 1mg/ml in degassed EtOH was prepared. 10 µl of degassed EtOH were added to 100 µg of the peptides, 5.175µl of solution A and 30 µl of solution B were added and mixture heated at 50 °C for 30 minutes. Analyzing the mixture at time 0 and after 36 h, with RP-HPLC method 40%-100% B (A: H2O 0.1% TFA; B: CH_3CN 0.1% TFA) chromatogram did not change. The complex is stable for 36 h at room temperature. The radiolabeling yield calculated via RP-HPLC is 56%.

Method B. Solution A Sodium gluconate: 0,0218g in 10 ml degassed H_2O milliQ. Solution B SnCl2: Immediately before the labeling procedure. 0.0189 g of $SnCl_2$ dissolved in 100 µl di HCl 1M diluted at 900 µl in degassed H_2O milliQ. $SnCl_2$ 0.1M in HCl 0.1M. 60 µl of degassed EtOH were added to 100 µg of the peptide, 1 µl of solution A and 2 of solution B and 40 µl of a solution of $^{99m}TcO4-$ in degassed saline solution (~1mCi) was added, the mixtures were heated for 30 minutes at 70° C. The mixture was analyzed at time 0 and after 24 h, with RP-HPLC method 40%-100% B (A: H2O 0.1% TFA; B: CH3CN 0.1% TFA) chromatogram did not change. The complex was stable for 24 h at room temperature. The radiolabeling yield calculated via RP-HPLC was 60%.

BFCA BiFunctional Chelating Agent

Boc *Tert*-Butoxycarbonyl

BSA Bovine Serum Albumine

c-AMP Cyclic Adenosine Monophosphate

COSY COrrelation SpettroScopY

CVFF Consisten Valence Force Field

DCM Dichloromethane

dhDsa-C, dehydrodiaminosuberic acid C-terminus

dhDsa-N, dehydrodiaminosuberic acid N-terminus

DMF N,N-dimethylformamide

DMSO Dimethyl Sulfoxide

DMSO-d6 Dimethyl Sulfoxide exa-deuterated

DNA Deoxyribonucleic Acid

DOTA 1,4,7,10,-tetraazacyclododecane-*N,N',N'',N'''*-tetraacetic acid

DQF-COSY Double Quantum Filtered Correlation SpettroscopY

Dsa-C diaminosuberic acid C-terminus

Dsa-N diaminosuberic acid N-terminus

DTCM dithiocarbamate

DTPA diethylenetriamine pentaacetic acid

EDT 1,2-ethanedithiol

ESI Electron Spray Ionization

Fmoc 9-Fluorenylmethoxycarbonyl

GEP Gastrointenteropancreatic

GH Growth Hormone

GPCRs G protein coupled receptors

Hag L-2-Allyl-glycine

HATU 1-[bis(dimethylamino)methylene]-1H-1,2,3-triazole(4,5-b)pyridinium 3-oxide hexafluorophosphate

I-Amp 4-(N.isopropyl)-aminomethylphenilalanine

IGF Insulin-like Growth Factor

MD Molecular Dynamics

MS Mass Spectrometry

NHC Nitrogen Heterocyclic Carbenes

NMM N-metilmorpholine

NMR Nuclear Magnetic Resonance

NOE Nuclear Overhauser Effect

NOESY Nuclear Overhauser Enhanced SpectroscopY

PE COSY Primitive Exclusive COrrelated SpectroscopY

PET Positron Emission Tomography

PRL Prolactin

QSAR Quantitative Structure-Activity Relationship

RCM Ring Closing Methatesis

R_f Ratio frontis

ROESY Rotational nuclear Overhouser Effect Spectroscopy

RP-HPLC Reverse Phase-High Performance Liquid Chromatography

SDS Sodium Dodecyl Sulphate

SPE Solid Phase Extraction

SPPS Solid Phase Peptide Synthesis

SRIF Somatostain Release Inhibiting Factor

SRIF-28 Somatostain Release Inhibiting Factor 28 amino acids.

Sst Somatostatin receptors subtype

TOCSY TOtal Correlated SpectroscopY

Trt Trityl

TSP 3-trimethylsilanylpropionic acid

UPLC Ultra Performance Liquid Cromatography

VIP Vasoactive Intestinal Peptide

SUPPLEMENTARY INFORMATION

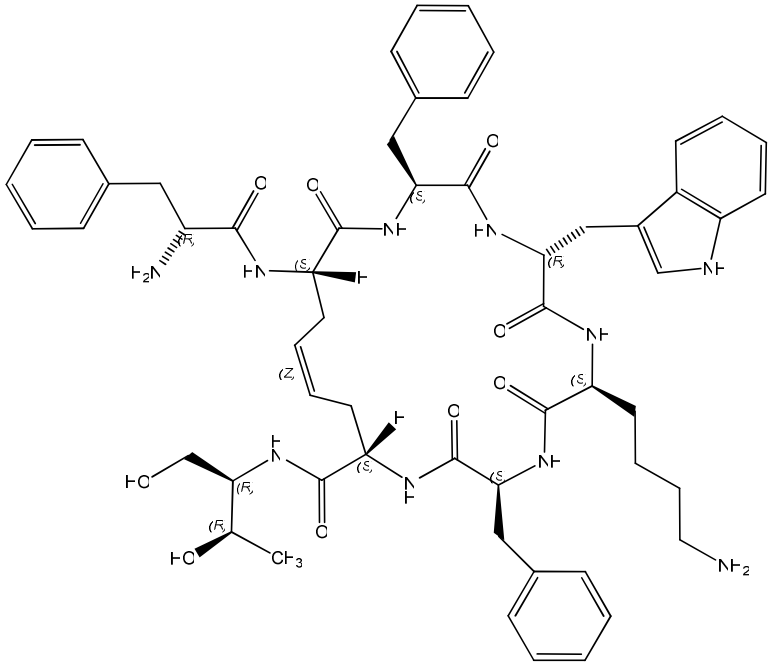

*Figure-S1. Peptide **27**.*

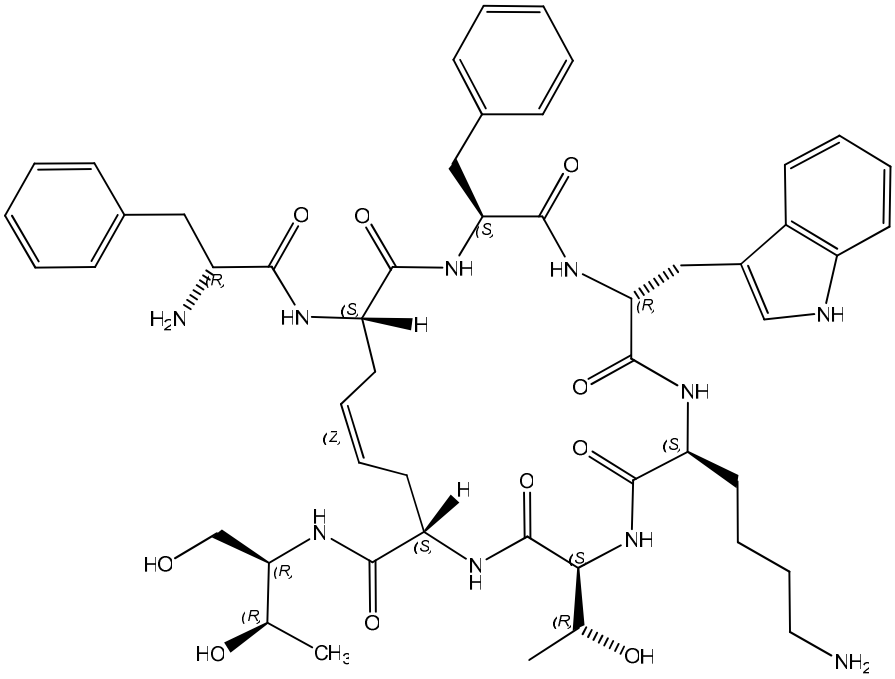

*Figure-S2. Peptide **28**.*

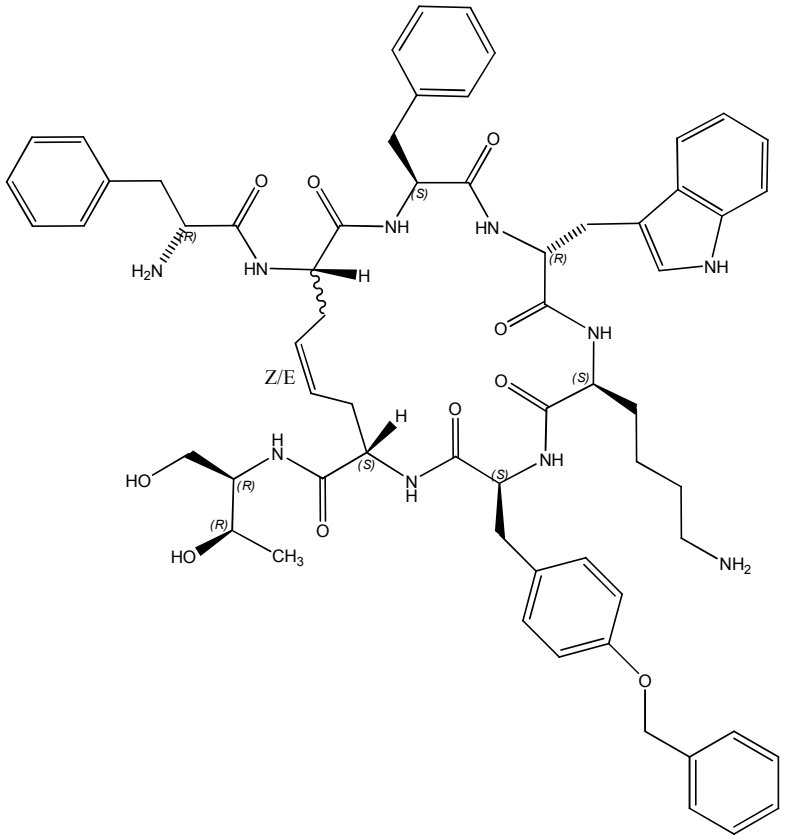

*Figure-S3. Peptides **29** (**E** and **Z**).*

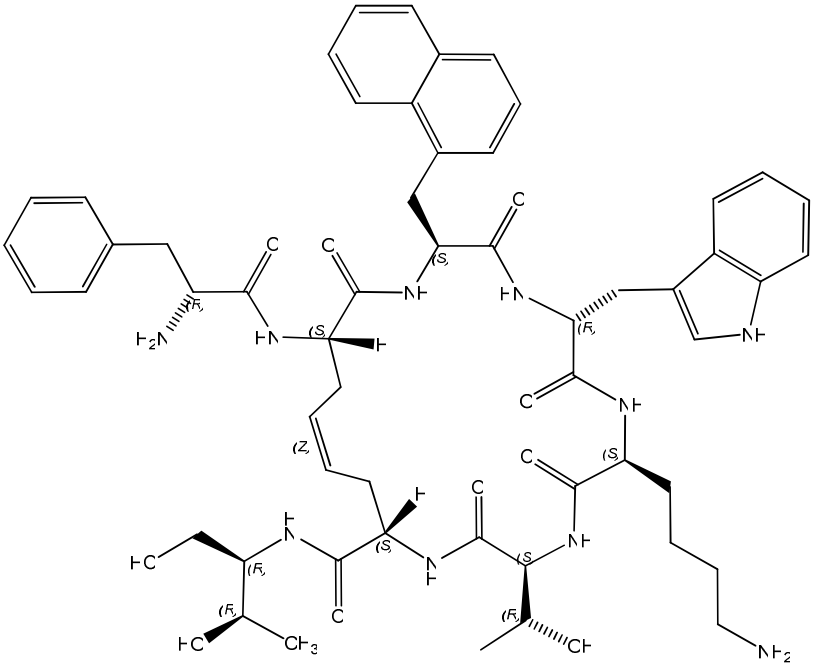

*Figure-S4. Peptide **30**.*

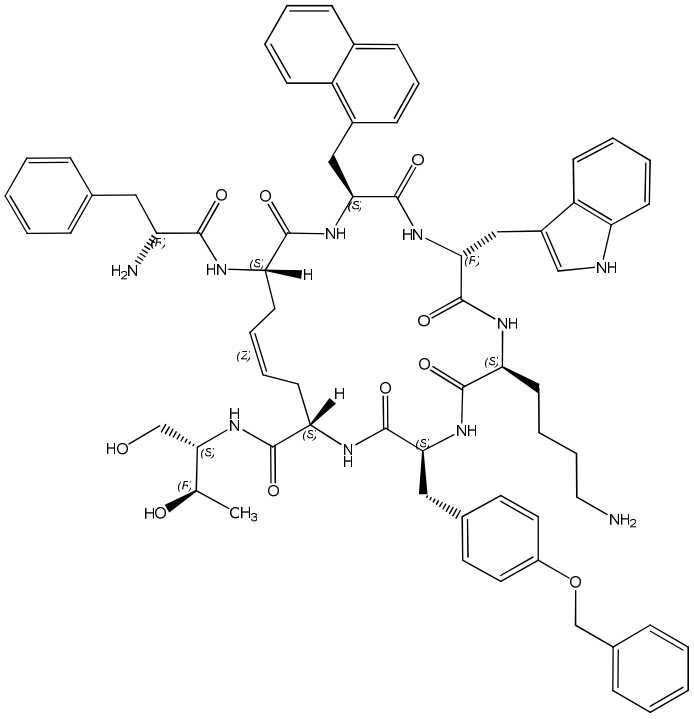

*Figure-S5. Peptide **31**.*

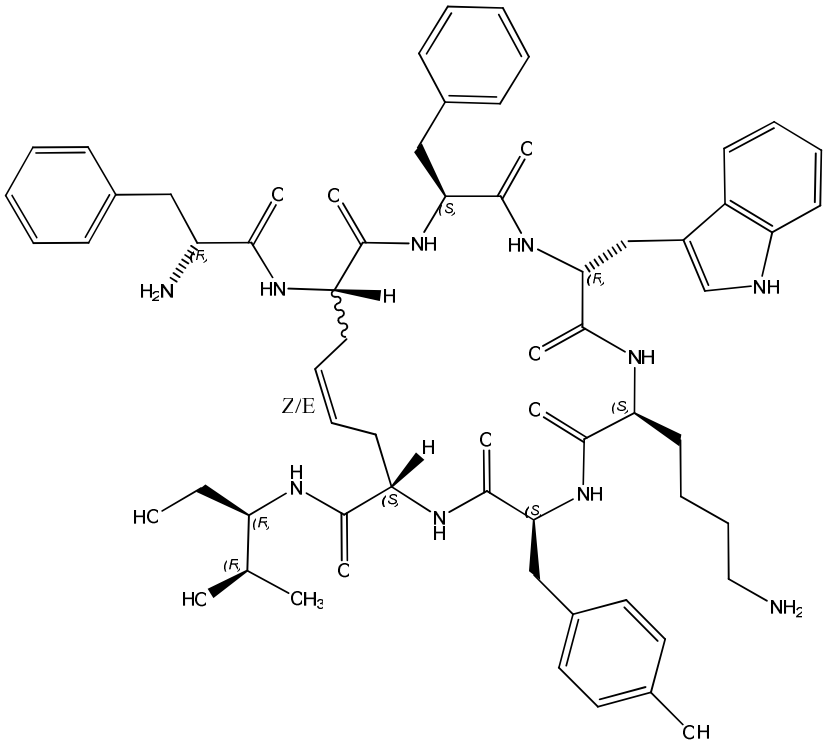

*Figure-S6. Peptides **32** (**E** and **Z**).*

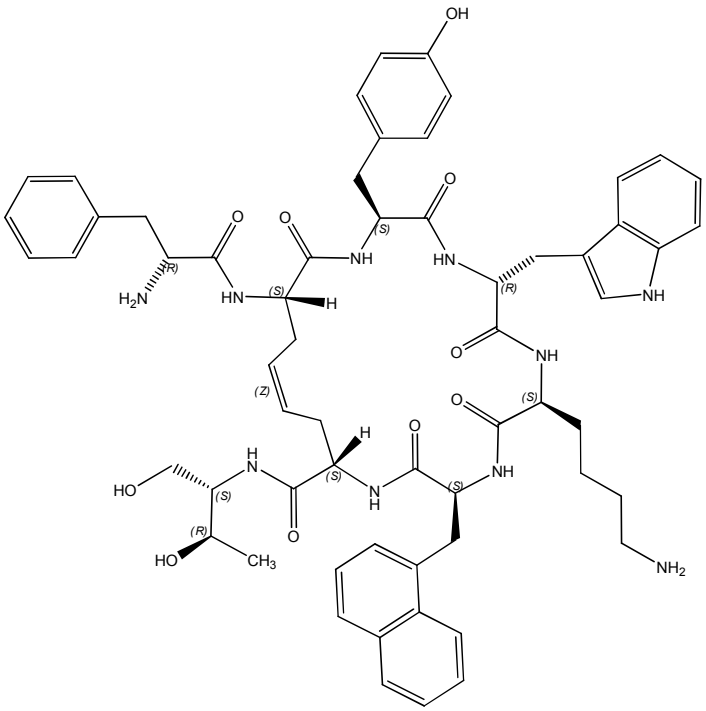

*Figure-S7. Peptide **33**.*

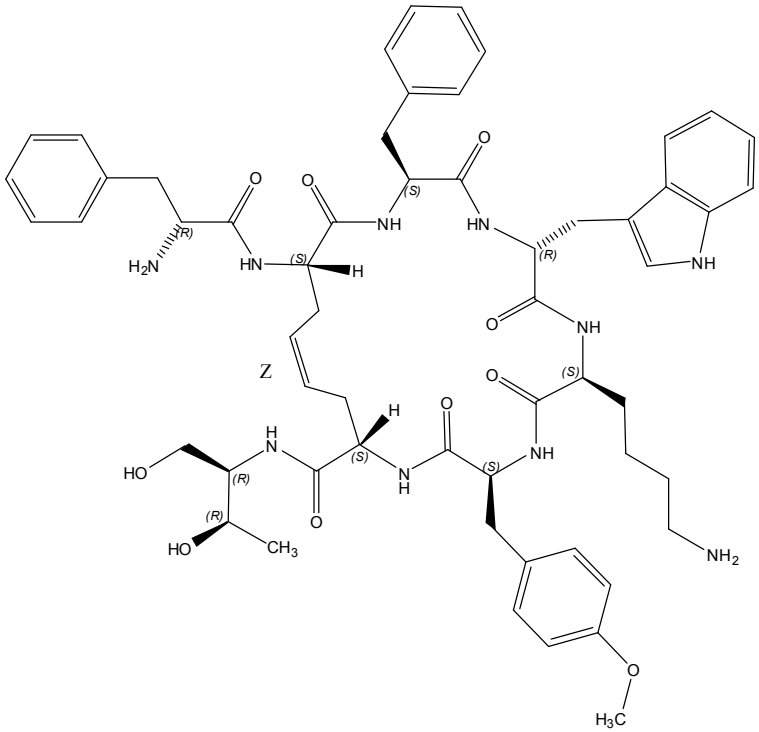

*Figure-S8. Peptide **34**.*

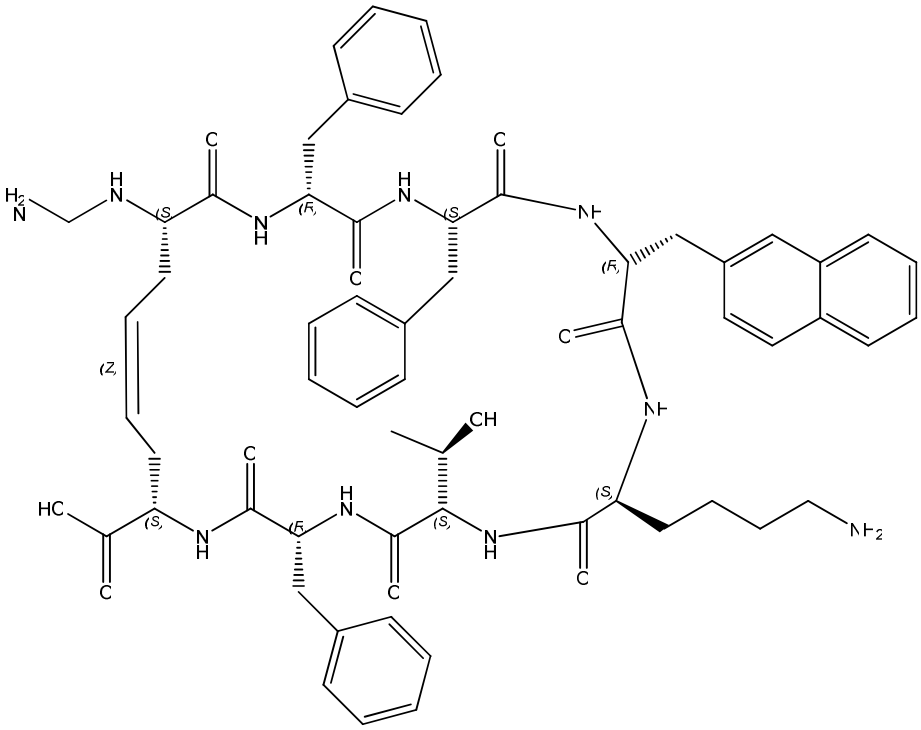

*Figure-S9. Peptide **36**.*

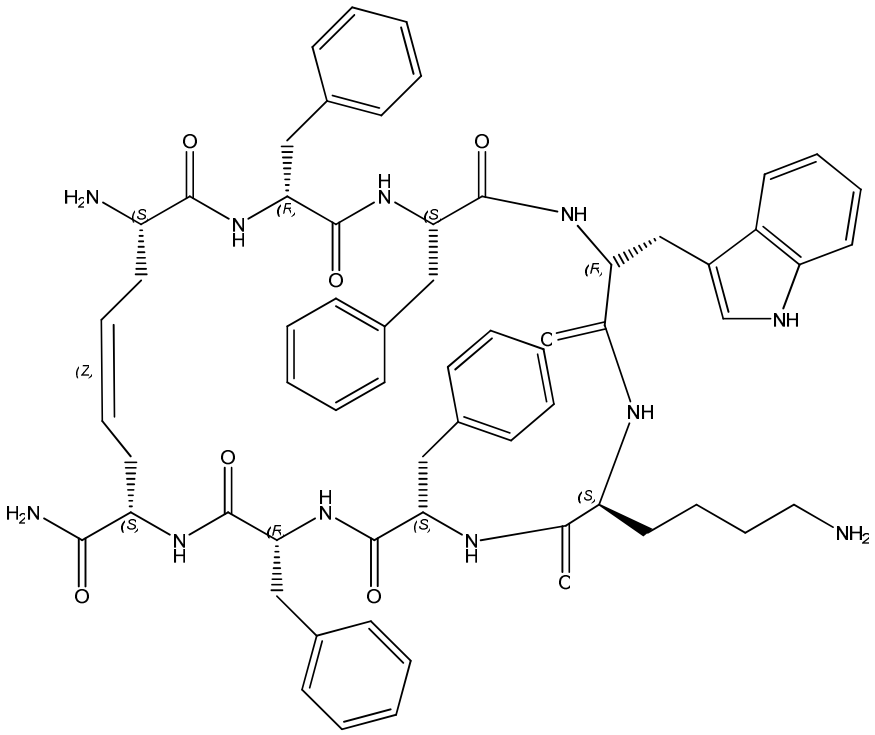

*Figure-S10. Peptide **37**.*

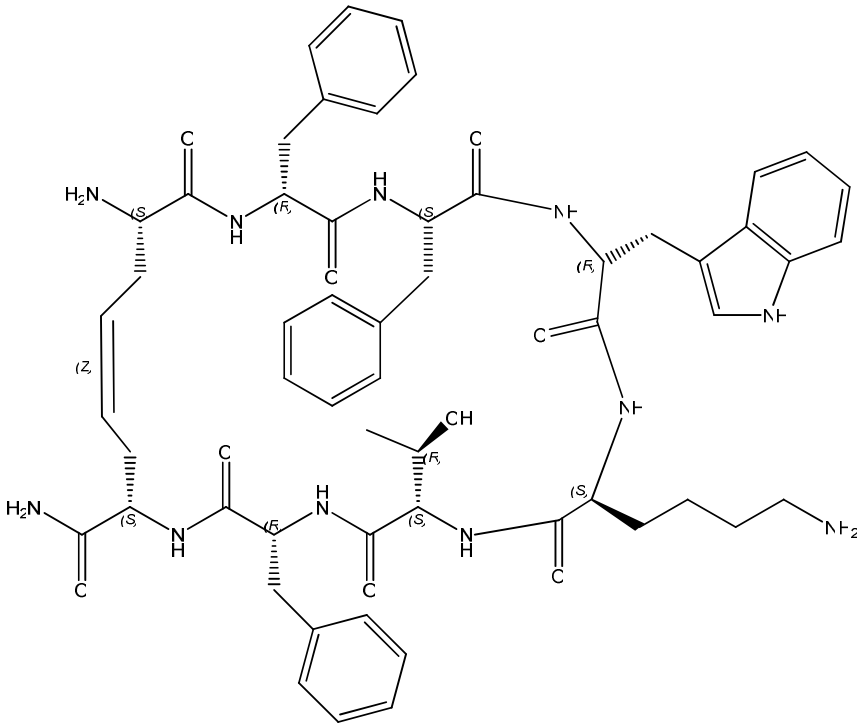

*Figure-S11. Peptide **38.***

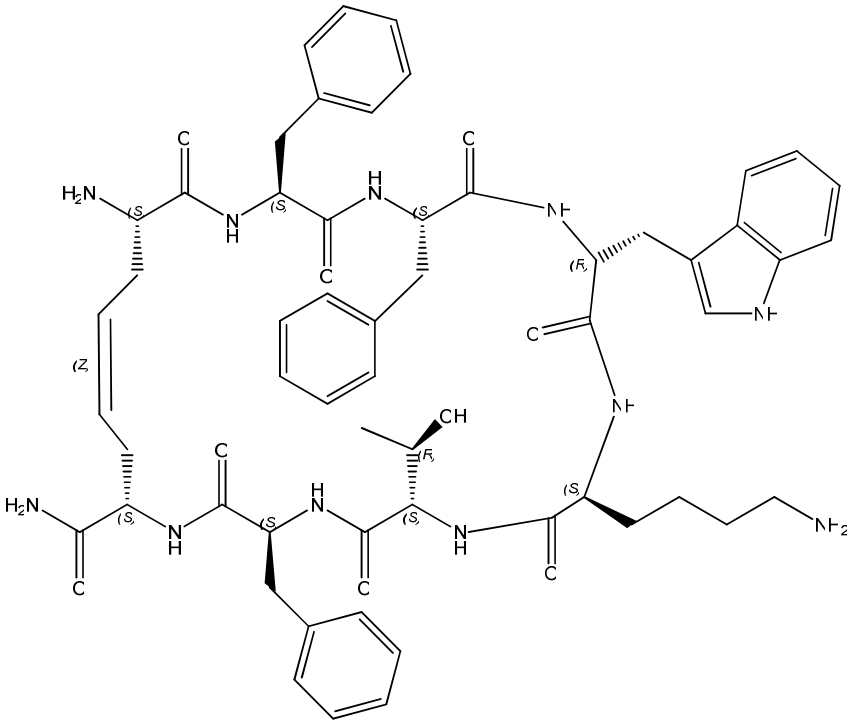

*Figure-S12. Peptide **39**.*

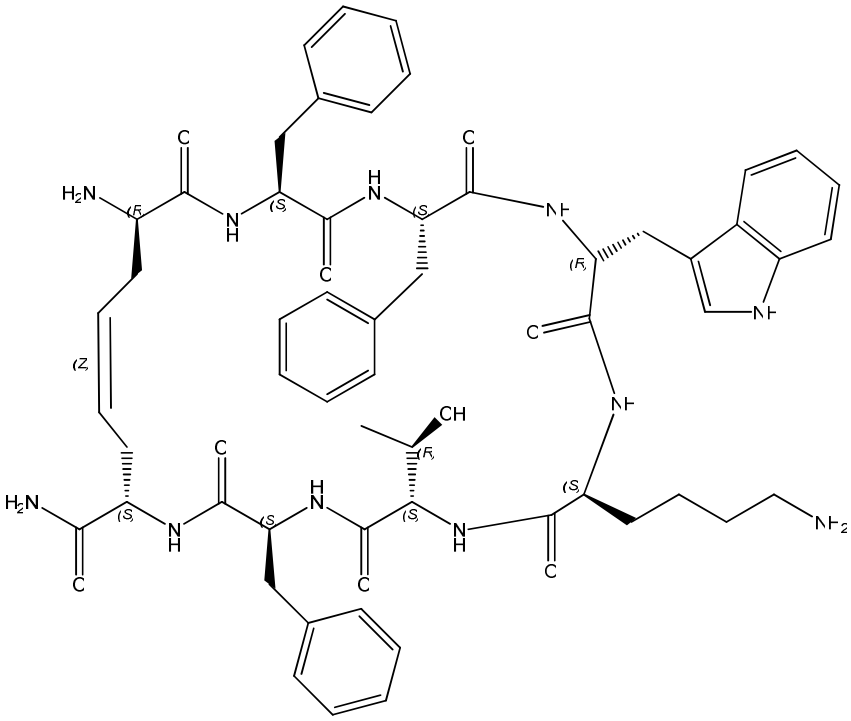

*Figure-S13. Peptide **40**.*

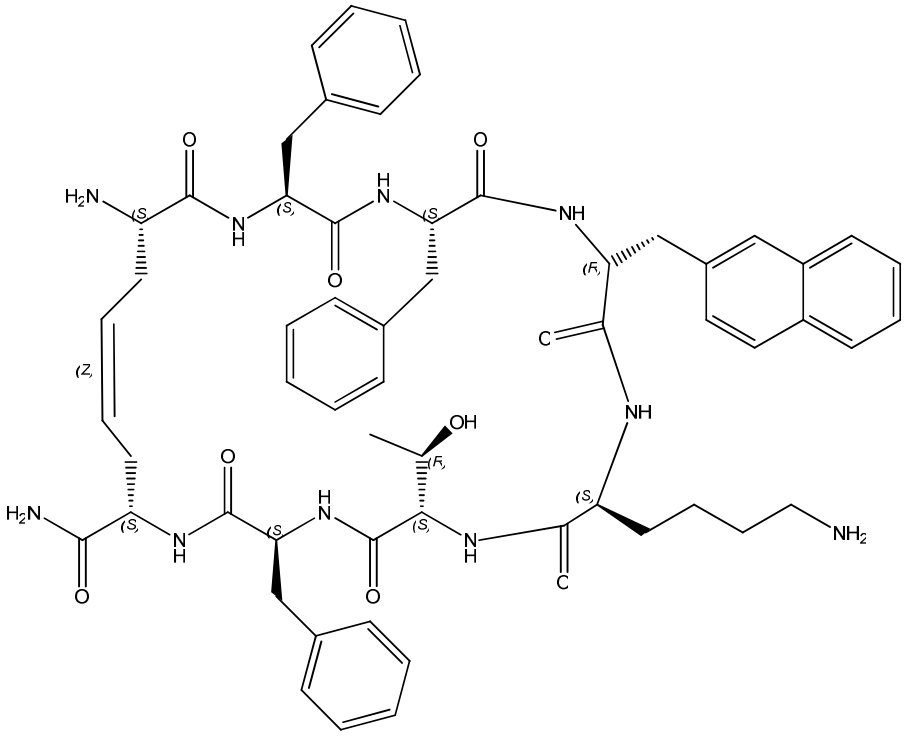

*Figure-S14. Peptide **41**.*

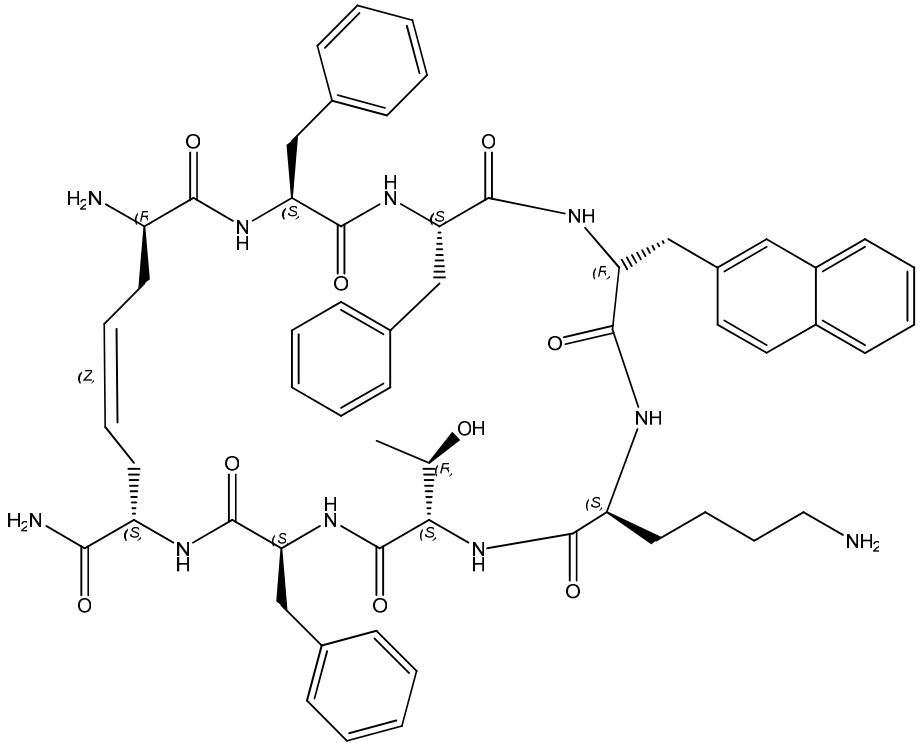

*Figure-S15. Peptide **42**.*

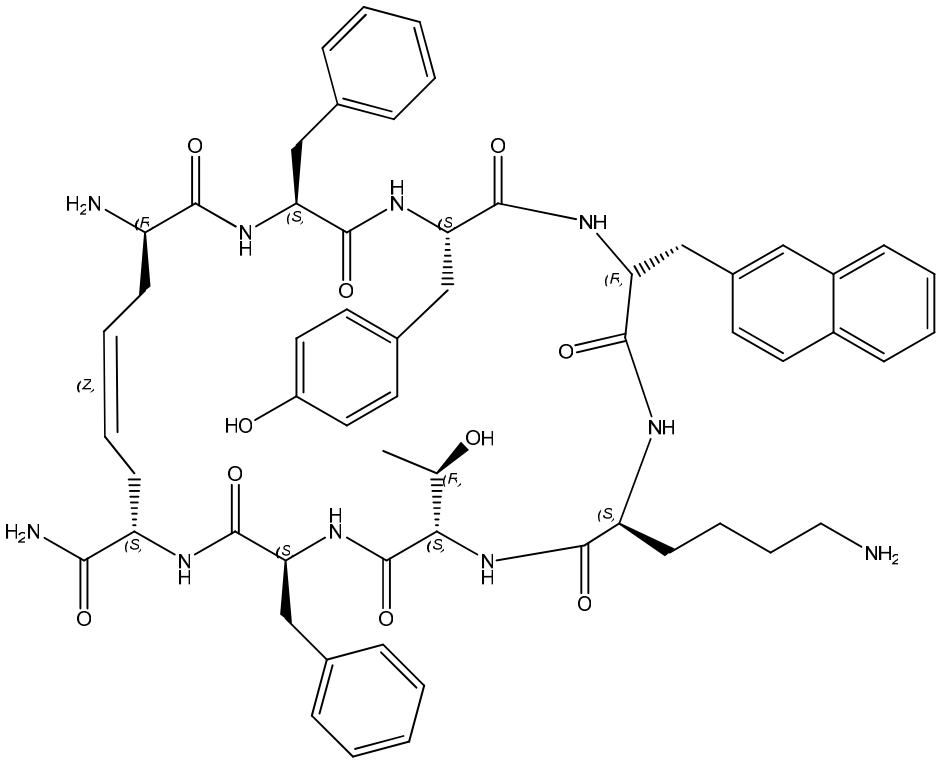

*Figure-S16. Peptide **43**.*

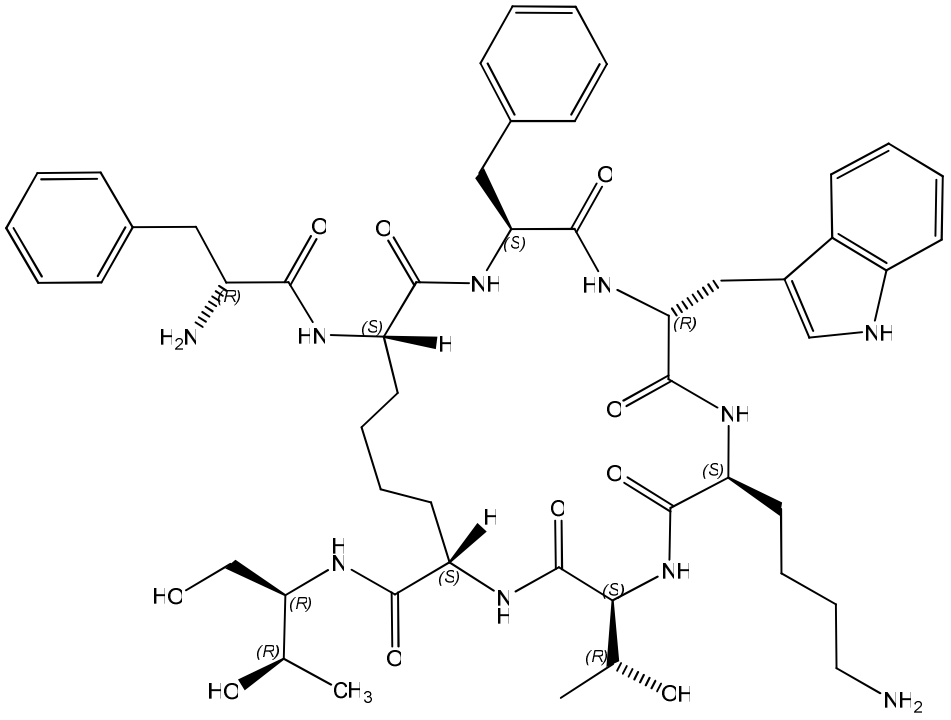

*Figure-S17. Peptide **45**.*

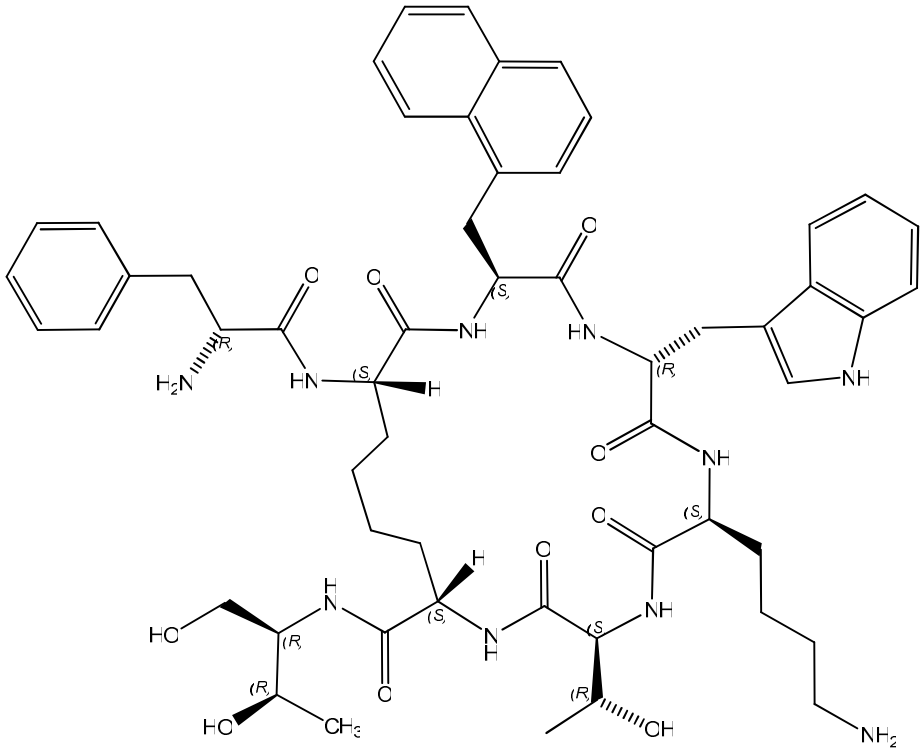

*Figure-S18. Peptide **46**.*

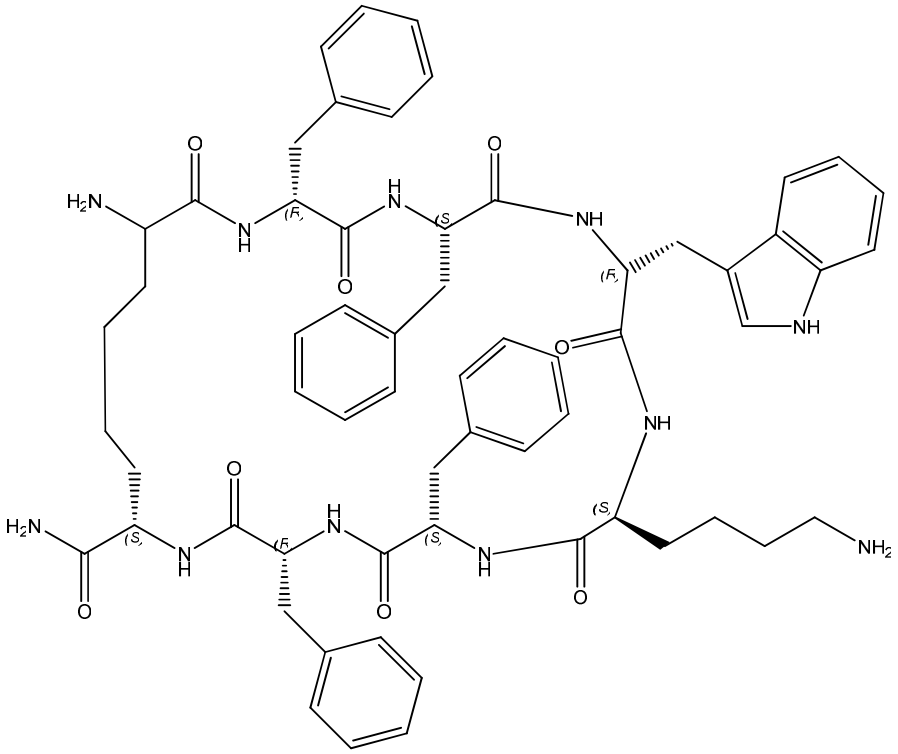

*Figure-S19. Peptide **47**.*

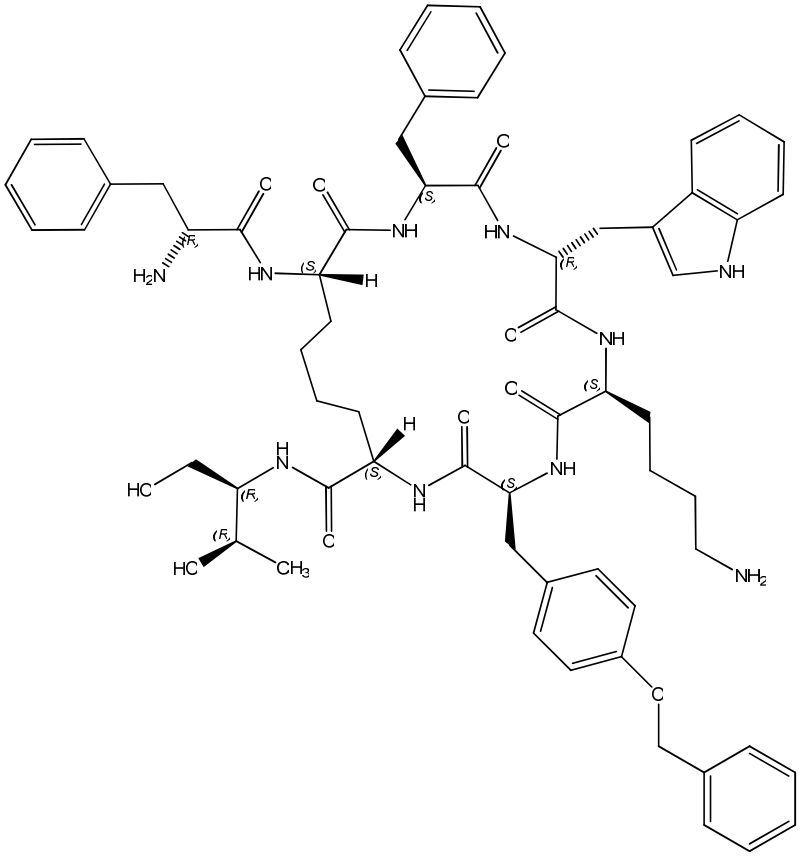

*Figure-S20. Peptide **48**.*

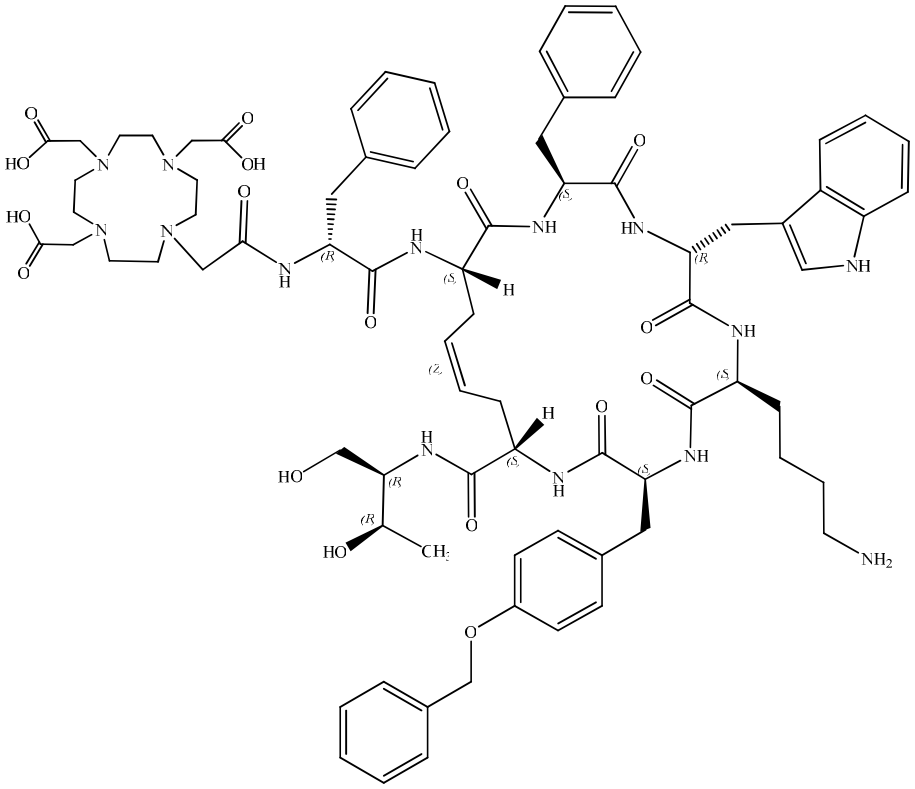

*Figure-S21. Peptide **49**.*

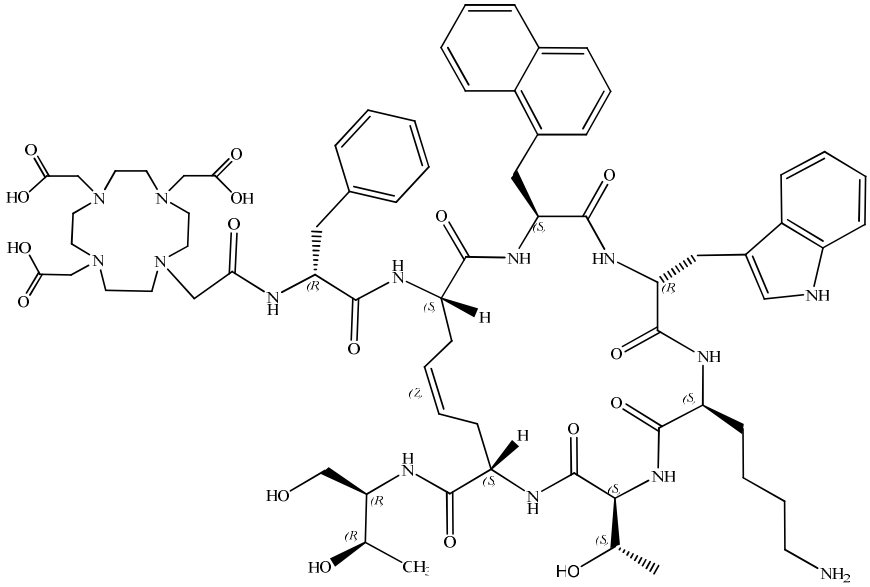

*Figure-S22. Peptide **50**.*

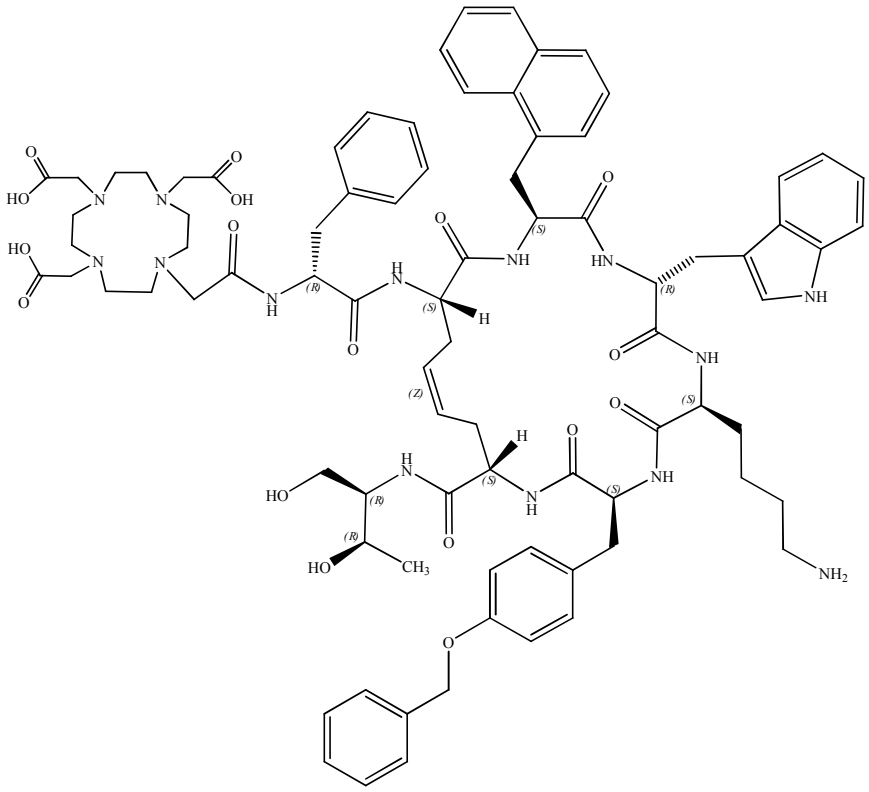

*Figure-S23. Peptide **51**.*

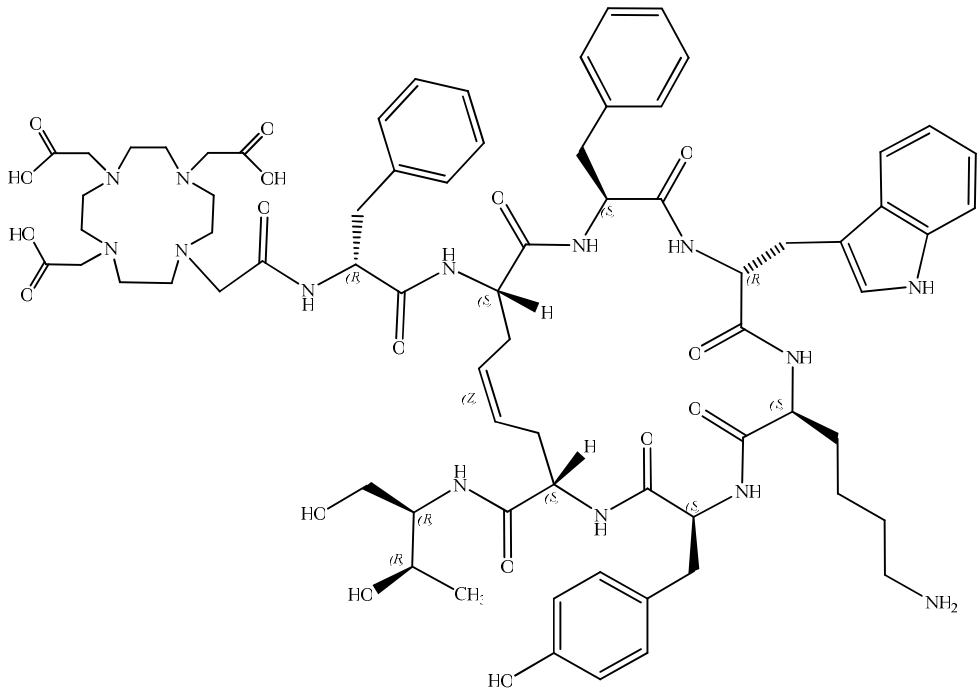

*Figure-S24. Peptide **52.***

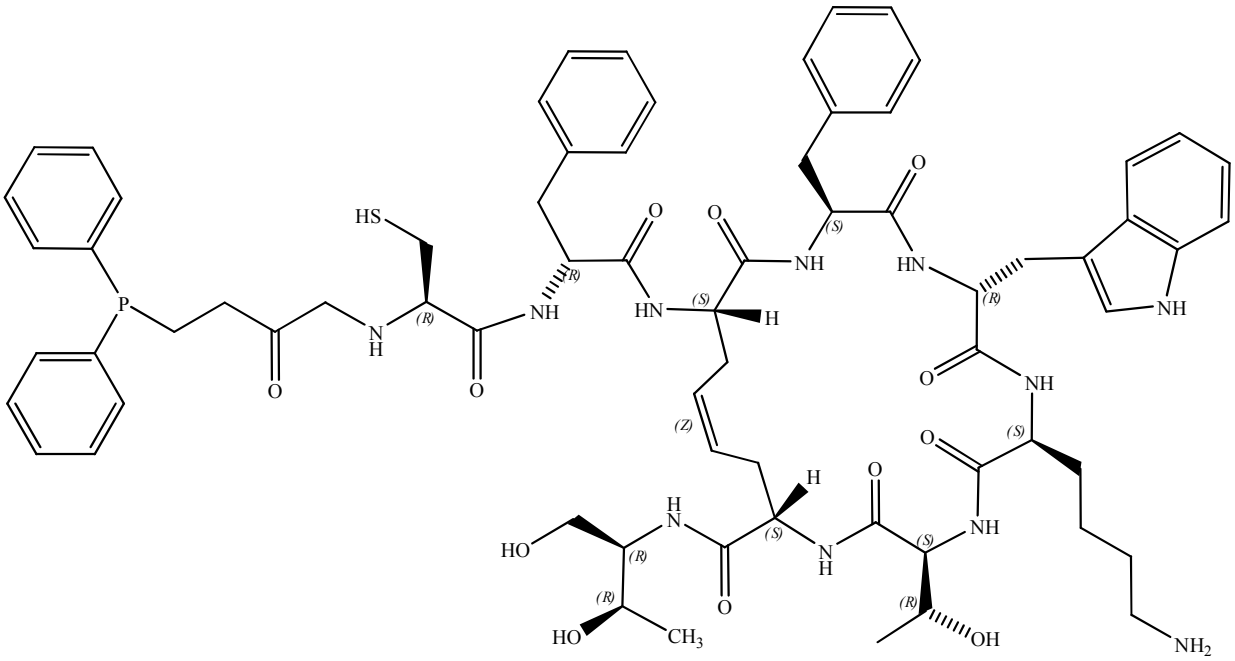

*Figure-S 25. Peptide **53**.*

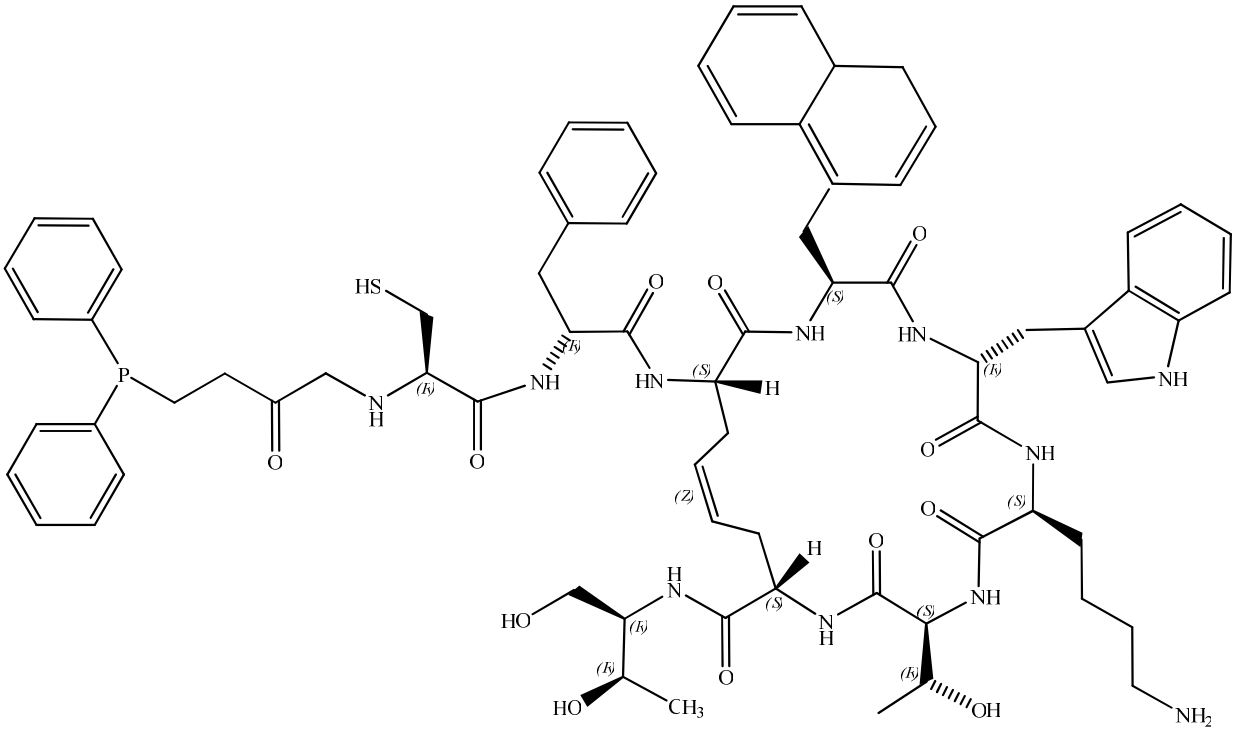

*Figure-S 26. Peptide **54**.*

Peptide Synthesis

Laboratory of Peptides & Proteins, Chemistry & Biology, Department of Organic Chemistry, University of Firenze

Prof. Mauro Ginanneschi
Prof. Anna Maria Papini

Conformational Analysis

Department of Pharmaceutical Chemistry and Toxicology, University Federico II, Napoli

Prof. Alfonso Carotenuto

Binding Essays

Institute of Pathology, Division of Cell Biology and Experimental Cancer Research., University of Bern, Bern, Switzerland

Prof. Jean Claude Reubi

^{99m}Tc Radiolabeling

Department of Pharmaceutical Sciences, University of Padova

Prof. Ulderico Mazzi
Dr. Elena Zangoni

^{111}In Radiolabeling

Regional Center of Nuclear Medicine, University of Pisa

Prof. Giuliano Mariani
Dr.Paola Erba
Dr. Chiara Manfredi

Molecular Modeling

Laboratory of Molecular Modeling, Cheminformatics & QSAR, University of Firenze

Prof. Fabrizio Melani